Role of Tandem Zinc Finger Proteins of *Arabidopsis thaliana* in plant stress responses

Dissertation

zur Erlangung des
Doktorgrades der Naturwissenschaften (Dr. rer. nat.)

der

Naturwissenschaftlichen Fakultät I – Biowissenschaften –

der Martin-Luther-Universität
Halle-Wittenberg,

vorgelegt

von Frau Manaswita Baruah

geb. am 31 December 1989 in Assam, India

Gutacher /in

1. Prof. Dierk Scheel, Leibniz Institute of Plant Biochemistry (IPB), MLU Halle

2. Prof. Sven-Erik Behrens, MLU Halle

3. Dr. Alok Krishna Sinha, NIPGR, India

Verteidigungsdatum: 04.02.2020

Contents

List of abbreviations

ABA	Abscisic acid
ActD	Actinomycin D
AGO1	ARGONAUTE 1
Amp	Ampicillin
ANK	Ankyrin
ARE	AU-rich element
At	*Arabidopsis thaliana*
ATP	Adenosine Triphosphate
BAK1	BRI1-associated Receptor Kinase
BiFC	Bimolecular fluorescence complementation assay
BIK1	Botrytis-induced kinase 1
BRI1	BR-INSENSITIVE 1
C/G/Y/RFP	Cyan/Green/Yellow/Red fluorescent protein
CaCl$_2$	Calcium Chloride
CCCH	Cysteine Cysteine Cysteine Histidine
CDPK	Ca^{2+}-dependent protein kinases
CERK1	Chitin Elicitor ReceptorKinase 1
Col-0	Arabidopsis accession Columbia
DAMP	Damage-Associated Molecular Pattern
DCP1	Decapping 1
DEPC	Diethylpyrocarbonate
DNA	Deoxyribo Nucleic Acid
EDTA	Ethylene Diamine Tetraacetic Acid
EFR	EF-Tu Receptor
EF-Tu	Elongation Factor Thermo Unstable
ERF	Ethylene Responsive Element Binding Factor
ETI	Effector Triggered Immunity
ETS	Effector-Triggered Susceptibility
flg22	Flagellin 22
FLS2	Flagellin insensitive 2
FRK1	Flg22-induced Receptor-like Kinase 1
GA	Gibberellic acid
GhZFP1	Cotton Zinc Finger Protein 1
HA	Hemagglutinin
HR	Hypersensitive response
hTTP	Human tristetraprolin
LB	Left Border
L/RP	left/right primer
LRR	Leucine-Rich Repeat
LysM	LysinMotif
MAMP	Microbe-Associated Molecular Pattern
MAPK/MPK	Mitogen Activated Protein Kinase
MAPKK	MAPK Kinase
MAPKKK	MAPK Kinase Kinase
MARD1	Mediator of ABA-Regulated Dormancy 1

MBP	Maltose binding protein
MEKK	Mitogen activated protein kinases kinase kinase
MKK	Mitogen activated protein kinases kinase
MKS1	Mitogen activated protein kinase substrate 1
MTI	MAMP-Triggered Immunity
NADPH	Nicotinamide Adenine Dinucleotide Phosphate
NES	Nuclear Export Signal
NLR	Nucleotide-binding and leucine-rich repeat domain
NLS	Nuclear Localization Signal
NMD	Nonsense mediated mRNA Decay
PAGE	Polyacrylamide Gel Electrophoresis
PAMP	Pathogen-Associated Molecular Pattern
PARN	Deadenylation enzymes
PAT1	Protein Associated with Topoisomerase II
PB	Processing Bodies
PBL	PBS1-Like Kinase
PCR	Polymerase Chain Reaction
PR1	Pathogenesis Related 1
PRR	Pattern Recognition Receptor
PTI	PAMP-Triggered Immunity
pUBQ10	Promoter, Ubiquitin10
pv.	pathovar
qRT-PCR	quantitative Real Time PCR
RDR6	RNA-dependent RNA polymerase 6
RLCK	Receptor Like Cytoplasmic Kinase
RLK	Receptor Like Kinase
RNA	Ribonucleic Acid
ROS	Reactive oxygen species
RT	Room Temperature
SA	Salicylic Acid
SAR	Systemic Acquired Resistance
SDS	Sodium Dodecyl Sulfate
SEM	Standard Error ofMean
SG	Stress granules
SGS3	Suppressor of Gene Silencing 3
siRNA	Short interfering RNA
SP	Serine Proline
SPCH	Speechless
Spec	Spectinomycin
TF	Transcription Factor
TZFs	Tandem Zinc Finger proteins
UPF	Up-frame shift proteins
UTR	Untranslated region
wt	Wild-type
XRN4	Exoribonuclease

1 Introduction

1.1 Plant innate immune system

Plants are sessile organisms and constantly encounter potential pathogens and pests which results in yield loss in economically important crops. As a first line of defence against pathogen attack, a surveillance system in plants is achieved by its innate immune system. The innate immune system in plants comprises of the recognition of constitutive and conserved molecules including peptides, metabolites, cell wall components, enzymes and toxins (Boller & Felix, 2009; Dodds & Rathjen, 2010; Giraldo et al., 2013; Wirthmueller, Maqbool, & Banfield, 2013) from pathogens (pathogen-associated molecular patterns; PAMPs) and also derived from non-pathogens (microbe-associated molecular patterns; MAMPs) (Ausubel, 2005) by specific receptors (pattern recognition receptors; PRRs): triggering defence responses and thereby transmitting the message of invasion into the downstream signaling cascades (Medzhitov & Janeway, 2002). They are involved in the perception of environmental signals and help plants to respond properly to defend themselves against potential pathogenic microbes or pests.

1.2 Pattern recognition receptors

PRRs are divided into surface and intracellular receptors. These include typically transmembrane or membrane-anchored proteins with structurally diverse extracellular domains, such as Leucine-rich Repeat (LRR), Lysin motif (LysM) or lectin domains. Plant PRRs are structurally and functionally analogous to animal Toll-like Receptors (TLRs) which recognizes PAMPs and damage-associated molecular patterns (DAMPs: plant derived molecules released during pathogen infection). PAMP/MAMP/DAMP detection is achieved by Receptor Kinases (RKs), Receptor Proteins (RPs) or extracellular binding proteins which bind to the epitopes with high specificity and sensitivity (Altenbach & Robatzek, 2007; Ranf, 2017). This recognition eventually activates Pattern-Triggered Immunity (PTI) and have diverse role in plant growth, development, reproduction, adaptation to abiotic stress, symbiosis (Morris & Walker, 2003; Tör, Lotze, & Holton, 2009).

Structurally, an RLK contains a single-pass transmembrane domain, an intracellular kinase domain, and an extracellular domain (ECD) to perceive extracellular molecules (Gómez-Gómez & Boller, 2000; Jianming & Joanne, 1997; Zipfel et al., 2006). On the other hand, RLPs only have a very short intracellular part lacking kinase domain (Liebrand, van den Burg, & Joosten, 2014). Based on the ECDs, these RLKs and RLPs are divided into multiple subfamilies based on their domains. These include LRR (largest group) (P.-L. Liu et al., 2016), LysM, Lectin, and epidermal growth factor-like (EGF) domains (Macho & Zipfel, 2014). There are ~ 410 RLKs and

170 RLPs in *Arabidopsis*, ~640 RLKs and 90 RLPs in rice (Fritz-Laylin, Krishnamurthy, Tör, Sjölander, & Jones, 2005; S.-H. Shiu & Bleecker, 2001; Shin-Han Shiu et al., 2004).

In *Arabidopsis,* LRR-containing RLKs are among the largest subfamilies in the genome with more than 230 members containing a ligand-binding extracellular LRR domain and a cytoplasmic serine/threonine kinase domain. Among the reported RLKs and RLPs, Arabidopsis RK Flagellin-Sensitive 2 (FLS2), Elongation Factor Tu Receptor (EFR), and rice LRR-RK XA21, recognizing a conserved 22 amino acid epitope (flg22) of bacterial flagellin (Gómez-Gómez & Boller, 2000), 18 amino acids of the N-terminus of Elongation Factor Tu (EF-Tu) (Kunze et al., 2004; Zipfel et al., 2006) and tyrosine-sulfated protein RaxX from *Xanthomonas oryzae* pv. *oryzae* (*Xoo*) species (Pruitt et al., 2017), respectively, have been shown to mediate perception of a variety of endogenous or exogenous signals (Tör et al., 2009). Also the two homologous LRR-RKs PEPR1 and PEPR2 act as receptors of AtPeps (A. Huffaker & Ryan, 2007; Krol et al., 2010; Yamaguchi, Huffaker, Bryan, Tax, & Ryan, 2010). Upon Pep perception, PTI signaling is amplified (Z. Liu et al., 2013; Tintor et al., 2013). PIP1, another plant endogenous peptide induced by a variety of pathogens and PAMPs, is perceived by the LRR-RK RLK7 and induces PIP1-mediated immune signaling (Hou et al., 2014). Brassinosteroid Insensitive 1 (BRI1) and BRI1-Associated Receptor Kinase 1 (BAK1, member of the Somatic Embryogenesis Receptor Kinase (SERK) family) are two LRR-RLKs that are involved in the brassinosteroid (BR)-signaling pathway after ligand binding to form ligand-induced heteromers with other RKs for subsequent signaling (Chinchilla, Shan, He, de Vries, & Kemmerling, 2009; J. Li et al., 2002; Nam & Li, 2002). However, BAK1 is not involved in chitin-induced Chitin Elicitor Receptor Kinase 1 (CERK1) signaling in *Arabidopsis*; rather, chitin induces CERK1 homodimerization for its activation (T. Liu et al., 2012). On the contrary, recently, AtLYK5 is reported as the primary receptor for chitin, heterodimerizing with AtCERK1 to induce plant immunity (Cao et al., 2014).

1.3 Pathogen/Microbe Associated Molecular Pattern-Triggered Immunity (PTI) and effector-triggered immunity (ETI)

Plants' innate immunity is achieved by two-tier perception system. The first layer of defense response refers to the basal resistance conferred by surface-localized PRRs leading to PAMP/pattern-triggered immunity (PTI) or MAMP-triggered immunity (MTI) (Ausubel, 2005; Boller & Felix, 2009; Dodds & Rathjen, 2010; Macho & Zipfel, 2015; Stael et al., 2015; Tsuda & Somssich, 2015). Apart from PAMPs/MAMPs, plants can also detect DAMPs which are endogenous molecules of the host plant or cell-wall degradation products such as oligogalacturonides from the action of invading pathogens (Boller & Felix, 2009), thereby resulting in immune responses similar to PTI (Ahrens et al., 2012; Seong & Matzinger, 2004). The second layer involves the host's ability to sense perturbations induced by bacterial toxins or

'effectors' via disease resistance proteins (R proteins) with the help of intracellular immune receptors, thereby inducing effector-triggered immunity (ETI), often resulting in hypersensitive responses. For long-term defense against a broad-spectrum of pathogens, plants also possess systemic acquired resistance (SAR). The second tier of plant immunity is triggered if PTI or MTI is insufficient to prevent infection by pathogens that can subvert PRR-mediated defenses, by recognizing the virulence effectors (molecules delivered by the pathogens in the extracellular matrix or into the plant cell to enhance its multiplication) resulting in high-amplitude activation of immune responses to terminate pathogen growth (Cui, Tsuda, & Parker, 2014; Jones & Dangl, 2006) (**Fig.1**).
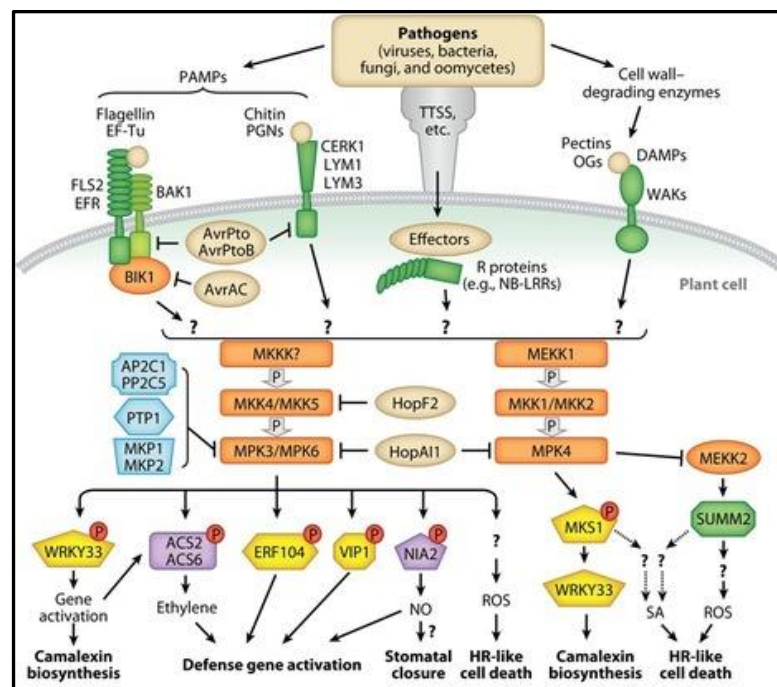
Fig.1 Activation of pathogen/microbe-associated molecular pattern (PAMP/MAMP) and damage-associated molecular pattern (DAMP) signaling.
The execution of immune responses upon ligand perception by the plant pattern recognition receptors (PRRs) and resistance (R) proteins triggers either PAMP-triggered immunity (PTI) or effector-triggered immunity (ETI), respectively. The pathogen-responsive Mitogen-activated protein kinases (MAPK) cascade is activated upon pathogen attack and is one of the earliest signaling events in PTI and ETI. This results in phosphorylation of downstream target proteins, including transcription factors and enzymes. (Source: (Meng & Zhang, 2013)).

1.4 Plant defence responses

In *Arabidopsis thaliana*, bacterial flagellin, elongation factor EF-Tu and fungal cell wall component chitin are recognized as PAMPs/MAMPs by the RLKs FLS2, EFR and CERK1 (Albert, 2013; Felix, Duran, Volko, & Boller, 1999; Gómez-Gómez & Boller, 2000; Kunze et al., 2004; Zipfel et al., 2006). The minimal elicitor-active epitopes are represented by flg22 and elf18 peptides or chitin octamers, respectively. The perception of flg22 and elf18 by FLS2 and EFR, respectively (Zipfel et al., 2006, 2004), leads to the association of another RLK, BAK1 for

activation of downstream immune responses (Chinchilla et al., 2007; Heese et al., 2007). BAK1 serves as a co-receptor for multiple PRRs, and along with the associated receptor-like cytoplasmic kinases (RLCKs) BIK1 (Botrytis–Induced Kinase 1) and its homolog PBL1 (PBS1-LIKE1), play critical roles in PTI (Böhm et al., 2014; Macho & Zipfel, 2014). These association of the FLS2/EFR-BAK1 complexes result in rapid phosphorylation of BIK1 and related PBL proteins, which in turn dissociate from the receptor complexes to regulate downstream signaling (W. Lin et al., 2013; Wenwei Lin et al., 2014; Z. Liu et al., 2013; J. Zhang & Zhou, 2010). BAK1 has dual regulatory function in both BRI1-regulated development processes (J. Li et al., 2002; Nam & Li, 2002) and PRR-dependent plant innate immunity (Boller & Felix, 2009).

Likewise, for perception of the DAMP peptides, *Arabidopsis* Pep epitopes (designated as AtPep1-AtPep8) which are derived from pro-peptides (PROPEPs; PROPEP1–PROPEP8 respectively) are perceived by the two homologous LRR protein kinases PEP1 RECEPTOR 1 (PEPR1)/ PEPR2 (Bartels et al., 2013; a. Huffaker, Pearce, & Ryan, 2006; A. Huffaker & Ryan, 2007; Yamaguchi et al., 2010). However, all the eight AtPeps have a similar function of inducing plant immunity with different expression patterns and localizations (Bartels et al., 2013). AtPeps are reported to have functional similarity as that of systemin (18-residue peptide identified in tomato) in playing a critical role in defense signaling (C. A. Ryan & Pearce, 2003). *At*Pep1 (23-amino acid peptide encoded by *Arabidopsis PROPEP1*), being mediated by PEPR1, activates expression of the defense gene *PDF1.2* (encoding defensin) and its own precursor gene, *PROPEP1*. This activation is achieved through the jasmonate/ethylene signaling pathway (A. Huffaker & Ryan, 2007). DAMP perception and signaling serve to intensify and/or propagate defence signaling for MAMP-triggered immunity against bacterial infection (Fontana & Vance, 2011; Ma, Walker, Zhao, & Berkowitz, 2012; C. a. Ryan, Huffaker, & Yamaguchi, 2007; Tintor et al., 2013).

Among the plant defence responses that follow PRR signaling are cellular responses like rapid and transient burst of Ca^{2+} and reactive oxygen species (ROS) (O'Brien, Daudi, Butt, & Bolwell, 2012), activation of Ca^{2+}-dependent protein kinases (CDPKs) and mitogen-activated protein kinases (MAPKs) (two central signaling modules that transduce early PTI signals into multiple intracellular defense responses) (Tena, Boudsocq, & Sheen, 2011). Among the other events following PRR signaling includes cell wall remodeling, callose deposition, stomatal closure (Melotto, Underwood, & He, 2008), production and secretion of antimicrobial compounds such as camalexin and defense-related proteins/peptides (Ahuja, Kissen, & Bones, 2012; Bednarek, 2012; Cowan, 1999; van Loon, Rep, & Pieterse, 2006), production of the phytohormones ethylene (ET) and salicylate (SA), programmed cell death (PCD) at the site of infection to limit

pathogen progression (Mur, Kenton, Lloyd, Ougham, & Prats, 2008) and extensive transcriptional reprogramming (Boller & Felix, 2009; Macho & Zipfel, 2014).

1.5 MAPK signaling cascade

Mitogen-activated protein kinases (MAPKs) are highly conserved signaling modules encoded by a large family of serine/threonine protein kinases in eukaryotes (Andreasson & Ellis, 2010; Ichimura et al., 2002; Pitzschke, 2015; Widmann, Gibson, Jarpe, & Johnson, 2017). MAPKs are activated by upstream MAPK kinases (MAPKK, MKK, or MEK) through phosphorylation of the conserved threonine and tyrosine residues. Upon ligand perception, MAPKKs activity is regulated by phosphorylation through upstream kinases that belong to the class of MAPKK kinases (MAPKKK or MEKK) (Meng & Zhang, 2013; Pitzschke, 2015; Juan Xu & Zhang, 2015). Regulation of the innate immune responses in plants involves the activation of the MAPK cascades (Pedley & Martin, 2005) and thereby MAPKs play critical role in plant defense against pathogens (Meng & Zhang, 2013; Sinha, Jaggi, Raghuram, & Tuteja, 2011).

In Arabidopsis, there are 20 MAPKs, 10 MAPKKs, and about 60 putative MAPKKKs (Ichimura et al., 2002). Upon PAMP/MAMP perception, two parallel MAPK cascades are activated: MEKK1/MAPKKK1-MKK4/5-MPK3/6 and MEKK1-MKK1/2-MPK4/11 (Asai et al., 2002; Meng & Zhang, 2013; Rodriguez, Petersen, & Mundy, 2010) (**Fig.2**). It has been reported that in Arabidopsis MPK3, MPK4 and MPK6 regulate cell cycle, cytokinesis, plant development and innate immunity (Rodriguez et al., 2010). In rice, fungal chitin triggers MPK3- and MPK6-mediated defense responses (J. Zhang & Zhou, 2010). Recently, MPK1, MPK11 and MPK13 were reported to be transiently activated in response to MAMP treatments (Eschen-Lippold et al., 2012; Nitta, Ding, & Zhang, 2014).
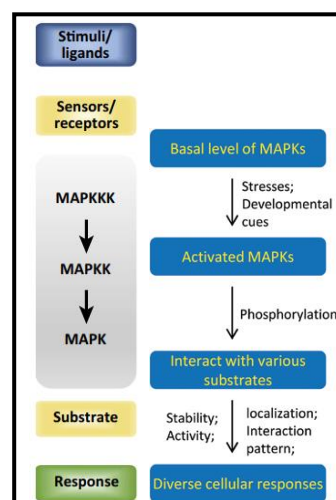

Fig.2 General scheme of Mitogen-activated protein kinase (MAPK) cascades showing the sequential phosphorylation steps.

MAPKs phosphorylate their substrates to execute the immune response. The phosphorylation event can modify major properties of downstream proteins, such as their enzyme activity, sub-cellular localization, as well as their stability and interaction with other proteins (Bigeard, Colcombet, & Hirt, 2015). (Source: (T. Zhang, Chen, & Harmon, 2016)).

1.5.1 MAPK substrates

MPK3 and MPK6 belong to group A of the MPK family and MPK4 to group B (Gao et al., 2008; Suarez-Rodriguez et al., 2007; H. Wang, Ngwenyama, Liu, Walker, & Zhang, 2007). As reported, MPK3 and MPK6 are functionally redundant in many physiological processes. Both are activated by MKK4/5, and share many common substrates (**Table.1**). The lethal phenotype exhibited in the *mpk3/mpk6* double mutant and not in either of the single mutants, depicts their redundancy (H. Wang et al., 2007). However, distinct non-redundant roles for MPK6 have also been described: Ethylene Response Factor 104 (ERF104) was shown to be phosphorylated by MPK6, but not by MPK3 (Bethke et al., 2009). On the other hand, MPK4 was initially identified as a negative regulator in plant defense (Petersen et al., 2000). However, several other roles of MPK4 in plant defense (Andreasson et al., 2005; Frei dit Frey et al., 2014), cytokinesis (Sasabe, Kosetsu, Hidaka, Murase, & Machida, 2011), mRNA stability (Roux et al., 2015) and regulation of DNA binding activity (B. Li et al., 2015a) highlight the diversity of MPK4 activity.

Various screening methods have been employed to identify MAPK substrates, these include protein arrays (Feilner et al., 2005) and MS-based approaches (Benschop et al., 2007; Hoehenwarter et al., 2013; Lampard, MacAlister, & Bergmann, 2008; Lassowskat, Böttcher, Eschen-lippold, Scheel, & Lee, 2014; Y. Liu & Zhang, 2004; Roux et al., 2015; Umezawa et al., 2013; P. Wang et al., 2013; Whisenant et al., 2010). Functional analyses of candidate proteins involve techniques like kinase (phosphorylation) assays, mutagenesis approaches at specific phosphorylation sites and the like. Some of the reported substrates of MAPKs are depicted in **Fig.3** and are listed in **Table 1**.
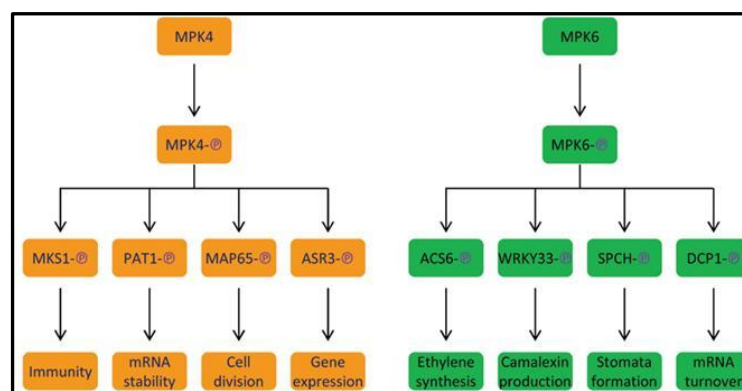

Fig.3 Downstream substrates of MAPK cascades.
The figure depicts the roles of the various substrates upon phosphorylation by the indicated MPKs. (Source: (T. Zhang et al., 2016)).

Table 1 MAPK substrates and their possible function

Substrate	MPK	Function	References
Arabidopsis SH4-Related 3 (ASR3)	MPK4	A transcription repressor closely related to Shattering 4 (SH4), which is a QTL controlling rice grain shattering	(B. Li et al., 2015b)
Topoisomerase II 1 (PAT1)	MPK4	Required for the decapping of mRNAs in plants	(Roux et al., 2015)
MAP kinase 4 substrate 1 (MKS1)	MPK4	Interacts with MPK4 and WRKYs in defense response	(Andreasson et al., 2005)
SUMM1	MPK4	Encodes MAPKKK9, which is also known as MEKK2	(Q. Kong et al., 2012)
Microtubule-Associated Protein 65 (MAP65-1/2/3)	MPK4	Role in cytokinesis	(Beck, Komis, Müller, Menzel, & Šamaj, 2010; Sasabe et al., 2011)
MAP65-1	MPK6	Role in cytokinesis	(Hoehenwarter et al., 2013; Popescu et al., 2009; Smertenko, 2006)
DCP1	MPK6	Promotes mRNA decapping under dehydration stress	(Jun Xu & Chua, 2012)
ACS6 (1 aminocyclopropane-1-carboxylic acid synthase)	MPK6	Ethylene biosynthesis	(Y. Liu & Zhang, 2004)
Ethylene Response Factor (ERF104)	MPK6	Defense against fungal pathogens	(Bethke et al., 2009)
Speechless (SPCH)	MPK3/MPK6	Basic helix–loop–helix transcription factor, involved in stomatal development	(Lampard et al., 2008)
WRKY34	MPK3/MPK6	Pollen-specific transcription factor	(Guan et al., 2014)
WRKY33	MPK3/MPK6	Camalexin biosynthesis in defense	(Guan et al., 2014; Mao et al., 2011)
WRKY22	MPK3/MPK6	Resistance to both bacterial and fungal pathogens	(Asai et al., 2002)
WRKY29	MPK3/MPK6	Resistance to both bacterial and fungal pathogens	(Asai et al., 2002)
Ethylene Response Factor 6 (ERF6)	MPK3/MPK6	Defense against fungal pathogens	(Meng et al., 2013)
Tandem Zinc Finger protein (TZF7)	MPK3/MPK6	Role in oxidative stress responses	(Feilner et al., 2005; Hoehenwarter et al., 2013; Lassowskat et al., 2014)
Tandem Zinc Finger protein (TZF9)	MPK3/MPK6	Role in PAMP-triggered immunity (PTI)	(Feilner et al., 2005; Maldonado-Bonilla et al., 2014)

1.6 Post-transcriptional regulation

Post-transcriptional regulation plays a crucial role in eukaryotic gene expression. It encompasses several steps linking transcription and translation, which includes 5' capping, splicing, polyadenylation, RNA modifications, regulation of RNA sub-cellular localization and degradation of RNA (X. Deng & Cao, 2017). RNA quality control, a surveillance mechanism in eukaryotes, selectively eliminates endogenous dysfunctional transcripts to guard against defects in gene expression, whereas RNA silencing degrades exogenous RNAs (D. Belostotsky, 2004; X. Chen, 2008; Chiba & Green, 2009; M. J. Moore, 2005; Schoenberg & Maquat, 2012) and is activated when the RNA surveillance cannot degrade aberrant RNAs in cells (De Alba et al., 2015; Gazzani, Lawrenson, Woodward, Headon, & Sablowski, 2004; Gy et al., 2007; Herr, Molnar, Jones, & Baulcombe, 2006; Lange et al., 2014; Moreno et al., 2013). Both these mechanisms are essential to ensure the correct partitioning of RNA substrates and, hence, are important for maintaining plant transcriptome integrity and proper plant development.

Degradation of mRNA or mRNA turnover is a tightly regulated process and is an important control point in the regulation of gene expression. The process of mRNA decay, as reported, can be divided into three steps *viz.*, targeting mRNA recognition, activation of the mRNA decay machinery, and its degradation. The first two steps are referred to as potential targets for regulation, and hence are essential to elucidate the regulation of mRNA turnover in modulating gene expression (Lykke-Andersen & Wagner, 2005). An important signal for rapid mRNA turnover in mammalian cells is the AU-rich element (ARE), which is a *cis*-acting element present in the 3′ UTR of many highly regulated mRNAs (C. Y. A. Chen & Shyu, 1995; Wilusz, Wormington, & Peltz, 2001) that encode many inflammation and cancer-associated genes and act as mRNA (in)/stability determinants by interacting with ARE-binding proteins (ARE-BPs) (Bevilacqua, Ceriani, Capaccioli, & Nicolin, 2003; C. Y. Chen et al., 2001).

1.6.1 RNA surveillance

In eukaryotes, there are three types of mRNA surveillance pathways, namely nonsense-mediated decay (NMD), non-stop decay (NSD), and no-go decay (NGD) (Chiba & Green, 2009; Isken & Maquat, 2007).

NMD is a surveillance mechanism that degrades aberrant mRNA transcripts and in plants, NMD is activated by the presence of premature termination codons (PTCs) arising as a consequence of mutation, transcription errors, or alternative splicing events (Chiba & Green, 2009; Schweingruber, Rufener, Zünd, Yamashita, & Mühlemann, 2013). The NMD machinery consists of three core components, UP FRAMESHIFT1 (UPF1), UPF2, and UPF3, which participate in NMD target recognition and the degradation of these aberrant RNAs either through decapping or

deadenylation pathways followed by exonucleolytic decay (Chiba & Green, 2009; Isken & Maquat, 2008; Kerényi et al., 2008; Lejeune, Li, & Maquat, 2003; Yoine, Nishii, & Nakamura, 2006) (**Fig.4**). It was reported that *Arabidopsis* UPF1 co-localized with both Processing body (P body) (see section **1.6.4.1**) and small interfering RNA (siRNA) body markers, suggesting UPF1's dual roles in RNA surveillance and RNA silencing (Moreno et al., 2013).
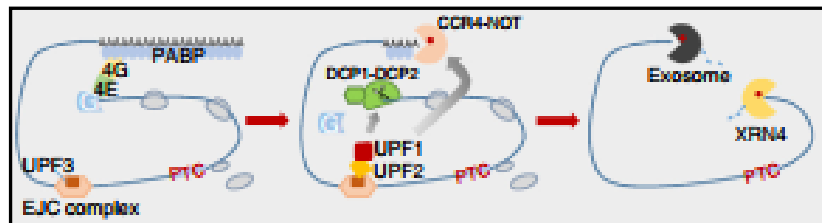

Fig.4 Non-sense mediated decay.
NMD is one of the major mRNA quality control pathways that degrade mRNAs in translation-dependent manner. Degradation of aberrant mRNAs by NMD occurs via premature termination codons (PTCs) involving UPF1, UPF2 and UPF3. (Source: (X. Zhang & Guo, 2017)).

1.6.2 RNA decay

In eukaryotes, degradation of messenger RNAs (mRNAs) is required for both mRNA quantity and quality control. The 5' cap and the 3' poly(A) tail are the primary determinants of mRNA stability and translation and these structures are bound by the eukaryotic initiation factor 4E (eIF4E) and poly(A) binding proteins (PABP), respectively. eIF4F forms a tight complex with the mRNA cap, along with eIF4G and cytoplasmic PABP, thereby circularizing the mRNAs into a stable and translatable entity (Amrani, Ghosh, Mangus, & Jacobson, 2008; Mangus, Evans, & Jacobson, 2003; Wells, Hillner, Vale, & Sachs, 1998). Hence, cytoplasmic mRNA degradation begins with deadenylation, the shortening or complete removal of the poly (A) tail by deadenylases. This results in shutting down mRNA translation and activating the mRNA degradation machinery (Eulalio, Behm-Ansmant, & Izaurralde, 2007; Parker & Sheth, 2007).

RNA decay in plants occurs through two mechanisms: 5'-3' degradation by XRN exonucleases and 3'-5' degradation by the multimeric exosome complex (Meyer, Temme, & Wahle, 2004; Shoemaker & Green, 2012). The key steps in both the mechanisms include deadenylation, decapping, and exonucleolytic degradation of mRNA (Chiba & Green, 2009) (**Fig.5**). The decay process is initiated by removal of the poly(A) tail (deadenylation), catalyzed by the 3'-5' poly(A)-specific ribonuclease (PARN) and carbon catabolite repressor 4 (CCR4) complex (Chiba et al., 2004; Dupressoir et al., 2001; Reverdatto, Dutko, Chekanova, Hamilton, & Belostotsky, 2004; Virtanen, Henriksson, Nilsson, & Nissbeck, 2013). After this, the 5' cap structure is removed by the decapping reaction, mediated by a set of conserved decapping proteins, including DECAPPING 1 (DCP1), DCP2, DCP5, VARICOSE (VCS), and DEA (D/H)-box RNA HELICASE

HOMOLOG 1 (DHH1); DCP2 being the catalytic subunit (Goeres et al., 2007a; Iwasaki, Takeda, Motose, & Watanabe, 2007; Jun Xu & Chua, 2009; Jun Xu, Yang, Niu, & Chua, 2006).

After the decapping step, the aberrant mRNAs are degraded irreversibly by 5'–3' exoribonuclease, e.g. XRN1 in yeast (Decker & Parker, 1993; Muhlrad & Parker, 1994), the nuclear XRN2 and XRN3 and the cytoplasmic XRN4/EIN5 in plants: XRN4 in *Arabidopsis* (Gazzani et al., 2004; Kastenmayer & Green, 2002; Nagarajan, Jones, Newbury, & Green, 2013; Rymarquis, Souret, & Green, 2011; Souret, Kastenmayer, & Green, 2004) and also by the 3'-5' exonucleolytic pathways.

The deadenylation and the decapping proteins and also the exoribonuclease, XRN4/EIN5, are reported to co-localize in cytoplasmic foci called RNA processing bodies (P bodies), the sites of RNA turnover (C. Y. A. Chen & Shyu, 2013; Maldonado-Bonilla, 2014; Souret et al., 2004; Weber, Nover, & Fauth, 2008a; Jun Xu & Chua, 2011).

1.6.3 RNA silencing

RNA silencing in plants is a nucleotide-sequence-specific gene regulation mechanism (Molnar, Melnyk, & Baulcombe, 2011). Transcriptional gene silencing (TGS) and post-transcriptional gene silencing (PTGS) are two major types of RNA silencing mechanisms which are involved in DNA methylation or histone modifications in the nucleus, and mRNA cleavage or translational repression in the cytoplasm (Law & Jacobsen, 2010; Matzke & Mosher, 2014) respectively. RNA silencing depends on the actions of small RNA molecules of 21–24 nt: microRNA (miRNA) and small interfering RNA (siRNA) (Carthew & Sontheimer, 2009; X. Chen, 2012; Poethig et al., 2006; Ramachandran & Chen, 2008). PTGS is triggered by the production of double-stranded RNAs (dsRNAs) by RNA-DEPENDENT RNA POLYMERASE 6 (RDR6) and the RNA stabilizing protein SUPPRESSOR OF GENE SILENCING 3 (SGS3), which are reported to accumulate in siRNA bodies in the cytoplasm (Jouannet et al., 2012a; Kumakura et al., 2009). The dsRNAs produced are further processed by DICER-LIKE 4 (DCL4) or DCL2 into siRNAs, which are then acted upon by Argonaute 1 (AGO1) to mediate the cleavage of the target mRNAs (Dalmay, Hamilton, Rudd, Angell, & Baulcombe, 2000; Gasciolli, Mallory, Bartel, & Vaucheret, 2005; Mourrain et al., 2000) (**Fig.5**).
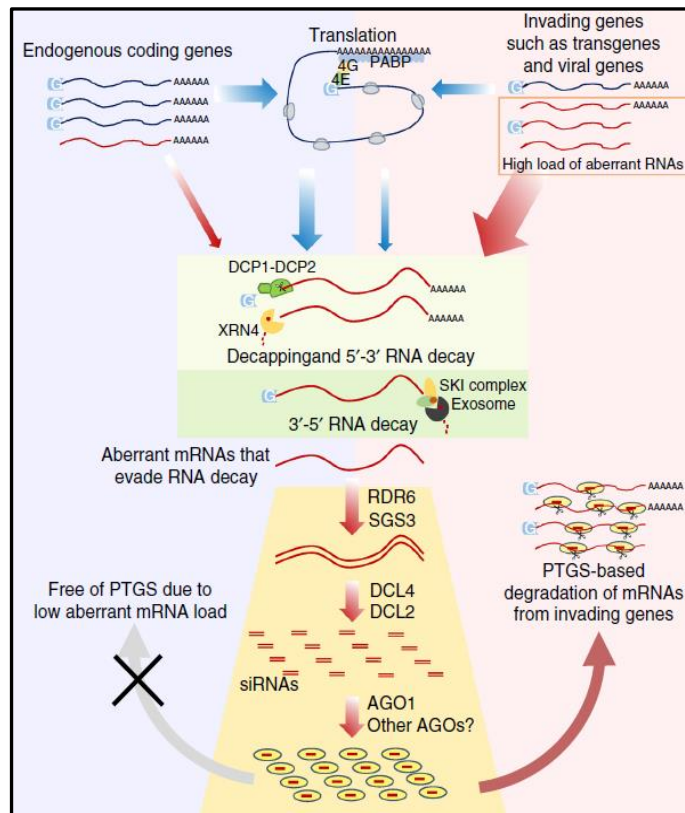
Fig.5 RNA degradation pathways in plants.
mRNA decay occurs through deadenylation-mediated RNA decay pathway followed by either XRN4-mediated 5'–3' digestion or exosome-mediated 3'–5' digestion and is also mediated by XRN4. On the other hand, accumulation of cellular aberrant mRNAs from invading genes such as transgenes and viral genes is directed to RDR6-mediated posttranscriptional gene silencing (PTGS) involving RDR6, SGS3, DCL2/DCL4 and AGO1. (Source: (X. Zhang & Guo, 2017)).

1.6.4 Processing bodies, Stress granules

Regulation of gene expression involves the process of packaging of cytoplasmic mRNA into discrete RNA granules to delay the translation of specific transcripts. In eukaryotic cells, these cytoplasmic messenger ribonucleo proteins (mRNPs) exist in three functional states, namely, translated mRNPs, untranslated stored mRNPs and mRNPs under degradation (Eulalio et al., 2007; Garneau, Wilusz, & Wilusz, 2007; Parker & Sheth, 2007). The non-translating mRNAs accumulate in two types of cytoplasmic mRNP granules: Processing or P bodies (containing the mRNA decay machinery) and stress granules (SG) (containing many translation initiation components) (Anderson & Kedersha, 2006; Franks & Lykke-Andersen, 2008; Parker & Sheth, 2007).

1.6.4.1 Components of SG

Stress granules are non-membranous cytoplasmic phase-dense structures that occur in eukaryotic cells when exposed to environmental stress like heat, viral infection, oxidative conditions, ultraviolet (UV) irradiation, hypoxia (N. L. Kedersha, Gupta, Li, Miller, & Anderson, 1999). The assembly of these stress-induced structures results when translation initiation is

impaired, either due to decreased translation initiation rates during a stress response involving the stress-induced phosphorylation of eukaryotic initiation factor eIF2a (N. L. Kedersha et al., 1999; Nancy Kedersha et al., 2000), or the addition of drugs blocking translation initiation (Dang et al., 2006; Rachid Mazroui et al., 2006; Mokas et al., 2009; Weber et al., 2008a), or due to reduced expression of specific initiation factors (Mokas et al., 2009), or overexpression of RNA-binding proteins that repress translation (De Leeuw et al., 2007; Gilks, 2004; Nancy Kedersha et al., 2005; R. Mazroui, 2002; Wilczynska, A., Aigueperse, C., Kress, M., Dautry, F., Weil, D., 2005).

The core constituents of SGs include poly(A)+mRNA, 40S ribosomal subunits, eIF4E, eIF4G, eIF4A, eIF4B, PABP, eIF3, and eIF2 (Anderson & Kedersha, 2006; N. Kedersha, 2002; N. L. Kedersha et al., 1999; Kimball, Horetsky, Ron, Jefferson, & Harding, 2003; Rachid Mazroui et al., 2006). Additionally, SGs contain translationally-stalled mRNAs, associated pre-initiation factors, specific RNA-binding proteins, and many signaling proteins that are recruited transiently to SGs and/or influence their assembly (Nancy Kedersha, Ivanov, & Anderson, 2013a) (**Fig.6**). Hence, the SGs serve as sorting sites, where mRNAs are targeted for storage, re-initiation or degradation by transfer to P bodies (Nancy Kedersha et al., 2005).
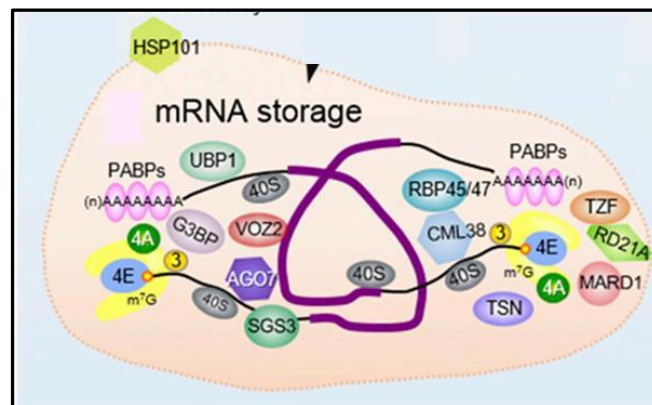
Fig.6 Composition of Stress granules (SG).
(Source: (Chantarachot & Bailey-Serres, 2018).

1.6.4.2 Components of P bodies

P bodies are cytoplasmic protein complexes involved in degradation and translational arrest of mRNAs and are enriched with translationally repressed mRNAs and mRNA silencing and degradation machineries (Parker & Sheth, 2007). P bodies comprise of RNA–protein complexes including factors involved in translation initiation (Andrei et al., 2005; Ferraiuolo et al., 2005), deadenylation (Cougot, Babajko, & Séraphin, 2004), decapping (Sheth & Parker, 2003), 5'→3' - exonucleolytic decay (Bashkirov, Scherthan, Solinger, Buerstedde, & Heyer, 1997), nonsense-

mediated decay (Sheth & Parker, 2006; Unterholzner & Izaurralde, 2004) and miRNA-mediated RNA decay (Sen & Blau, 2005). In yeast and animals, the core constituents of P body include subunits of decapping complex (DCP1, DHH1p, EDC3, SCD6, PAT1, and LSM1-7) which mediate the activity of the catalytic subunit DCP2. In *Arabidopsis,* the catalytic subunit DCP2, and the subunits DCP1, DCP5, and VCS, the 5'-exoribonuclease (in yeast: XRN1; in *Arabidopsis*: XRN4), and deadenylases (PARN and the carbon catabolite repressor 4 (CCR4)-associated factor 1 (CAF1) complex) are prominent markers of P body in eukaryotic organisms (**Fig.7**).
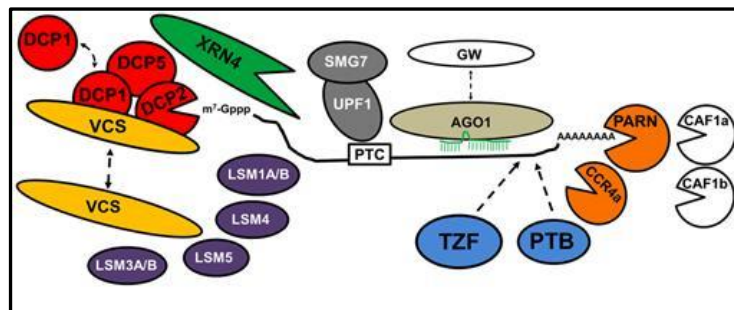
Fig.7 Composition of Processing body (P body).
(Source: (Maldonado-Bonilla, 2014)).

Both P bodies and SGs are conserved and are distinct from HSGs (Heat stress granules) (Weber et al., 2008a) and they are important for post-transcriptional regulation and epigenetic modulation of gene expression (Anderson & Kedersha, 2009; D. A. Belostotsky & Sieburth, 2009; Muench, Zhang, & Dahodwala, 2012; Jun Xu & Chua, 2009).

1.7 Tandem Zinc Finger Proteins

1.7.1 Zinc finger proteins
The zinc finger motif is a small protein motif; being first recognized in *Xenopus* transcription factor IIIA (TFIIIA) (Miller, McLachlan, & Klug, 2001) and the first TFIIIA-type zinc-finger protein in plants (ZPT2-1, renamed from EPF1) was identified from petunia (H. Takatsuji, Mori, Benfey, Ren, & Chua, 1992). Zinc finger genes constitute a large and diverse gene family characterized by the presence of zinc-containing 'finger-like' structural protein folds of conserved cysteine and histidine residues (Laity, Lee, & Wright, 2001). Zinc finger proteins are among the most abundant proteins in eukaryotic genomes and these vary widely in structure, as well as in function. Among the diverse cellular functions, DNA recognition, RNA packaging, transcriptional activation, regulation of apoptosis, protein folding and assembly, transcription, mRNA degradation, protein-protein interaction, membrane association and lipid binding have been reported (Laity et al., 2001). In animals, the zinc finger proteins have been reported to function

mainly in mRNA turnover (P. J. Blackshear, 2002; Hall, 2005). Structurally, based on the number and arrangement of cysteine and histidine residues, zinc finger proteins are classified as C_2H_2, C_2HC, C_2HC_5, C_3HC_4, CCCH, C_4, C_4HC_3, C_6, and C_8 (Jenkins, Li, Scutt, & Gilmartin, 2005; M. Moore & Ullman, 2003; Schumann et al., 2007; Hiroshi Takatsuji, 1999). In plants, zinc finger families include RING-finger, ERF, WRKY, DOF and LIM families (Arnaud, Déjardin, Leplé, Lesage-Descauses, & Pilate, 2007; Freemont, 1993; Kosarev, Mayer, & Hardtke, 2002; Lijavetzky, Carbonero, & Vicente-Carbajosa, 2003; Rice, Nakano, Suzuki, Fujimura, & Shinshi, 2006; Y. Zhang & Wang, 2005).

1.7.2 CCCH Zinc finger proteins

Among the different types of zinc finger proteins, the CCCH zinc finger proteins are conserved and present in diverse eukaryotic organisms ranging from man to yeast (Carrick, Lai, & Blackshear, 2004; De et al., 1999; DuBois, McLane, Ryder, Lau, & Nathans, 1990; Gomperts, Pascall, & Brown, 1990; Mello et al., 1996; Nie, Maclean, Kumar, McKay, & Bustin, 1995; Seydoux et al., 1996; Taylor et al., 1991; Thompson, Lai, Taylor, & Blackshear, 1996; D. Wang et al., 2008a). Genome-wide analyses have identified 67 CCCH zinc finger protein genes in rice (D. Wang et al., 2008a), 68 genes in maize (Peng et al., 2012), 34 genes in Medicago (Cuiqin Zhang et al., 2013) and 91 genes in poplar (Chai et al., 2012). In the *Arabidopsis* genome, there are 68 members of the 'CCCH-type' zinc finger proteins and these are divided into 11 subfamilies based on their finger structure and spacing (D. Wang et al., 2008a). The subfamily IX (**Fig.8**), also known as tandem zinc finger (TZF), has 11 members- being uniquely characterized by two tandem CCCH-type ($C-X_{7-8}-C-X_5-C-X_3-H$ and $C-X_5-C-X_5-C-X_3-H$) zinc fingers separated by 16 amino acids and a conserved 50 amino acid stretch upstream of the CCCH motifs (M. C. Pomeranz et al., 2010a). Five of these TZFs, TZF7–TZF11, are reported to contain two ankyrin repeats (Mosavi, Cammett, Desrosiers, & Peng, 2004) as potential protein–protein interaction domains.
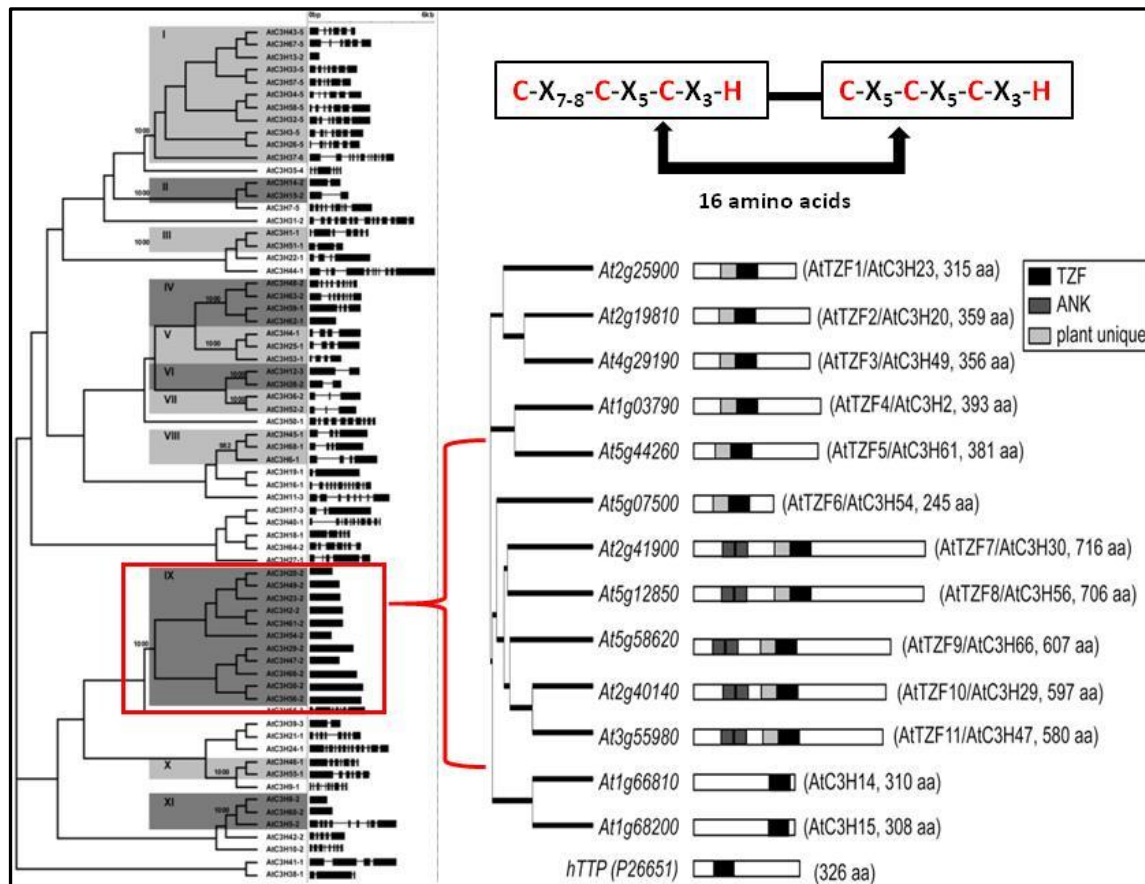
Fig.8 Phylogenetic tree of 11 subfamilies of *Arabidopsis* CCCH-TZFs.
The tree shows the 11 major phylogenetic subfamilies and the subfamily IX is shown in enlarged view. All the members of the subfamily IX comprise of two CCCH type zinc-finger domains and additionally the subgroup TZF7-TZF11 comprises of two ankyrin domains. (Source: (M. C. Pomeranz et al., 2010a; D. Wang et al., 2008a)).

1.7.3 Abiotic and biotic responses of TZFs

In animals and yeast, these arginine-rich tandem CCCH zinc finger proteins (TZFs) act as post-transcriptional regulators of gene expression. In plants, these have been characterized in relation to hormone-mediated developmental processes, environmental or abiotic cues, such as cold, salt, and drought as well as in the biotic context, in response to bacterial flagellin. Among the various reports on the sub-family IX of *Arabidopsis*, AtTZF1 acts as a positive regulator of Abscisic acid (ABA)/sugar responses and a negative regulator of GA responses and overexpression resulted in late flowering and enhanced tolerance to cold and drought stress (P. C. Lin et al., 2011). *AtTZF2* and *AtTZF3* are induced by ABA and abiotic stresses such as salt, mannitol and cold (Lee, Jung, Kang, & Kim, 2012). Also, AtTZF3 is described as a negative regulator of seed germination in the presence of NaCl and ABA (Gupta, Sengupta, & Gupta, 2016). AtTZF4, AtTZF5 and AtTZF6 are reported as negative regulators of light-dependent seed germination, loss-of-function mutants are characterized by reduced levels of ABA and elevated levels of GA (Bogamuwa & Jang, 2013a; Kim et al., 2008). AtTZF6 is involved in embryogenesis

(Z. Li & Thomas, 2007) and AtTZF7 (OXS2) is described as having multiple roles in regulating vegetative growth, activating stress tolerance and being involved in stress-induced flowering (Blanvillain, Wei, Wei, Kim, & Ow, 2011). AtTZF9 is involved in PTI responses (Maldonado-bonilla et al., 2014) and both AtTZF10 and 11 act as positive regulators of salt tolerance (Sun et al., 2007). Also the mutants of AtTZF10 have shown increased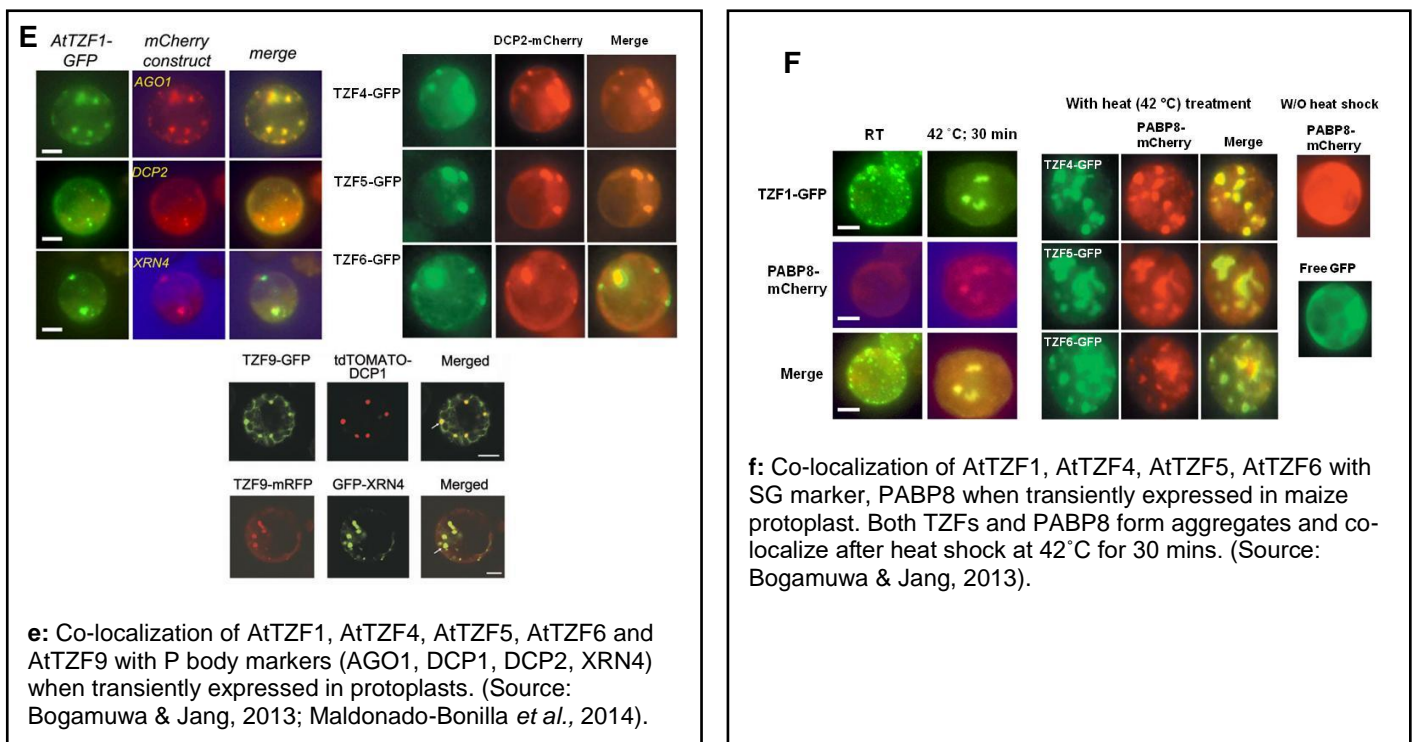 local susceptibility to *Botrytis cinerea* and sensitivity to germination in the presence of ABA (AbuQamar et al., 2006).

1.7.4 Localization of TZFs

When transiently expressed under the control of the strong 35S promoter in maize mesophyll protoplasts, all 11 members of the *Arabidopsis* TZF family were reported to localize in cytoplasmic foci resembling P bodies or SG (M. Pomeranz, Lin, Finer, & Jang, 2010) (**Fig.9(a)**). After treatment with cold, ABA, Leptomycin B (an antibiotic that inhibits exportin1 protein required for nuclear export of other proteins), CHX/cycloheximide (an antibiotic that inhibits translation) or ActD (a transcriptional inhibitor), TZF1, TZF7 and TZF9 were reported to accumulate in nuclei suggesting shuttling between the nucleus and cytoplasm (Blanvillain et al., 2011; Maldonado-bonilla et al., 2014; M. C. Pomeranz et al., 2010a) (**Fig.9(b)**). AtTZF2 and AtTZF3 localized in the plasma membrane (Huang et al., 2011a, 2012; Lee et al., 2012) (**Fig.9(c)**) and also in cytoplasmic foci (M. Pomeranz et al., 2010) (**Fig.9(a)**). AtTZF11 was reported as being localized to the nucleus in onion epidermal cells (Sun et al., 2007) (**Fig.9(d)**), and also in cytoplasmic foci in maize protoplasts (M. Pomeranz et al., 2010) (**Fig.9(a)**). Like AtTZF1 (M. C. Pomeranz et al., 2010a), AtTZF4, 5, 6 and 9 co-localize with markers of P bodies (AGO1, DCP1, DCP2, XRN4) and SG (PABP8) in plant cells, and the morphology of these cytoplasmic foci resembles that of mammalian P bodies and SGs (Bogamuwa & Jang, 2013a; Maldonado-bonilla et al., 2014) (**Fig.9(e)**).

A

Fig.9 Sub-cellular localization of TZF proteins.
a: *Arabidopsis* CCCH TZFs (subfamily IX) and hTTP (human tristetraprolin, mammalian homolog of TZFs) are localized in cytoplasmic foci when transiently expressed in protoplasts. (Source: Pomeranz *et al.,* 2010).

B

b: AtTZF1, AtTZF7 and AtTZF9 accumulate in nuclei after treatment with CHX, ActD or LepB when transiently expressed in protoplasts. (Source: Pomeranz *et al.,* 2010; Blanvillain *et al.,* 2011; Maldonado-Bonilla *et al.,* 2014)

C

D

c & d: Plasma membrane localization of AtTZF2 and AtTZF3 in *Arabidopsis* root cells (**c**). AtTZF11 localizes to the nucleus in onion epidermal cells (**d**). (Source: (Huang et al., 2011a, 2012; Lee et al., 2012; Sun et al., 2007)).

E

e: Co-localization of AtTZF1, AtTZF4, AtTZF5, AtTZF6 and AtTZF9 with P body markers (AGO1, DCP1, DCP2, XRN4) when transiently expressed in protoplasts. (Source: Bogamuwa & Jang, 2013; Maldonado-Bonilla *et al.,* 2014).

F

f: Co-localization of AtTZF1, AtTZF4, AtTZF5, AtTZF6 with SG marker, PABP8 when transiently expressed in maize protoplast. Both TZFs and PABP8 form aggregates and co-localize after heat shock at 42˚C for 30 mins. (Source: Bogamuwa & Jang, 2013).

The co-localization of most AtTZFs with P body and SG markers suggests a role in mRNA regulation as these marker proteins were previously reported to be conserved and important for mRNA processing in plants (D. A. Belostotsky & Sieburth, 2009; Muench et al., 2012; M. C. Pomeranz et al., 2010a; Jun Xu & Chua, 2009). Among the TZFs, AtTZF1 can bind both DNA and RNA *in vitro* (M. C. Pomeranz et al., 2010a) and can trigger mRNA decay in a sequence specific manner by binding to RNA. These binding events are dependent on the presence of zinc (Qu, Kang, Wang, Musier-Forsyth, & Jang, 2014). *In vivo*, AtTZF1 was shown to be involved in the decay of ARE-containing mRNAs (Qu et al., 2014). For AtTZF2 and AtTZF3, RNase activity *in vitro* was reported (Lee et al., 2012) and AtTZF9 is known to bind RNA (Maldonado-bonilla et al., 2014).

AtTZF7 and AtTZF9 were also previously identified as *in vitro* MPK3/6 substrates (Feilner et al., 2005). AtTZF9 was validated to be an MPK3/6 substrate, it interacts with two PAMP activated MAPKs, MPK3 and MPK6, in both the cytoplasm and the nucleus and is assumed to be involved in post-transcriptional gene regulation (Maldonado-bonilla et al., 2014). Previously, AtTZF7 was reported to be a nuclear-localized transcription factor rather than being in P bodies (Blanvillain et al., 2011). Interestingly, TZF7 was recently shown to be phosphorylated after *in vivo* MPK3/6 activation (Lassowskat et al., 2014) suggesting it is also an MPK3/6 substrate in plants.

Thus, CCCH TZFs may have pivotal roles in controlling gene expression, cell fate specification, and various developmental processes and also abiotic stresses including drought tolerance, salt responses, stress-induced flowering, etc. However, the molecular mechanisms underlying the TZFs function are unknown.

1.8 Aims

Due to the discrepancies in various reports of TZF7 localization and the recent evidence of a link between TZF7 and MAPK cascades, the aims of this project are to clarify TZF7 cellular localization and to understand how MAPKs affect TZF7 function. For comparison and completeness, the analysis is expanded to include the related members from the TZF7-TZF11 subfamily (i.e. TZF8, TZF9, TZF10 and TZF11).

Hence, the proposal of the thesis focuses on the following objectives:

   A. Investigation of TZFs as MAPK targets (*in vitro* and *in vivo*)
   B. Determination of TZFs' sub-cellular localization
   C. Role of the TZFs in pathogen/PAMP/stress responses

2 Materials and methods

2.1 Gene expression analysis

2.1.1 RNA extraction
Two-week-old *Col-0* seedlings were grown in 0.5 MS medium supplemented with 0.5% sucrose and 1 mM MES. Seedlings were elicited with flg22, harvested at the indicated time points in **Fig.10** and frozen in liquid nitrogen. Samples were homogenized until a fine powder was obtained, resuspended in 1 ml of Trizol solution **(Appendix III (A) provided in CD)** and thawn by vortexing to mix vigorously. Upon incubation for a minimum time of 5 mins at RT, the supernatant was extracted with 200 ml of chloroform; vortexed vigorously for about 20 secs and incubated for 2-3 mins at RT. Following centrifugation at 12,000 x g for 15 mins (4°C) to separate the phases, top aqueous phase was collected into new tubes. RNA was precipitated from the aqueous phase using 0.5 ml (per 1 ml Trizol) isopropyl alcohol after incubating for 10-15 mins at RT and centrifuging at 12,000 x g for 15 mins (4°C). The RNA pellet was washed with 70% ethanol and resuspended in RNase free H_2O. To assist solubility, the resuspended RNA pellet was incubated at 60°C for 15 mins.

2.1.2 cDNA synthesis
To remove contaminating genomic DNA prior to reverse transcription (RT), RNA was treated with Deoxyribonuclease I (Thermo Scientific) for 30 mins at 37°C, followed by addition of 25mM EDTA and incubation at 65°C for 10 mins. The first strand cDNA synthesis was performed by incubating the DNAse I-treated RNA with oligo d(T) primer, ribonuclease inhibitor, 10 mM dNTP mix, Reverse Transcriptase and 5x Reverse Transcriptase buffer for 5 mins at 37°C followed by incubation at 42°C for 1 hour. The reaction was stopped by incubating at 70°C for 10 mins. The resulting cDNA product was used for further PCR analysis.

2.1.3 Quantitative RT-PCR
Quantitative analysis of gene expression was performed with 14-day old seedlings of *Col-0*, which were elicited with 100 nM flg22. Relative transcript levels of the *TZFs* were determined using the Mx3005P real time PCR detection system (Agilent) and quantified using the comparative CT method with four biological replicates for each time point. qRT-PCR was performed in 10 µl reaction volume using the 5x QPCR Mix EvaGreen® (Bio & Sell) according to the manufacturer's protocol (PCR conditions and the primers are listed in **Appendix II Table S1.1 and S1.6**, respectively). The expression levels were normalized using the CT values obtained for the reference gene, *PP2A* (*Protein phosphatase*, At1g69960).

2.2 Molecular cloning

2.2.1 Polymerase Chain Reaction (PCR)

Amplification of the genes of interest was carried out using a high fidelity Phusion DNA Polymerase with 3' to 5' proof-reading activity (ThermoFisher) (PCR conditions and the primers are listed in **Appendix II Table S1.2 & S1.6, respectively**). The final reaction mixes were of 20 µl with 1x buffer (including 2 mM $MgCl_2$ provided by ThermoFisher with enzymes), 200 µM dNTPs, 1 µM forward and reverse primers, 10-100 ng template DNA and 0.5 U of the enzyme.

2.2.2 Purification of PCR products

The amplified PCR products were electrophoresed in EtBr-containing 1% agarose gels. Purification was performed to remove excess primers and salts by excising the desired band (under UV light) using a commercially available kit (Invisorb Spin DNA Extraction Kit, Stratec), prior to digestion and subsequent ligation of the genes of interest into the required vector.

2.2.3 Cloning of TZFs into pENTR-TOPO vector and transformation

Full-length *TZF7*, *TZF8*, *TZF10*, *TZF11*, *PAB2*, *PAB8* with stop codons and TZF9, DCP1, DCP2, AGO1, PARN, XRN4 without a stop codon (cloned by Naheed Tabassum), were PCR-amplified from genomic DNA using specific primers with a CACC extension at the 5' end of the forward primers. The blunt-end PCR products were cloned into pENTR™/D-TOPO vector (Invitrogen) according to the manufacturer's instructions. The reaction mix was transformed into DH5α cells (transformation protocol as described in **2.2.5.1**).

2.2.4 Cloning into destination vectors

Expression constructs were generated by performing "LR recombination reactions" between the entry clones and a Gateway destination vector of choice. LR reactions were performed by mixing 50-150 ng Entry clone, 150 ng Destination vector, TE buffer: pH 8.0 (to 5 µl) and 1 µl LR Clonase™ II enzyme-mix in the tube and incubation at 25°C for 1 hr. The reaction mixes were then transformed into DH5α cells and the plasmids isolated from DH5α cells were re-transformed into KRX competent cells (Promega) for protein expression related experiments (transformation protocol as described in **2.5.1**). Destination vectors used in the present study are as follows: pDESTN110 vector (Dyson, Shadbolt, Vincent, Perera, & McCafferty, 2004): for expression of the recombinant protein (TZF7/TZF8/TZF10/TZF11); pUGW14 (TZF9) (cloned by Naheed Tabassum) and pUGW15 (Nakagawa et al., 2007): 3xHA tagged vector (TZF7/TZF8/TZF10/TZF11/PAB2/PAB8): for transient expression in protoplasts; pUBN-GFP (TZF7-TZF11), pUBN-RFP (DCP2/AGO1/PARN/XRN4/PAB2/PAB8), pUBN-CFP (DCP1) tagged vector (Grefen et al., 2010); pE-SPYNE (TZF7/PAB2/PAB8/MPK3/MPK4/MPK6/MPK8), pE-SPYCE (TZF7/TZF8/TZF10/TZF11/PAB2/PAB8), pUC-SPYCE (Walter et al., 2004) (TZF9)

(cloned by Naheed Tabassum): for transient expression in protoplasts (microscopy). The expression constructs were introduced into the appropriate host (e.g. bacteria) and the recombinant proteins were expressed for further analysis.

2.2.5 Selection of correct transformants

2.2.5.1 Transformation in E. coli (DH5α and KRX) cells and colony PCR
The cloning reaction mix was transformed into *E. coli* (DH5α) by mixing with 50 µl thawed cells and incubation on ice for 30 mins. The cells were then subjected to heat-shock at 42°C for 30 secs and then incubated at 37°C for 1 hr with shaking (120 rpm) after adding 250 µl LB medium to the cells. After this, the transformed cells were plated onto selective LB-agar plates containing the respective antibiotics and incubated at 37°C overnight. The overnight grown colonies were randomly picked and pre-checked for the presence of the inserts by colony PCR using DreamTaq DNA polymerase (ThermoFisher) (PCR conditions listed in **Appendix II Table S1.3**) by suspending the colonies in the PCR master mix (50 µl of final reaction volume).

2.2.5.2 Plasmid DNA purification
For plasmid purification of pre-selected bacterial colonies (those positive in colony PCR), 2 ml liquid LB medium **(Appendix III (E) provided in CD)** with appropriate antibiotics were inoculated and incubated at 37°C with constant shaking, 120 rpm, for 12–16 hrs overnight. The overnight cultures were transferred into 2 ml microcentrifuge tubes and the plasmids were isolated through Invisorb® Spin Plasmid Mini Two kit as per the prescribed protocol (Stratec). Quantification of plasmid DNA and estimation of purity was done with the help of a spectrophotometer (Nanodrop8000, Thermo Scientific).

2.2.5.3 Restriction digestion and DNA sequencing analysis
Purified plasmid DNA for each of the constructs cloned into entry/destination vectors was digested with the appropriate type II restriction enzymes by incubating overnight at 37°C or as recommended for each of the restriction enzymes. To check the predicted digested products (using Vector NTI software, Thermo Scientific) after restriction digestion, 1% agarose gels **(Appendix III (P) provided in CD)** were used with midori green nucleic acid stain (Biozym) or ethidium bromide (Roth) for detection. The selected plasmids were sequenced (Sanger sequencing, GATC-biotech Ltd.).

2.3 Localization, co-localization and interaction analysis

2.3.1 Plasmid purification
For plasmid purification, bacterial cells harbouring high-copy plasmids were cultivated in 250 ml LB medium under appropriate antibiotic selection to ensure plasmid propagation and incubated

at 37°C with constant shaking, 120 rpm, for 12–16 hrs overnight. Maxipreps were prepared using a commercial kit provided by Qiagen.

2.3.2 Protoplast preparation

For protoplast preparation, plants were grown on soil in growth chambers under short-day conditions (8 hrs light, 16 hrs darkness). Well-expanded leaves were used to cut into leaf strips of <0.5 mm with razor blades upon removal of the leaf stalks. The cut leaf strips were transferred into the prepared enzyme solution; dipping completely into the solution by using a pair of flat-tip forceps and then vacuum-infiltrated for 30 mins in the dark using a desiccator (covered with a black cloth). After which, enzyme digestion was carried out without shaking, for at least 2.5 hrs at 20-22°C in the dark; followed by gentle shaking for 30 mins to release the protoplasts. Then the protoplast suspension was filtered through a nylon mesh (100 µm mesh size) into 12 ml cell culture tubes on ice. Tubes were centrifuged for 1 min at 200 g (4°C) and the supernatant removed. The protoplast suspension was resuspended by addition of 2 ml W5 per tube and by gently inverting the tubes. Protoplasts were kept on ice for 40 mins in the dark to settle on the bottom of the tube by gravity. The supernatant was removed from protoplast pellet followed by a second wash with another 2 ml W5 and incubated on ice for another 40 mins (in the dark). The protoplast pellet obtained after removing the supernatant was resuspended in MMG solution and diluted to working concentration at RT (20-22°C) by mixing gently by inverting. Composition of the protoplast preparation solutions are listed in **Appendix III (B) provided in CD**.

2.3.3 PEG-mediated transformation of DNA into protoplasts

Required amount of plasmid DNA for transformation (10 µg plasmid prep/100 µl pp) was pipetted at the bottom of the tubes and mixed gently by carefully inverting the tubes after adding protoplasts to DNA. Following addition of 1.1x pp volume of PEG solution to the tube, the tubes were mixed gently by inverting the tubes and were incubated at RT (20-22°C) for 5-10 mins. To stop the transformation process, 4.4x pp volume of W5 was added and mixed by gently inverting the tubes, followed by centrifugation for 1 min at 200 g (4°C). After removing the supernatant, 1x pp volume of WI was added and mixed by gently inverting the tubes. For microscopic observation (tubes positioned horizontally) and western-blot (0.3 ml aliquot of transformed samples), the tubes were incubated in the dark at RT (20-22°C) overnight.

2.3.4 Sub cellular localization analysis

For localization studies, isolated Arabidopsis protoplasts were transformed with the various TZFs (TZF7-TZF11) cloned in pUBN-Dest, GFP tagged and with PAB2 and PAB8 cloned in pUBN-Dest, RFP tagged, for ubiquitin10 promoter-driven expression. GFP and RFP fluorescence was visualized with an LSM780 confocal microscope (Carl Zeiss) using a 488 nm argon laser to

excite GFP and 561 nm argon laser to excite RFP. Captured images were processed by using ImageJ and Adobe Photoshop.

2.3.5 Sub cellular co-localization analysis
For co-localization studies, isolated Arabidopsis protoplasts were transformed with the various TZFs (TZF7-TZF11) cloned in pUBN-Dest, GFP tagged (for ubiquitin10 promoter-driven expression) along with the P-body markers *viz.* CFP-DCP1, RFP-DCP2, RFP-XRN4, RFP-AGO1, RFP-PARN (for ubiquitin10 promoter-driven expression); siRNA body markers *viz.* RFP-SGS3 and RFP-UPF1 (for CaMV 35S promoter-driven expression; generously provided by Alexis Maizel); SG markers *viz.* RFP-PAB2 and RFP-PAB8 (for ubiquitin10 promoter-driven expression). GFP, RFP and CFP reporter fusion proteins were used to document sub cellular co-localization patterns with an LSM780 confocal microscope (Carl Zeiss) using a 488 nm argon laser to excite GFP, 561 nm argon laser to excite RFP and 405 nm argon laser to excite CFP, respectively. Captured images were processed by using ImageJ and Adobe Photoshop.

2.3.6 Sub cellular localization change analysis
For alterations in the sub cellular localization of the various TZFs (TZF7-TZF11) cloned in pUBN-Dest, GFP tagged (for ubiquitin10 promoter-driven expression), transformed protoplasts were treated with 1µM flg22 after around 12 hrs of transformation. For this purpose, several z-planes were chosen and changes were monitored until 1 hr after treatment; images being captured for every z-plane after every 5 mins until an hour. Water treatment (until 1 hr) was used as a control in each of the TZFs' organizational change experiment. GFP fluorescence was visualized with an LSM780 confocal microscope (Carl Zeiss) using a 488 nm argon laser to excite GFP. Captured images were processed by using ImageJ and Adobe Photoshop.

2.3.7 Bimolecular Fluorescent Complementation (BiFC) assay
For the BiFC assays, the proteins of interest were expressed as fusions with the N-terminal and C-terminal fragments of YFP, respectively, and transformed into isolated Arabidopsis protoplasts: TZF7 (cloned in pE-SPYNE and pE-SPYCE), TZF9 (cloned in pUC-SPYCE), TZF8/TZF10/TZF11 (cloned in pE-SPYCE) along with PAB2 (cloned in pE-SPYNE and pE-SPYCE), PAB8 (cloned in pE-SPYNE and pE-SPYCE), DCP1 (cloned in pE-SPYNE), MPK3 (cloned in pE-SPYNE), MPK4 (cloned in pE-SPYNE), MPK6 (cloned in pE-SPYNE), MPK8 (cloned in pE-SPYNE). To detect interactions of each of the TZFs with the PABs, DCP1 and with the MPKs, reconstitution of the YFP signals was visualized with an LSM780 confocal microscope (Carl Zeiss) using a 514 nm argon laser to excite YFP after around 12 hrs incubation in the dark. Captured images were processed by using ImageJ and Adobe Photoshop.

2.4 Protein work and immunoblot analysis

2.4.1 *In vitro* protein phosphorylation assay

2.4.1.1 Protein extraction and purification by denaturing method

<u>Bacterial cultures for protein extraction</u>: For detection of phosphorylation in the various full length proteins, TZF7/TZF8/TZF10/TZF11-6xHis and TZF9-MBP-10xHis were expressed in *E. coli* KRX (Promega) harbouring a rhamnose-inducible system for protein expression. A small liquid culture of 5 ml LB media and antibiotics (Ampicillin @ 100 µg/ml) was incubated overnight at 37°C, 120 rpm. The overnight grown culture was diluted to 1:20 (i.e. 5 ml overnight culture in 100 ml media) with TB media **(Appendix III (F) provided in CD)** with Ampicillin @ 100 µg/ml and incubated for 3 hrs at 37°C, 120 rpm (OD$_{600}$: 0.8-1). After the required OD was achieved, recombinant protein was induced by addition of 0.1% Rhamnose and the culture was incubated overnight at 25°C, 120 rpm. Following harvesting of cells by centrifugation for 20 mins at 4°C @5000 rpm, the bacterial pellet obtained was used for purification.

<u>Protein extraction and purification</u>: About 100-150 µl lysis buffer **(Appendix III (H) provided in CD)** (per ml of culture) was added to bacterial pellets. Following resuspension, samples were vortexed and mixed at RT for 30 mins in a rotor. After centrifugation to pellet bacterial debris for 10-15 mins at maximum speed (4°C), the supernatants (lysate) obtained were collected in new tubes. To the collected lysates, 50 µl NiNTA–Agarose (1:2 diluted in Lysis Puffer, Qiagen) was added and mixed gently for 1-2 hr(s) to allow binding of proteins to beads at RT. The supernatant (unbound fraction) was collected after centrifugation for 2 mins @2000 rpm and the pellet was washed 3 times with wash buffer **(Appendix III (H) provided in CD)** with centrifugation steps in between.

<u>Refolding of proteins</u>: The bead-bound proteins were resuspended in 100 µl wash buffer and then neutralized with 1/3 volume of 1M Tris 7.5 <u>(33 µl)</u> by placing it on ice. Native buffer **(Appendix III (H) provided in CD)** of 1 volume (130 µl) was added and after 10-20 mins, another volume (260 µl) of native buffer was added; following addition of another volume (520 µl) of native buffer after 10-20 mins and kept overnight for proper refolding of proteins. Following centrifugation, the refolded proteins were washed with 1 ml native buffer and the supernatant was removed. After which, the purified proteins were resuspended in Tris buffer (100 µl) for downstream assays.

2.4.1.2 Kinase assay

For detection of phosphorylation in the various full length purified recombinant TZF proteins, MAPK assays were performed by incubating active MPK3/4/6 and TZF7/TZF8/TZF10/TZF11-6xHis, TZF9-MBP-10xHis in 2x substrate buffer **(Appendix III (I) provided in CD)** for 30 mins at

37°C. Phosphorylated proteins were detected by autoradiography after SDS-PAGE and staining of gels with coomassie solution **(Appendix III (J) provided in CD)**, followed by destaining with destaining solution **(Appendix III (K) provided in CD)**.

2.4.2 *In vivo* protein phosphorylation assay

For detection of phosphorylation, isolated Arabidopsis protoplasts were transformed with the various TZFs (pUGW15-TZF7/TZF8/TZF10/TZF11, pUGW14-TZF9; CaMV 35S promoter-driven expression). After around 12 hrs of incubation, transformed protoplasts were treated with 100 nM flg22 for 15 mins and 1 hr and the reduced mobility of the proteins due to phosphorylation was detected by SDS-PAGE separation followed by western blot analysis (as described in **2.4.4**), as compared to the unelicited samples.

2.4.3 *In vivo* protein dephosphorylation assay

For the dephosphorylation assay (to show that the mobility shift after flg22 treatment was due to phosphorylation), isolated Arabidopsis protoplasts were transformed with the various TZFs (same constructs as used for the phosphorylation assay). After around 12 hrs of incubation, transformed protoplasts were treated with lambda-phosphatase (1x buffer, 10 mM DTT, 1U enzyme (NEB)) for 10 min at 30°C. The extracts were then subjected to western blot analysis (as described in **2.4.4**) after incubating with 2x loading buffer **(Appendix III (L) provided in CD)** at 95°C for 5 mins.

2.4.4 Western Blot

Western blot analysis was performed after protein separation using 8% SDS-PAGE and transferring to nitrocellulose membrane (Porablot NCL; Macherey & Nagel) using transfer buffer **(Appendix III (Q) provided in CD)**. The blots were blocked using TBST **(Appendix III (R) provided in CD)** containing 5% skimmed milk for 1hr at RT. After which the blots were incubated with primary antibody at 4°C overnight and then with secondary antibody for 1 hr at RT followed by subsequent washing in TBST containing 3% skimmed milk, after each incubation with the respective antibodies. The list of antibodies used is summarized in **Appendix II Table S1.5**.

2.5 Plant growth and treatment

2.5.1 Selection of T-DNA insertional (SALK) lines

T-DNA insertion mutants of the genes of interest (AtTZF7: SALK_N120825; AtTZF8: SALK_N004272; AtTZF9: SALK_ N510842; AtTZF10: SALK_N024800 and AtTZF11: SALK_N141550) were obtained from the SALK Institute collection. Quadruple (*tzf7tzf8tzf9tzf10*) and the penta (*tzf7tzf8tzf9tzf10tzf11*) mutants were generously provided by Blanvillain (previously from the David W Ow lab). The T-DNA insertion mutants and the wild type

accession, *Col-0*, were grown at the same time in growth chambers in short day conditions at 22°C. Leaf samples were harvested for further analysis.

2.5.2 DNA extraction for PCR
DNA was extracted from leaf materials homogenized using a Precellys 24 homogenizer (Peqlab) without thawing by addition of 400 µl of extraction buffer **(Appendix III (C) provided in CD)**. The supernatant, around 300-350 µl, obtained after centrifugation at maximum speed for 5-10 mins was transferred to new tubes.DNA was precipitated with 1 volume of isopropanol and the supernatant obtained after centrifugation for 5-10 mins was discarded. The DNA pellet was washed with 70% ethanol and resuspended in sterile water.

2.5.3 PCR screening for homozygous T-DNA insertion lines
To obtain homozygous lines of the T-DNA mutants of each gene, the insertion lines were identified by PCR genotyping (PCR conditions listed in **Appendix II Table S1.4**) using specific T-DNA primers **(Appendix II Table S1.6)**, consisting of LP (left genomic primer), RP (right genomic primer), LBa1 (left border primer of T-DNA insertion) and also the gene specific primers of the respective TZF insertion mutants.

2.5.4 PEG precipitation of the PCR products
The PCR products (50 µl) of the various T-DNA insertion lines of the TZFs were mixed with 150 µl of TE **(Appendix III (D) provided in CD)**. After adding 100 µl of PEG/MgCl$_2$ **(Appendix III (D) provided in CD)**, the samples were centrifuged for 15 mins at 10,000 rcf at RT and supernatant removed to obtain a pellet. The pellet obtained was dissolved in sterile water.

2.5.5 Sequencing for confirmation of the T-DNA positions
To determine the exact location of the T-DNA insertion, the PCR products were sequenced (using LBb1.3 and RP primers) to obtain flanking sequence information.

2.5.6 Germination analyses
For the germination assays, *tzf* mutant seeds and the wild type accession were at first surface sterilized by 70% ethanol for 1 min, 35% NaClO+ 3 drops 10% TritonX-100 for 8 mins, and then rinsed for 4-5 times with sterilized distilled water. After surface sterilization, the stored seeds in sterile water were individually spotted onto MS plates **(Appendix III (T) provided in CD)**. To determine the effects of ABA, MS plates were supplemented with or without 10 µM ABA (Sigma). Plates were kept in the dark at 4°C for 3 days and then incubated vertically at 22°C under a 16 hrs light, 8 hrs dark photoperiod in the growth cabinet. Germination kinetics were determined by scoring the time of radicle emergence and recorded after 8 days of incubation in the growth cabinet. Two experiments, with about 50 seeds per genotype, were used for each treatment.

2.5.7 PAMP induced root growth inhibition assays

To determine PAMP induced root growth inhibition, surface sterilized *tzf* seeds and the wild type accession, *Col-0* stratified at 4°C for 2 days were individually spotted on ATS **(Appendix III (S) provided in CD)** agar plates. Seedlings were grown vertically on agar plates for 5 days and then transferred onto ATS plates supplemented with or without 1 μM flg22 for 9 days. Photographs were taken on the 14th day and data recorded were depicted as percentage root growth inhibition compared with the control.

2.5.8 ABA induced root growth inhibition

To determine ABA induced root growth inhibition, surface sterilized *tzf* seeds and the wild type accession, *Col-0*, stratified at 4°C for 2 days and were individually spotted on MS agar plates. After stratification, the plates were incubated vertically at 22°C under a 16 hrs light, 8 hrs dark photoperiod in the growth cabinet. Five day old seedlings grown on MS medium were transferred to plates supplemented with or without 10 μM ABA and the photographs were taken after 12 days of the transfer.

2.6 Statistical significance:

Statistical significance of the data was evaluated with GraphPad Prism software package (using statistical tests indicated in the figure legend).

3 Results

3.1TZFs' gene expression is PAMP inducible

*TZF*s' gene expression was observed to be PAMP inducible (**Fig.10**). Relative transcript levels of the *TZF*s were assessed by qRT–PCR in 14-day old seedlings of *Col-0* and the result obtained was consistent with prior microarray analyses (Genevestigator, https://www.genevestigator.com) that expression of all the five *TZF*s are inducible upon flg22 elicitation. *TZF7* and *TZF9* were observed to be induced late with a significant one-fold and two-fold induction, respectively, after 3 hrs of PAMP elicitation (**Fig.10 (A & C)**). *TZF8* gene expression was observed to be intermediate with a highly significant one-fold induction after 1 hr of PAMP elicitation (**Fig.10 (B)**). On the other hand, both*TZF10* and *TZF11* were induced early with about significant ten-fold induction each after 15 mins of flg22 elicitation and each with thirty-fold induction after 30 mins of elicitation. The gene induction in *TZF10* and *TZF11* was observed to gradually decrease with increased time points (**Fig.10 (D & E)**). Hence, in the current study, the expression patterns observed for each of the *TZFs* implies that they might play a role in the response of plants to PAMP.
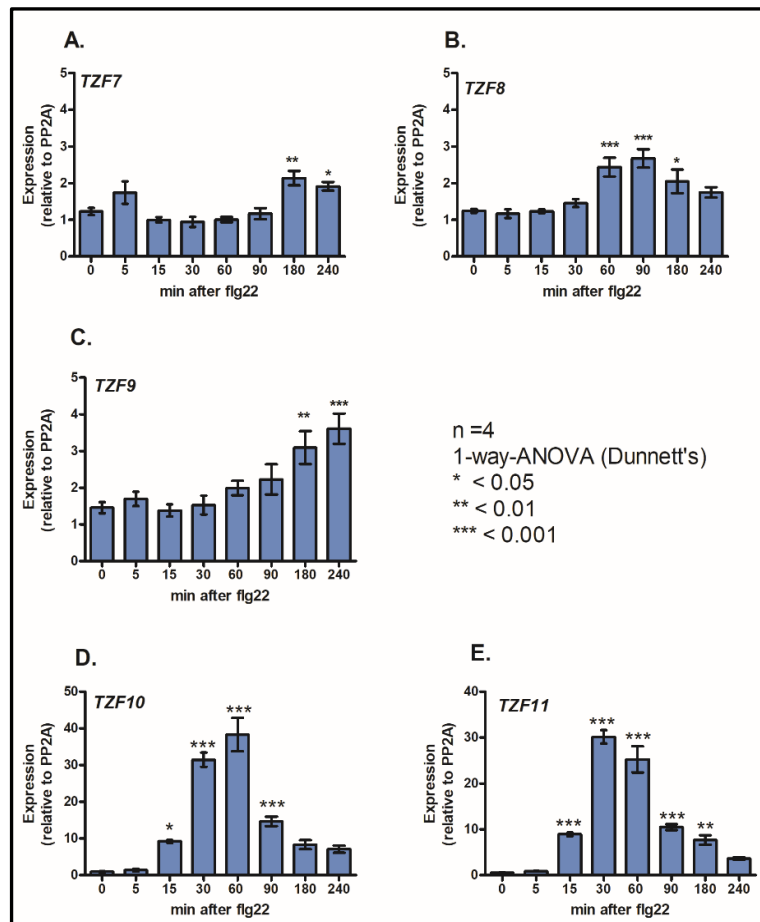
Fig.10 *TZFs'* gene expression is PAMP inducible.

Quantitative analysis of gene expression was performed with 14-day old seedlings of *Col-0*, which were elicited with 100 nM flg22 for the indicated time points. Relative transcript levels of *TZF*s were assessed by qRT–PCR. The bars represent the mean ± SE of one of the two independent experiments with four biological replicates. Statistical significance was evaluated by 1-way-ANOVA (*$P<0.05$; **$P<0.01$, ***$P<0.001$) with Dunnett's post test compared to time point zero.

- **A.** *TZF7*: late gene expression after flg22 elicitation
- **B.** *TZF8*: intermediate gene expression after flg22 elicitation
- **C.** *TZF9*: late gene expression after flg22 elicitation
- **D.** *TZF10*: early gene expression after flg22 elicitation
- **E.** *TZF11*: early gene expression after flg22 elicitation

3.2 Dynamic sub-cellular localization of the TZFs

Previous analyses of the TZF family suggest they play distinct roles in plant development and environmental responses (Guo et al., 2009; Kim et al., 2008; Z. Kong, Li, Yang, Xu, & Xue, 2006; Lee et al., 2012; P. C. Lin et al., 2011; Sun et al., 2007). To ascertain the molecular functions of the TZF proteins in the present study, determination of the proteins' sub-cellular localization was necessitated. This was achieved by transiently expressing the TZFs in *Arabidopsis* mesophyll protoplasts and then visualized under a fluorescent microscope.

In the present study, the TZFs' (TZF7-11) localization was observed to be varied, appearing as speckled cytoplasmic foci or non-speckled (cytoplasm and/or nucleus) signals. **Fig.11** shows the percentage of distribution for each of the TZFs as calculated after observing many protoplasts (n=27-72). The localization of the TZFs in cytoplasmic foci is in accordance with the previous report (Maldonado-bonilla et al., 2014; M. Pomeranz et al., 2010). Nuclear localization was reported previously in TZF7 (upon treatment of cold, ABA or leptomycin B (LMB)) (Blanvillain et al., 2011), TZF10 and TZF11 (Sun et al., 2007). However, current study reveals a major portion of the proteins' localization in the cytoplasmic foci nearly 50% (in case of TZF7 and TZF11) or more (in case of TZF8, TZF9 and TZF10). As observed, these cytoplasmic foci varied in size, shape, fluorescence intensity and numbers, possibly depending on the conditions of individual cells due to unintended stress or from different handling conditions of the protoplasts.
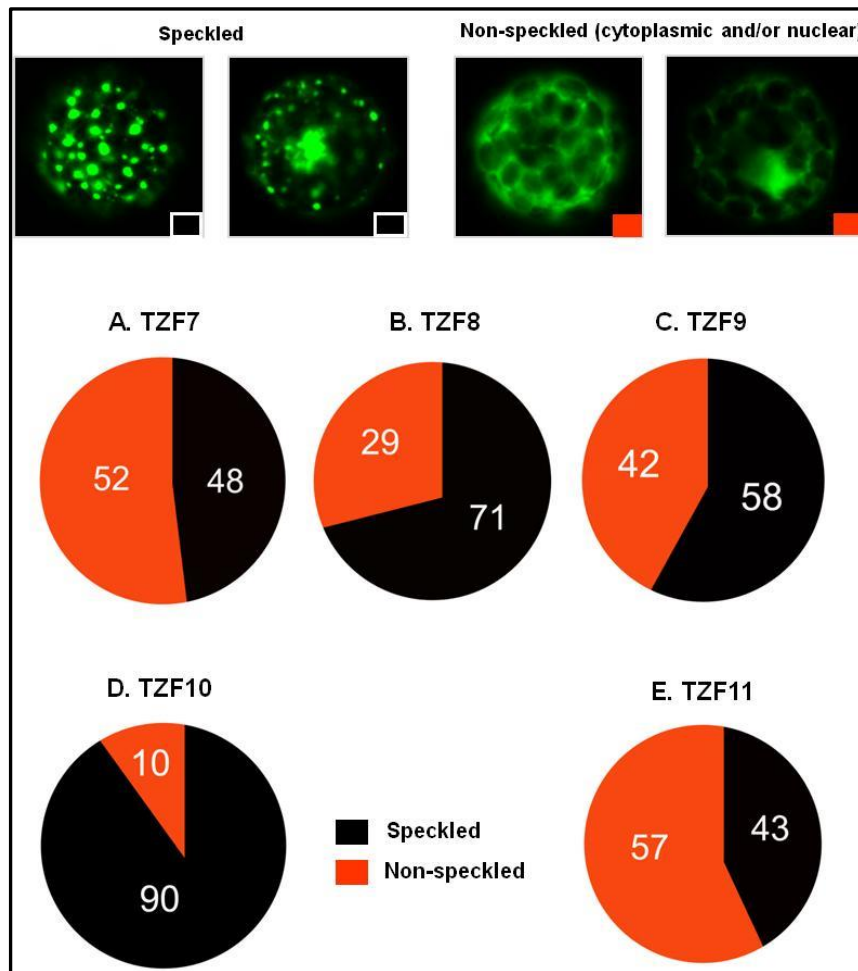
Fig.11 Sub-cellular localization of the TZFs.

Pie diagram showing distribution pattern of the TZFs in percentage when transiently expressed in mesophyll protoplasts of *Arabidopsis*. (**A**) TZF7 localization, n=27 (**B**) TZF8 localization, n=71 (**C**) TZF9 localization, n=74 (**D**) TZF10 localization, n=72 (**E**) TZF11 localization, n=67. (n= number of observed protoplasts)

As from previous reports of TZFs' association with P body markers and SG markers (TZF1, TZF4, TZF5, TZF6, TZF9) (Bogamuwa & Jang, 2013a; Maldonado-bonilla et al., 2014; M. C. Pomeranz et al., 2010a), localization of the TZFs in the current study as speckled structures might indicate their association with P bodies, siRNA bodies or stress granules and as such also suggests the TZFs' role in post-transcriptional regulation. And also this variable localization in the different compartments of the cell suggests that the TZFs have diverse functions in the respective compartments: post-transcriptional regulation (being localized in cytoplasmic foci) or transcriptional regulation (being localized in the nucleus).

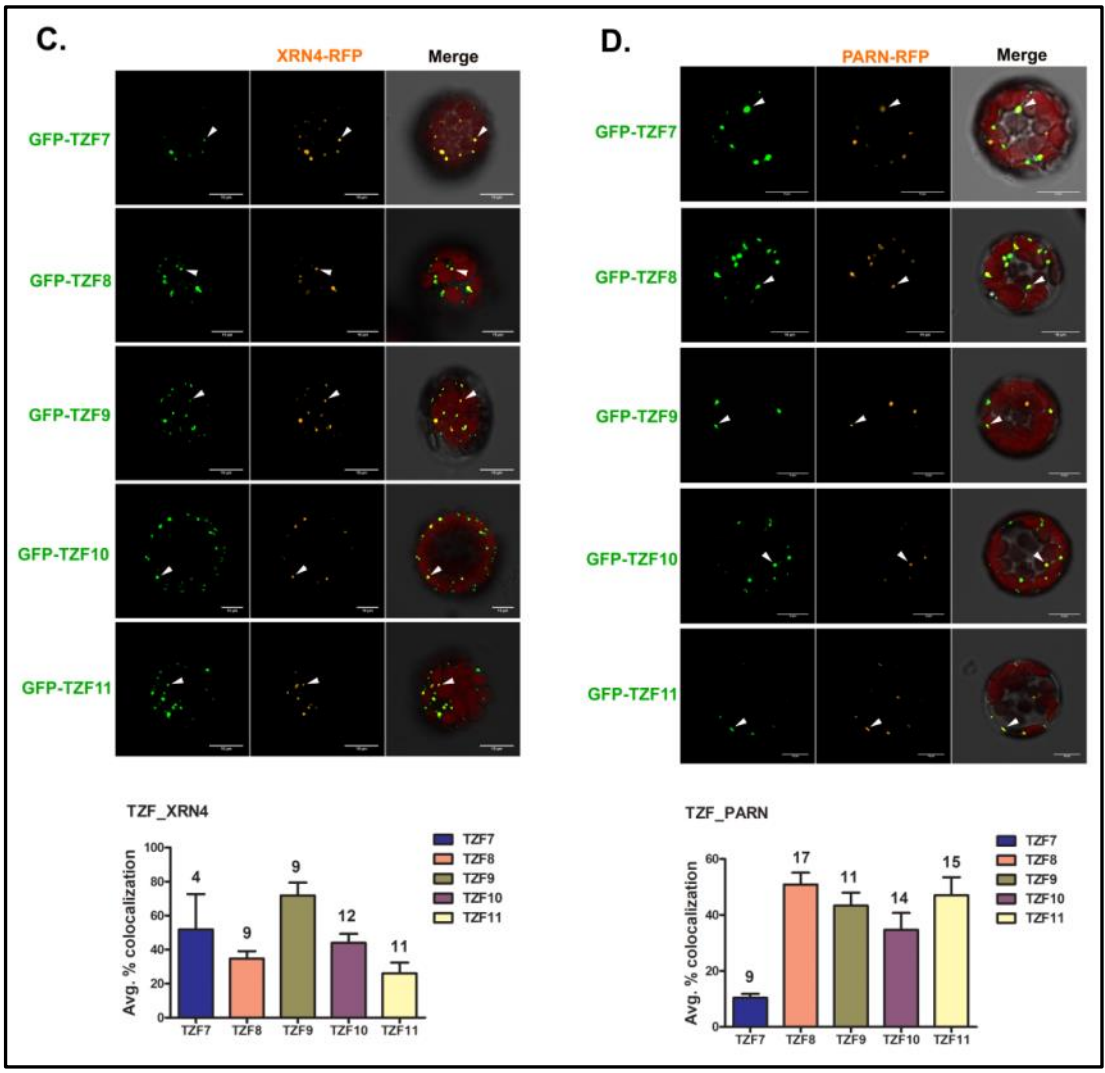### 3.3 Association of the TZFs with P bodies, siRNA bodies, stress granules

To ascertain the nature of the speckled localization of the TZFs, co-localization analyses with the different established markers proteins of P bodies, siRNA bodies and SG, was conducted using

the transient *Arabidopsis* protoplast system. P body markers used in the present study include DCP1 (Decapping 1), DCP2 (Decapping 2), XRN4 (Exoribonuclease 4), AGO1 (Argonaute 1), PARN (PolyA Ribonuclease); siRNA markers used are SGS3 (Suppressor for Gene Silencing 3), UPF1 (Upframeshift 1); SG markers included are PAB2 (Poly A Binding Protein 2) and PAB8 (Poly A Binding Protein 8).

3.3.1 TZFs localizes within P bodies and siRNA bodies

The observation from the co-localization experiments with P body markers and siRNA body markers was that the TZFs co-localize (as indicated with arrowheads in white) partially with the respective markers (**Fig.12 (A-E) & Fig.13 (A & B)**). The bar graphs below each of the representative photographs of TZF co-localization with the respective P bodies and siRNA bodies indicate the average percent co-localization per protoplasts with no perfect co-localization in all the cases.

C.

XRN4-RFP | Merge

GFP-TZF7

GFP-TZF8

GFP-TZF9

GFP-TZF10

GFP-TZF11

TZF_XRN4

D.

PARN-RFP | Merge
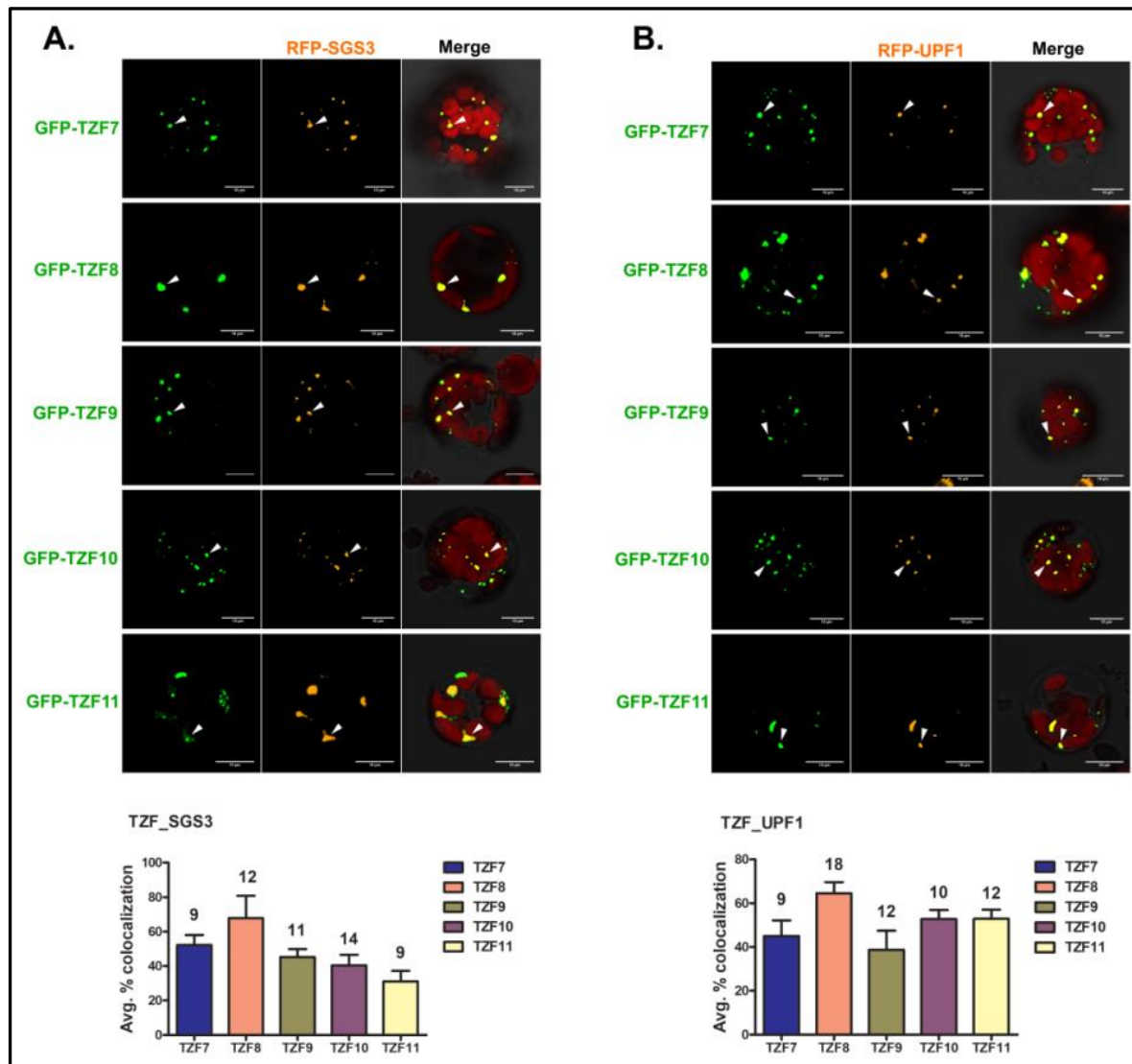
GFP-TZF7

GFP-TZF8

GFP-TZF9

GFP-TZF10

GFP-TZF11

TZF_PARN
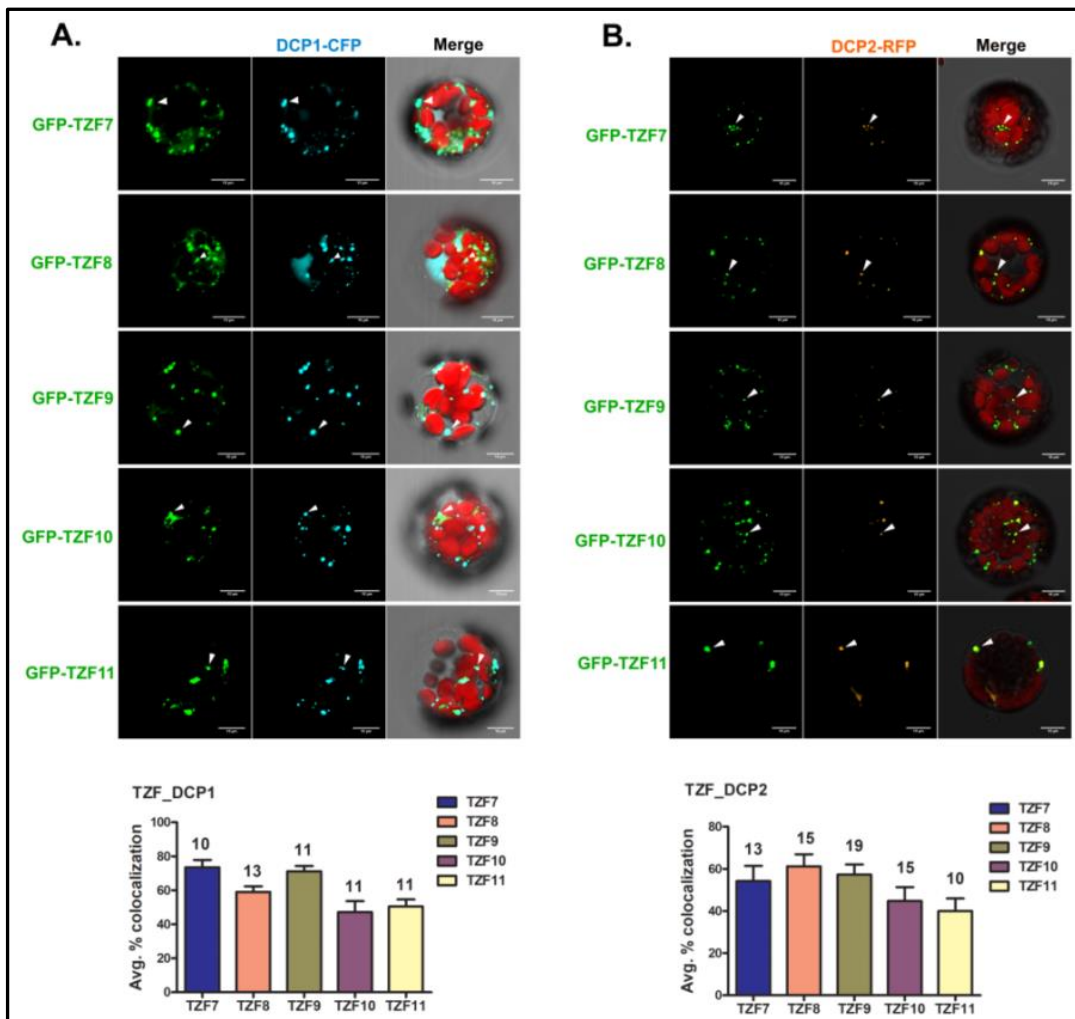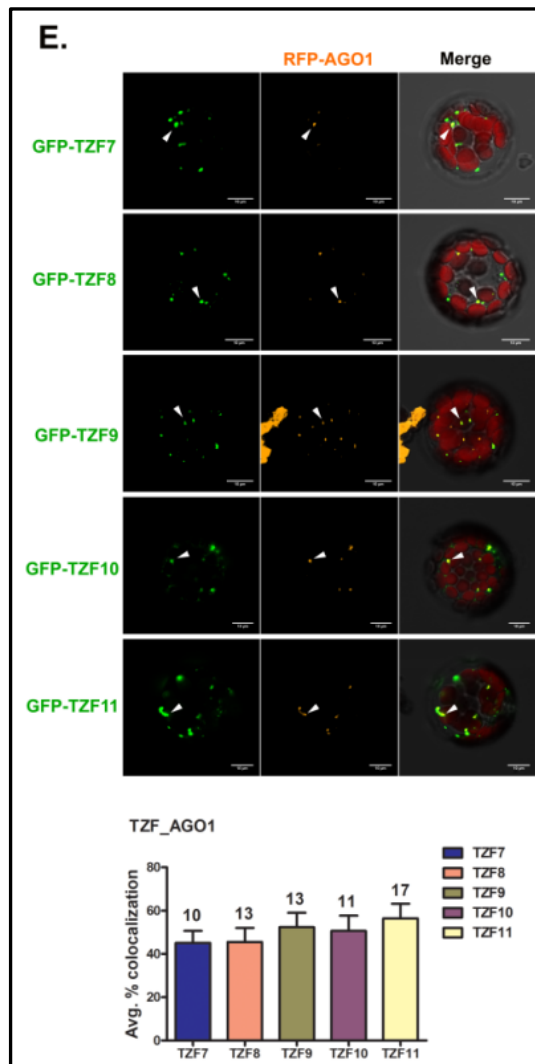
Fig.12 TZFs are associated with putative P bodies.

Representative photographs of TZFs' co-localization with P body markers (as indicated with arrowheads in white), DCP1 (**A**), DCP2 (**B**), XRN4 (**C**), AGO1 (**D**), PARN (**E**) are shown above. Mesophyll protoplasts were co-transfected with indicated constructs and observed by confocal microscopy 12 hrs post-transfection. Scale bars=10 µm. Merged field includes chlorophyll alongwith the respective localized proteins. TZF7-11 co-localized partially with P body markers which are quantified and represented in the graph below showing the average percent co-localization per protoplast. The numbers above the bars indicate the number of protoplasts used for the analysis.
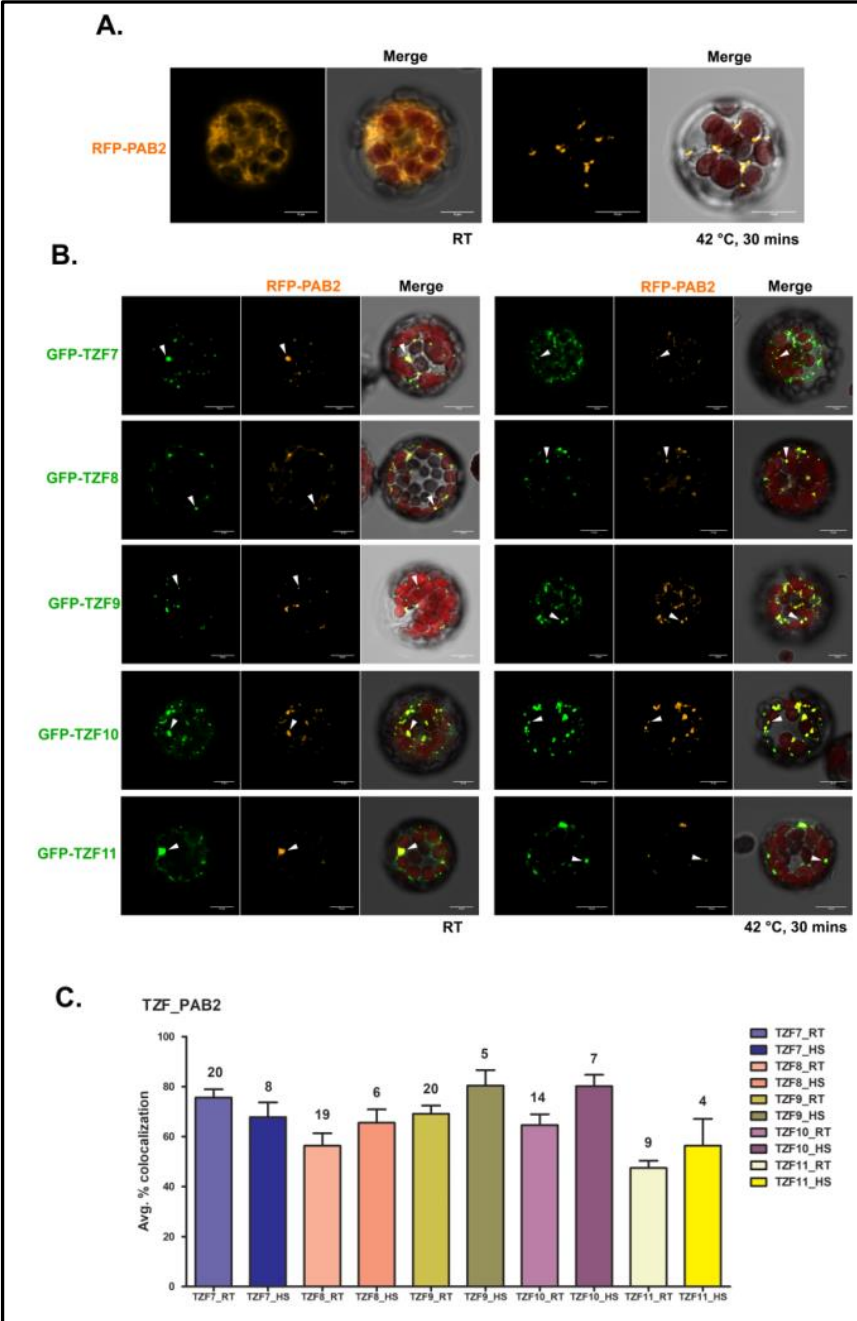
Fig.13 TZFs are associated with putative siRNA bodies.

Representative photographs of TZFs' co-localization with siRNA-body markers (as indicated with arrowheads in white), SGS3 (**A**), UPF1 (**B**) are shown above. Mesophyll protoplasts were co-transfected with indicated constructs and observed by confocal microscopy 12 hrs post-transfection. Scale bars=10 μm. Merged field includes chlorophyll alongwith the respective localized proteins. TZF7-11 co-localized partially with siRNA body markers which are quantified and represented in the graph below showing the average percent co-localization per protoplast. The numbers above the bars indicate the number of protoplasts used for the analysis.

No perfect co-localization was observed with the marker proteins (P body and siRNA body). Partial co-localization of the TZFs observed in experiments performed with P body markers implies that TZF protein accumulates in cytoplasmic foci distinct to P bodies, suggesting co-localization with siRNA bodies presumably. Thus, TZF proteins co-localizing with both P body and siRNA body markers might suggest their dual roles in RNA surveillance and RNA silencing.

3.3.2 TZFs co-localizes with SG markers even at room temperature

Stress granules (SG) are induced by heat treatment (42°C, 30 mins) as depicted in **Fig.14 (A) & (D) (right panel).** In the current study, the TZFs also co-localizes (as indicated with arrowheads in white) partially with the SG markers, PAB2 (**Fig.14 (B)**) and PAB8 (**Fig.14 (E)**) interestingly even at room temperature; unlike the previously reported co-localization of TZF1, 4, 5 and 6 (Bogamuwa & Jang, 2013a; M. C. Pomeranz et al., 2010a) with SG markers only after heat treatment. Also additionally, in the present study, heat treatment (for 30 mins at 42°C) stimulated more cytoplasmic granule formation for all the TZFs and PABs (**Fig.14 (B & E); right panel**) as indicated with the bar graphs showing the average percent co-localization per protoplast (**Fig.14 (C & F)**).

3.3.3 TZFs' recruitment of PABs to cytoplasmic foci

The variation in the localization of the PABs (PAB2/PAB8) into cytoplasmic granules at room temperature might suggest that the TZFs recruit the target mRNAs bound to PABs into the granule structures. To ascertain if the altered change in localization of the PABs was due to presence of TZF and not an artifact of the overexpression system, experiments were conducted to check for the localization of the PABs both at room temperature and after heat treatment. It was observed that both the PABs localized to cytoplasm at room temperature in the absence of the TZFs (**Fig.14 (A & D), left panel**) and formed granules only upon heat treatment (**Fig.14 (A & D), right panel**).
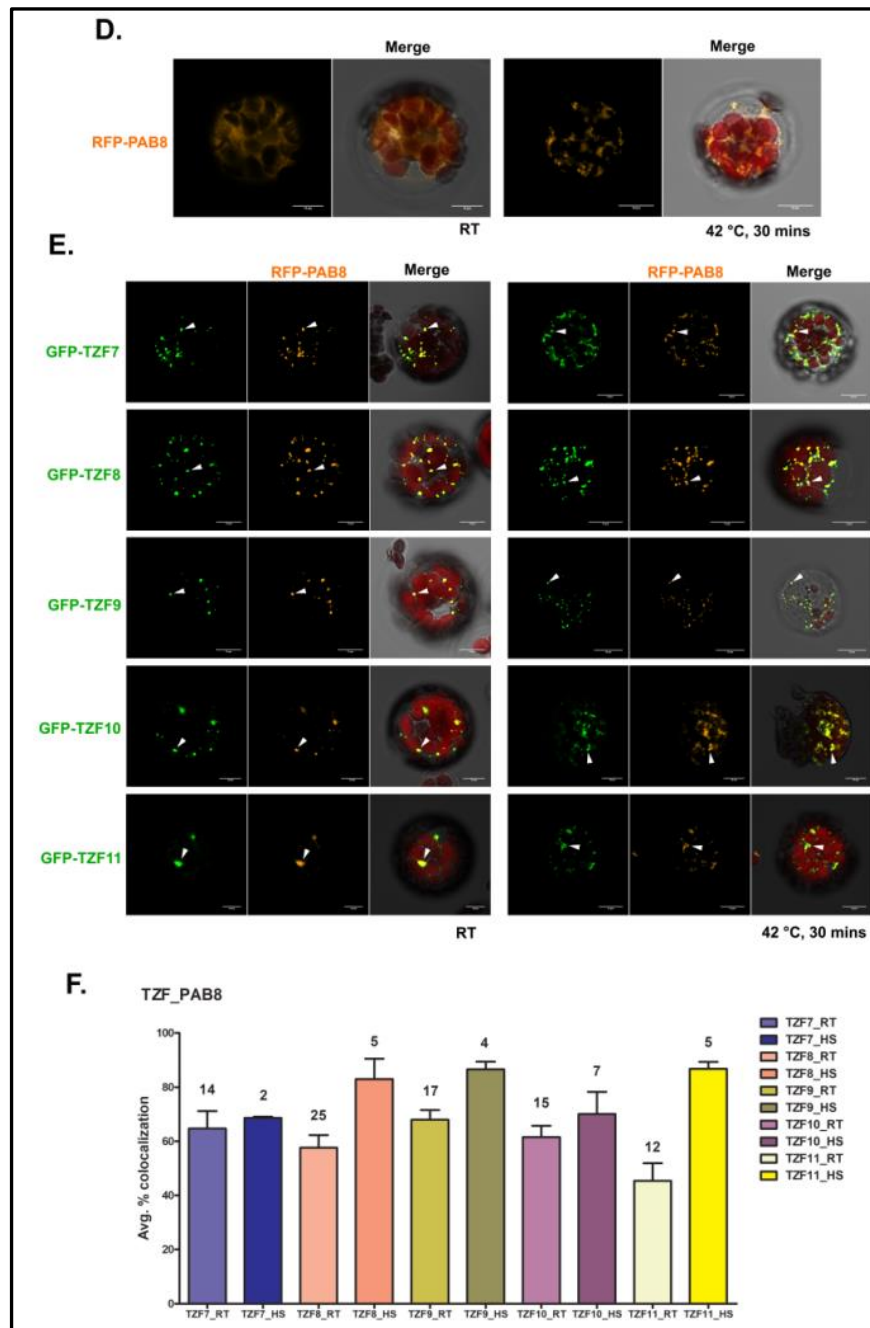
Fig.14 TZFs are associated with putative SGs.
Representative photographs of PAB2 (**A**) and PAB8 (**D**) localization in cytoplasm at room temperature (**left panel**) and localization in cytoplasmic granules (**right panel**) after heat treatment (42˚C, 30 mins) are shown.
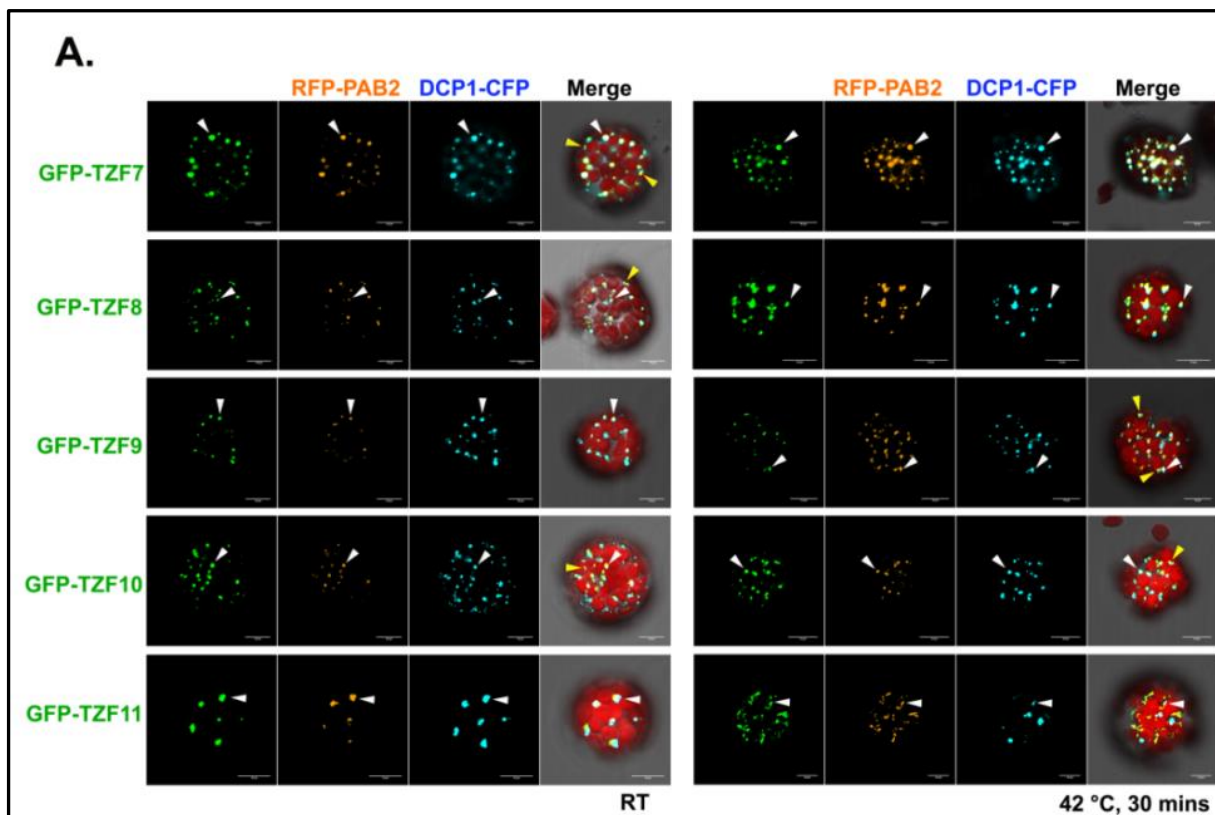Representative photographs of TZFs' co-localization (as indicated with arrowheads in white) with stress granule component, PAB2 (**B**) and PAB8 (**E**) even at room temperature (**left panel**) and increased granule formation after heat treatment; 42˚C, 30 mins (**right panel**) in co-transformed protoplasts are shown.
Mesophyll protoplasts were co-transfected with indicated constructs and observed by confocal microscopy 12 hrs post-transfection. Scale bars=10 µm. Merged field includes chlorophyll along with the respective localized proteins.
TZF7-11 induces the localization change of PABs into cytoplasmic granules both with and without heat treatment which are quantified and represented in the graphs (**C & F**), showing the average percent co-localization per protoplast. The numbers above the bars indicate the number of protoplasts used for the analysis.

From the co-localization analyses of the TZFs with the PABs, it was observed that cytoplasmic granules were formed regardless of heat treatment (**Fig.14**). As shown in **Fig.14 (C & F),** the quantification of the associations indicated that in all the cases (be it with PAB2 or PAB8 co-transformation with the TZFs), heat stress induced higher rates of average percent co-localization in all the associations, except that in TZF7 and PAB2, wherein association after heat treatment decreased (**Fig.14 (C)**). This might suggest that heat stress either induced an increment in the association of the TZFs with the PABs or an increased PABs' aggregation after heat treatment.

The altered localization of the PABs (forming granule structures even at room temperature) led to determine the nature of those punctated structures. So to determine the nature of the PAB containing structures under basal conditions, triple localization experiments were conducted. In these experiments, when DCP1, a P body marker was co-expressed, it was observed that the partially associated TZFs and PABs were also associated with DCP1 both with and without heat stress (partial association, as indicated with arrowheads in white) (**Fig.15 (A & B)**). The yellow arrowheads in **Fig.15** indicate TZFs' co-localized PABs clustering adjacent to DCP1 labeled foci. TZFs were observed either to be associated with both PABs and DCP1 in the same cluster at the same time or adjacent to DCP1, co-localizing with PABs.
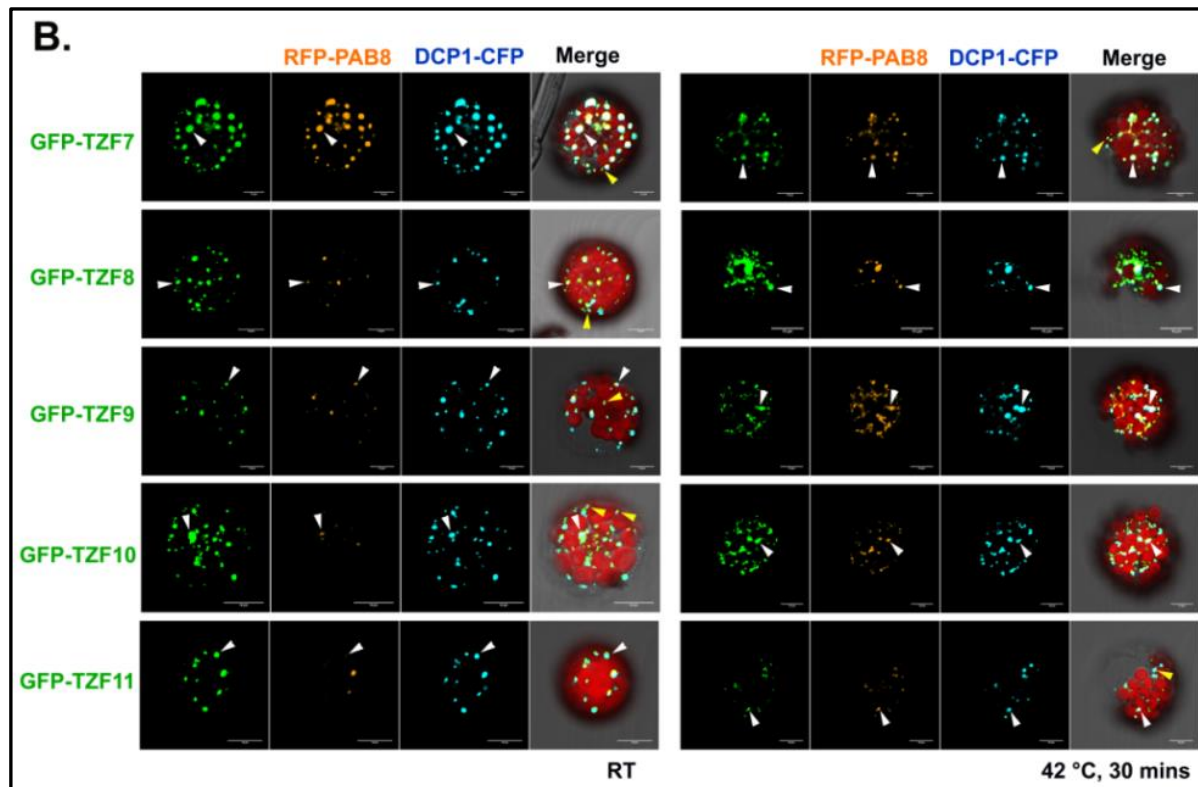
Fig.15 TZF's recruitment of PABs into P bodies with and without any stress.
Representative photographs of PAB2 (**A**) and PAB8 (**B**) recruitment into DCP1 labeled cytoplasmic granules in the presence of TZF7-TZF11 at room temperature (**left panel**) and after heat treatment at 42°C for 30 mins (**right panel**) are shown. The white arrowheads indicate co-localization of TZF with both PABs and DCP1 (with and without heat stress) and the yellow arrowheads indicate TZFs' co-localized PABs clustering adjacent to DCP1 labeled foci.
Mesophyll protoplasts were co-transfected with the indicated constructs and observed by confocal microscopy 12 hrs post-transfection. Scale bars=10 μm. Merged field includes chlorophyll along with the respective localized proteins.

Another speculation might be that *CaMV35S* or *UBQ10* promoter could produce artifacts due to high expression levels and might result in co-localization of all the TZFs for all the markers tested. Reliability of the protoplast transient system was determined by uniform distribution of free GFP, free CFP and free RFP in the cytoplasm (**Fig.16**). The protoplast transient expression systems appeared to be reliable, as free GFP/CFP/RFP was uniformly distributed in the cytoplasm.
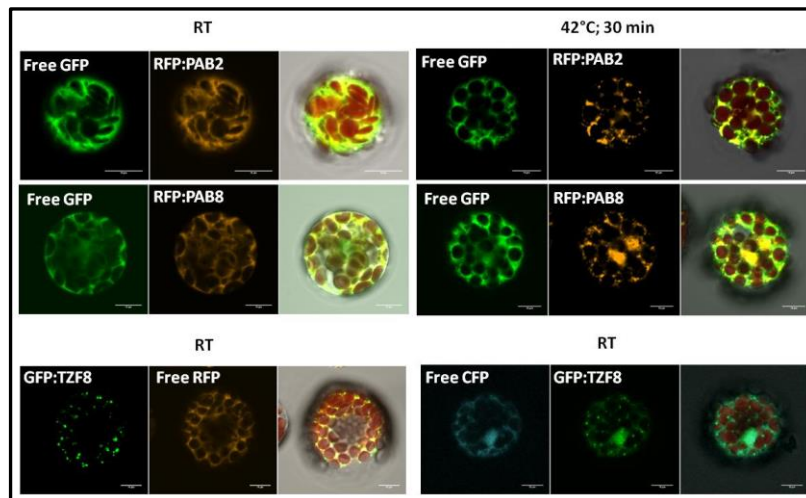
Fig.16 Distribution of free GFP, free CFP and free RFP.
Representative photographs offree GFP, free CFP and free RFP being uniformly distributed in the cytoplasm at room temperature are shown.
Mesophyll protoplasts were co-transfected with the respective constructs and observed by confocal microscopy 12 hrs post-transfection. Scale bars=10 µm. Merged field includes chlorophyll alongwith the respective localized proteins.

3.3.4 TZFs interact with the PABs in cytoplasmic foci

Another speculation of the altered localization of the PABs might be that TZFs and the PABs interact with each other and hence SG formations are observed even in the absence of stress. Hence, to determine if granule structures are formed due to interaction of the TZFs with the PABs, thereby altering the localization of the PABs, split YFP experiments were conducted and it was observed that PABs do interact with all the five TZFs in the cytoplasm and notably also in foci (**Fig.17 (A & B)**). The interactions observed between the PABs and the TZFs are still intact after heat stress and there appeared to be more speckles, suggesting further formation of stress granules containing TZF-PAB complexes.
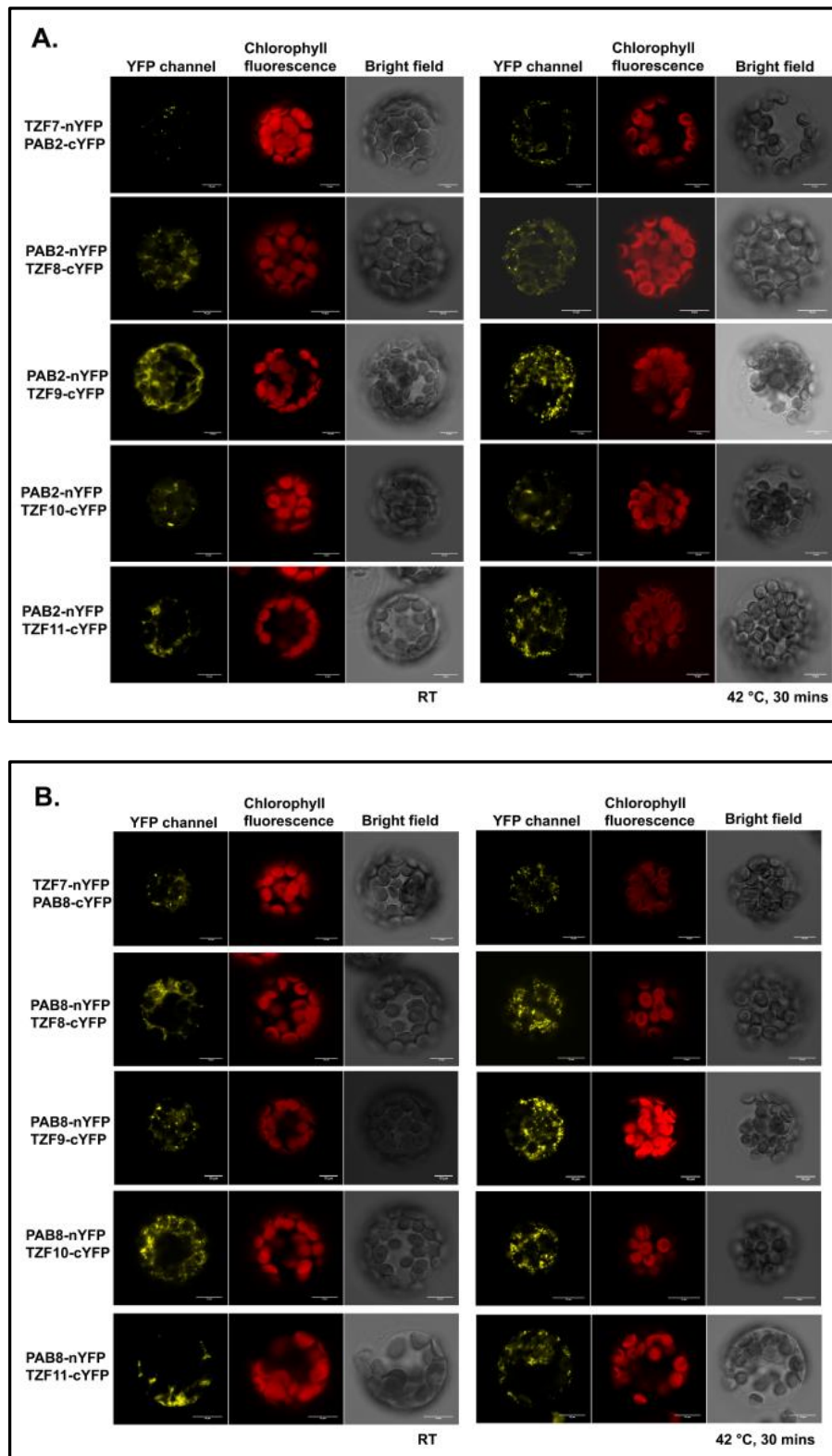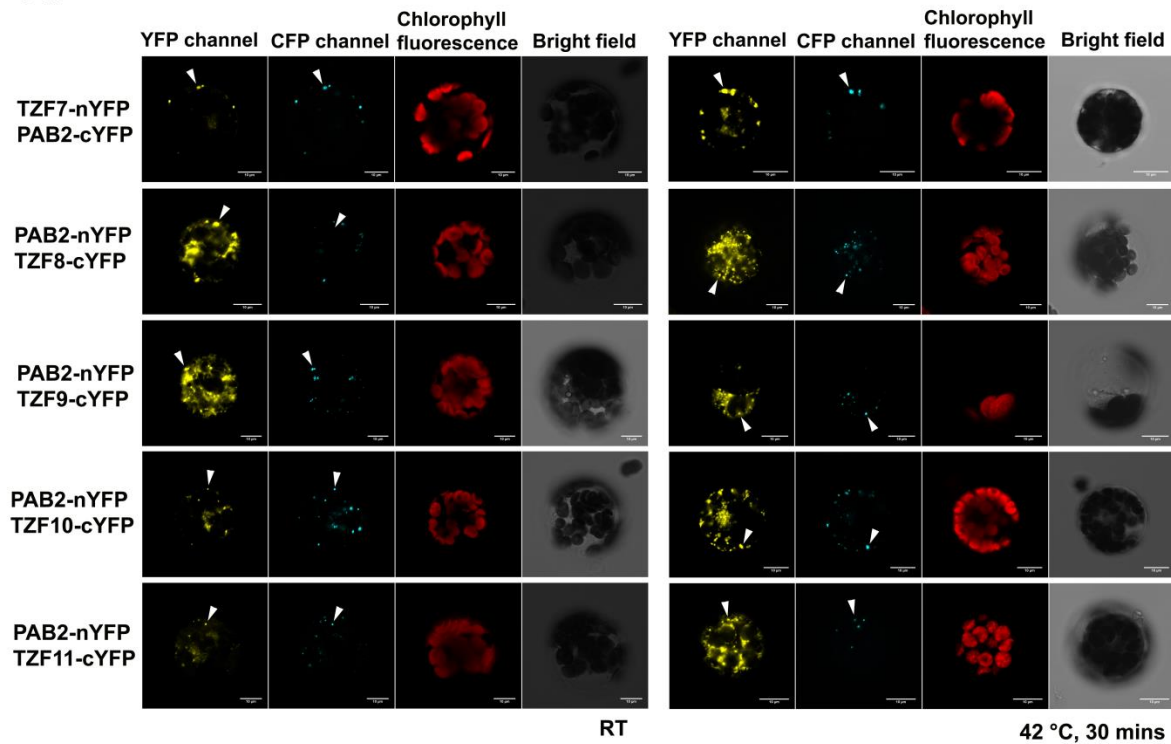
Fig.17 PABs interact with the TZFs *in vivo.*
A & B. Visualization of *in vivo* interactions by bimolecular fluorescence complementation (BiFC) analysis (YFP channel) by transiently expressing the respective protein fusions to N- or C-terminal YFP fragments (nYFP or cYFP, respectively) in *Arabidopsis* protoplasts. The respective TZFs (TZF7-TZF11) and PAB2 (**A**)/ PAB8 (**B**) (N-YFP-/C-YFP-tagged proteins) were pair-wise tested with (**right panel**) and without (**left panel**) heat treatment. Scale bars=10 μm.

The speckled split-YFP signals resulting from interaction between the PABs and the TZFs co-localizes with CFP-labeled DCP1 as shown in **Fig.18 (A & B)**). To check if this may be due to direct interaction of DCP1 with TZFs or PABs, additional split-YFP-based interaction assays were conducted. As shown in **Fig 19**, no direct interaction of DCP1 was observed with the TZFs (**Fig.19 (A)**) and the PABs (**Fig.19 (B)**). Western blot to prove the integrity of the fusion proteins is shown in supplementary **Fig.S1.1** with amido black staining of the membrane to show equal protein loading.
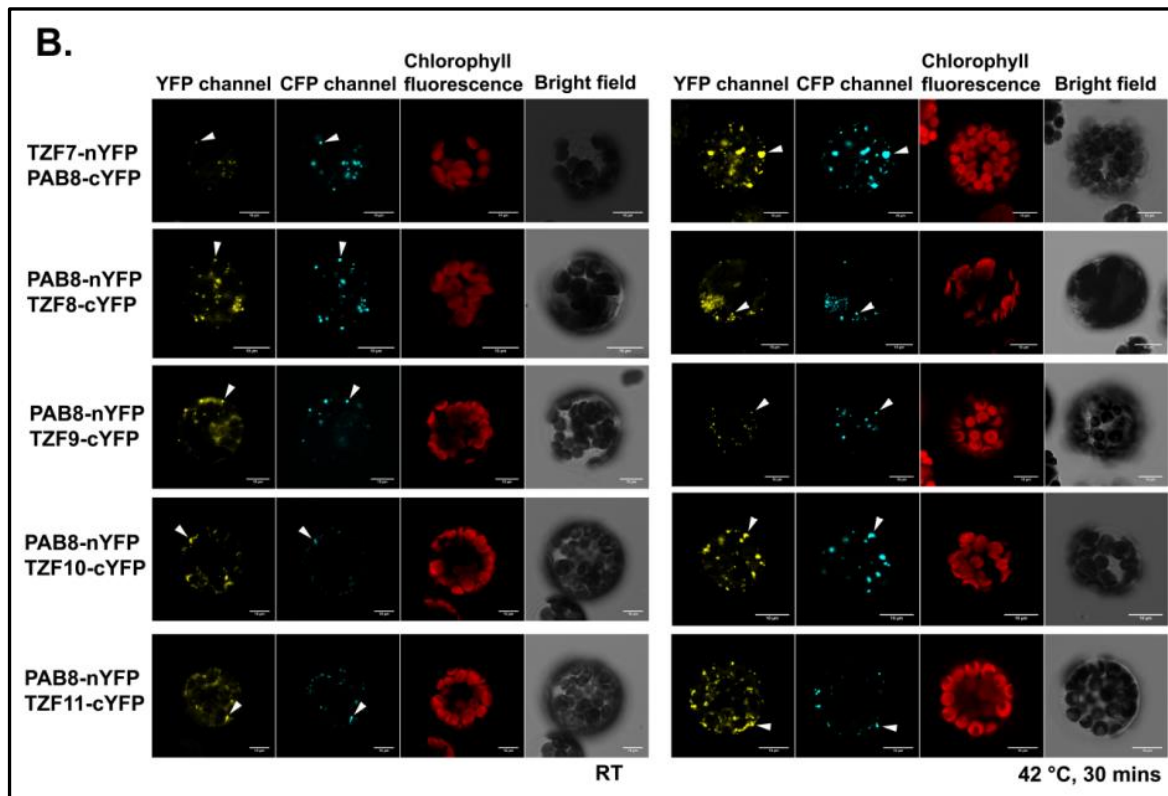
Fig.18 *In vivo* interaction of PABs with the TZFs in DCP1 labeled foci.
A & B. Visualization of *in vivo* interactions was analyzed by bimolecular fluorescence complementation (BiFC) analysis (YFP channel) by transiently expressing the respective protein fusions to N- or C-terminal YFP fragments (nYFP or cYFP, respectively) in *Arabidopsis* protoplasts. The respective TZFs (TZF7-TZF11) and PAB2 (**A**)/ PAB8 (**B**) (N-YFP-/C-YFP-tagged proteins) were pair-wise tested with (**right panel**) and without (**left panel**) heat treatment. Scale bars=10 µm.
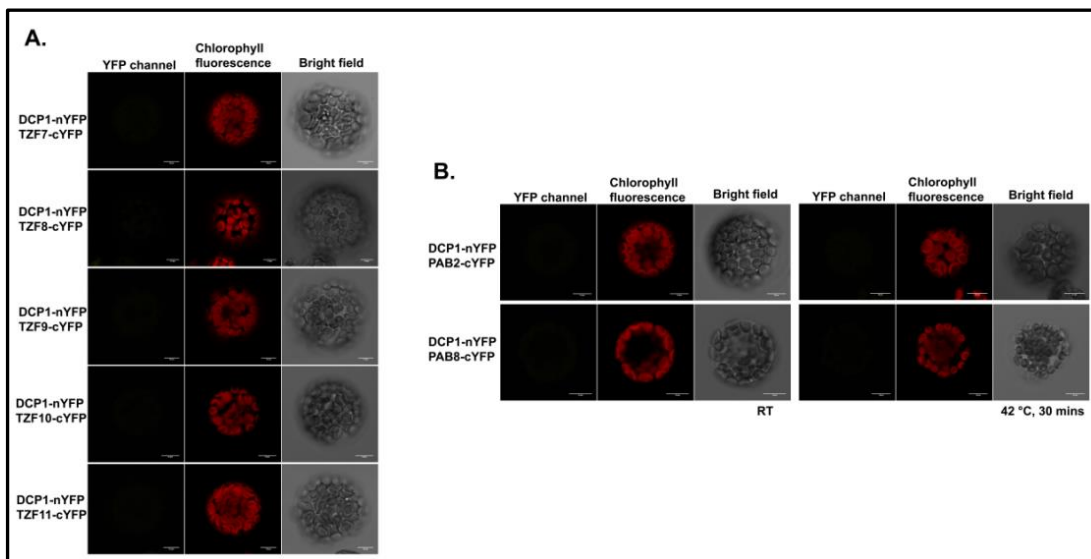

Fig.19 P body marker, DCP1 do not interact with the TZFs and PABs *in vivo.*
A & B. Visualization of *in vivo* interactions was analyzed by BiFC analysis (YFP channel) by transiently expressing the respective protein fusions to N- or C-terminal YFP fragments (nYFP or cYFP, respectively) in *Arabidopsis* protoplasts. The respective TZFs (TZF7-TZF11) and DCP1 (N-YFP-/C-YFP-tagged proteins) were pair-wise tested **(A)**. PAB2/PAB8 and DCP1 (N-YFP-/C-YFP-tagged proteins) **(B)** were tested with (**right panel**) and without (**left panel**) heat treatment. Scale bars=10 µm.
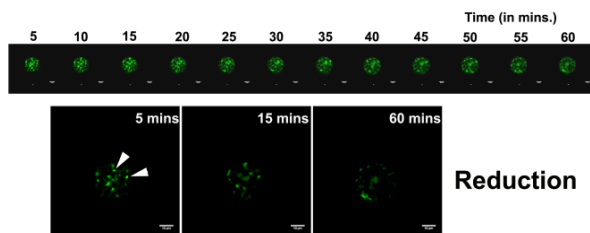
Hence, co-localization of the GFP tagged TZFs with the various markers suggest a potential role of the TZFs in post-transcriptional regulation (similar to the functions of the P bodies, siRNA bodies and SG). No perfect co-localization observed with all the marker proteins (P body, siRNA body and SG) might indicate that the TZFs have diverse functions at the same time co-localizing to the different bodies.

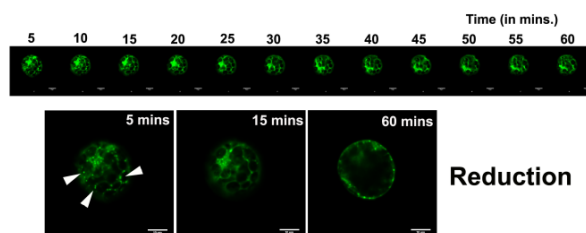## 3.4 TZF localization changes after flg22 elicitation

As gene expression of *TZF*s is induced after PAMP (flg22) elicitation, TZFs may be involved in PTI response. The organizational changes in the TZFs upon PAMP elicitation was checked based on previous reports of TZFs as nucleocytoplasmic shuttling proteins i.e. upon treatment with cold, ABA, Leptomycin B, CHX or ActD, led to relocalization of TZF1, TZF7 and TZF9 from cytoplasmic foci to the nucleus (Blanvillain et al., 2011; Maldonado-bonilla et al., 2014; M. C. Pomeranz et al., 2010a). In additional studies, treatment of mesophyll protoplasts with cycloheximide led to a marked reduction in number of TZF9-containing cytoplasmic foci (Maldonado-bonilla et al., 2014). To determine if the TZF-labeled speckle structures are affected by PAMP treatment, images of individual protoplasts transiently expressing the proteins were taken every 5 mins after flg22 elicitation (in different z-planes, for 1 hr). Looking at each protoplast individually is needed as there is too much variation in distribution at the population level and also to focus on those showing cytoplasmic foci to check for any changes in their localization. PAMP elicitation was tested for changes in size, quantity or distribution of the speckled structures within the cell.

In general, elicitation with flg22 caused a reduction in the number of the speckled structures of the TZFs within 15 mins (in most of the protoplasts, see summary of responsiveness below, **Table 20 (F)**). However, different patterns of transient reduction/fusion/reappearance of the speckled structures were observed (**Fig. 20**). TZF7 and TZF8 have shown only the reduced pattern of localization change after flg22 elicitation (after 15 mins) as shown in **Fig.20 (A & B)** respectively (indicated with arrowheads in white). TZF9 and TZF11 have shown two patterns: reduction (indicated with arrowheads in white) and reappearance (indicated with arrowheads in yellow) of the cytoplasmic foci as shown in **Fig.20 (C & E)** respectively. TZF10 has shown three patterns: reduction (indicated with arrowheads in white), reappearance (indicated with arrowheads in yellow) and fusion (indicated with arrowheads in red) of the cytoplasmic foci as shown in **Fig.20 (D)** (enlarged images of the protoplasts from a single z-plane for each of the TZFs are shown at three different time points).
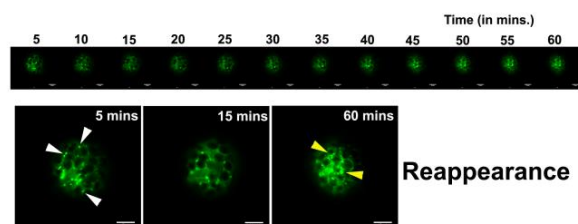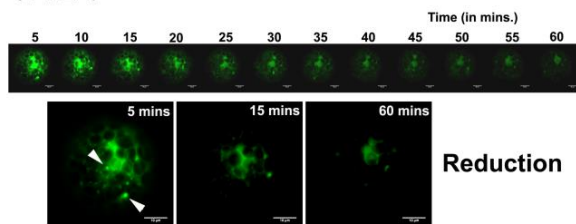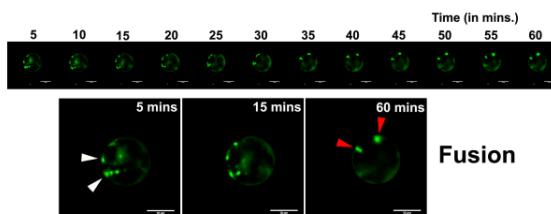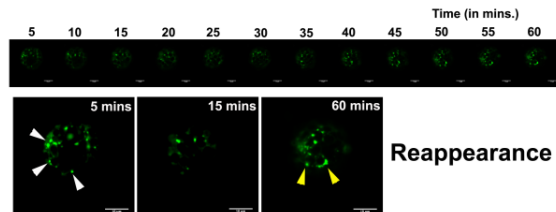
A. TZF7

Reduction

B. TZF8

Reduction

C. TZF9

Reduction

Reappearance

D. TZF10

Reduction

Reappearance

Fusion

E. TZF11

Reduction

Reappearance
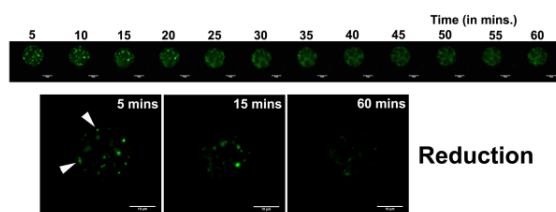
Fig.20 Changes in TZF labeled structures after PAMP elicitation.
Transiently transformed protoplasts were treated with flg22 (1 μM) and the photographs were taken after every 5 mins until 60 mins. Experiments are repeated at least 9 times for each of the proteins. The numbers above indicate time (in mins) for changes in a single protopla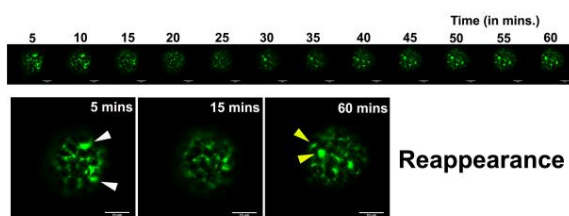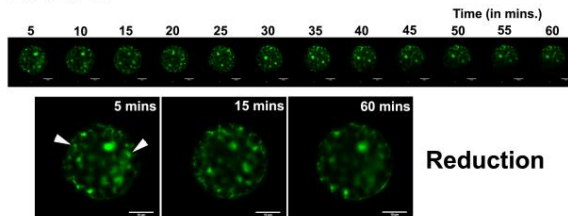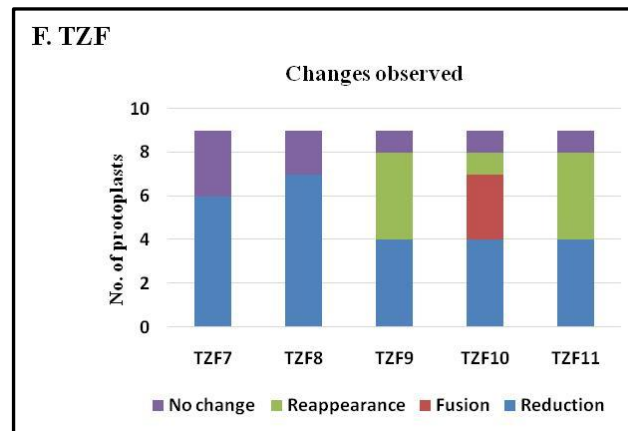st in a single z-plane. Water treatment was used as control (not shown above, data provided in CD). All the data for the time series experiments for each of the TZFs are provided in CD with the folder named 'PAMP induced changes'.

A. TZF7 localization changes after flg22 treatment: reduction in the number of TZF labeled structures over time
B. TZF8 localization changes after flg22 treatment: reduction in the number of TZF labeled structures over time
C. TZF9 localization changes after flg22 treatment: reduction in the number of TZF labeled structures after 15 minutes and gradual increase until 60 mins of treatment
D. TZF10 localization changes after flg22 treatment: reduction in the number of TZF labeled structures after 15 minutes/aggregation after 60 mins treatment/gradual increase until 60 mins of treatment
E. TZF11 localization changes after flg22 treatment: reduction in the number of TZF labeled structures over time and gradual increase until 60 mins of treatment
F. Table representing the type of changes observed in the various TZFs after flg22 elicitation (60 mins)

In **Table 20 (F)**, changes observed in all the TZFs after flg22 elicitation has been summarized along with the total number of protoplasts where the changes were observed. In TZF7, 6 out of 9 protoplasts have shown the above mentioned changes upon PAMP elicitation; 7 out of 9 protoplasts in TZF8; and 8 out of 9 protoplasts in TZF9/TZF10/TZF11. The protoplasts where such changes were not observed might point to the fact that those protoplasts were already stressed or were not responsive to flg22 treatment.

PAMP elicitation changes the number of TZF labeled structures, possibly through phosphorylation of the TZFs (as seen in TZF9 where no localization change of phospho-site mutant was observed after flg22 elicitation; Naheed Tabassum, personal communication). Hence, the changes in TZF localization presumably alter their functions.

3.5 TZFs are phospho-targets of MPKs

As shown, PAMP elicitation renders a change in the number of TZF labeled structures. Also validation of the previous reports of TZF7 and TZF9, as being putative phospho-proteins (Feilner et al., 2005), was performed. As TZF9 is a MPK3/MPK6 substrate (Maldonado-bonilla et al., 2014), similar experiments were conducted for the other TZFs (TZF7, 8, 10 and 11).

3.5.1 TZFs are involved in MAPK cascade and show mobility shift upon flg22 treatment

To find out whether the other TZFs are being phosphorylated by PAMP-activated MAPKs, kinase assays (*in vitro*) were conducted with recombinant purified His-tagged TZF proteins after incubation with pre-activated recombinant MAP kinases. It was observed that the TZFs (TZF7/8/10/11) are substrates of MPK3/4/6 with the exception that TZF10 being the substrate of MPK3 and MPK4 and not MPK6 (**Fig.21,** indicated with red arrows).
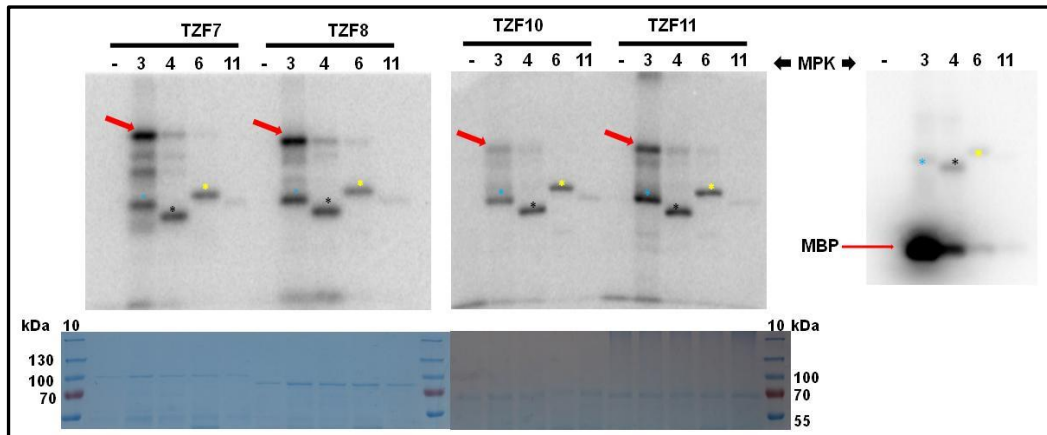

Fig.21 TZFs (TZF7/8/10/11) are substrates of MPKs (MPK3/MPK4/MPK6) *in vitro*.
Recombinant purified His tagged TZF7/8/10/11proteins are *in vitro* phosphorylated by MPK3, MPK4 and MPK6 (except TZF10). Phosphorylated proteins are indicated with the red arrows for the respective proteins. Auto-phosphorylated MPKs are indicated with blue (MPK3), black (MPK4) and yellow (MPK6) asterisks. MBP phosphorylation was used as control and the bottom panel is a Coomassie brilliant blue staining used as a loading control.

On the other hand, *in vivo* phosphorylation of the TZFs was tested by PAMP (100 nM flg22) elicitation in protoplasts expressing epitope-tagged TZFs and harvested after 15 mins and 60 mins. Untreated transformed protoplasts were used as control. From the experiments conducted, it was observed that upon flg22 elicitation, all the five TZFs (TZF7-11) show a mobility shift in SDS-PAGE gels 15 mins post treatment (possibly indicating modification by phosphorylation) (**Fig.22**).
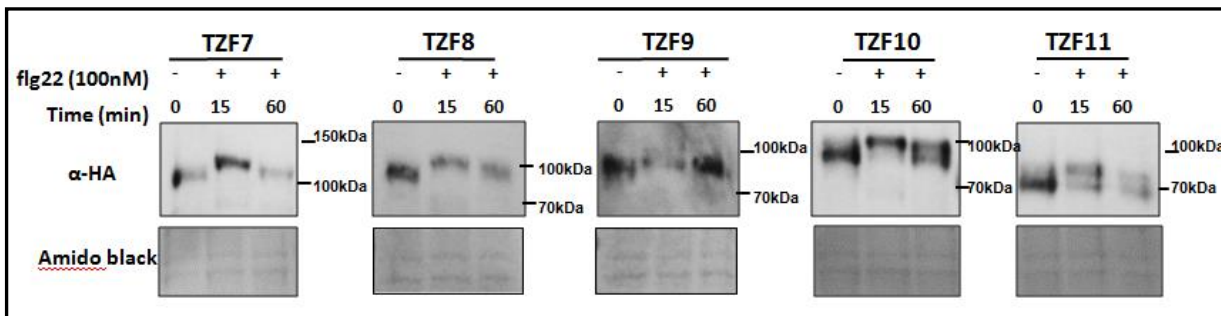
Fig.22 *In vivo* post-translational modification of the TZFs (TZF7-11) after PAMP elicitation.
Protoplasts expressing HA tagged TZFs were treated withflg22 (100 nM) for the indicated times, which were then lysed and the extracts were run on a SDS-PAGE gel and blotted against α-HA antibody. A mobility shift of the proteins is observed in SDS-PAGE after 15 mins post flg22 treatment (as visualized in α-HA blot) for each of the proteins. Amido black staining of the membrane is used as the loading control.

Hence, from both *in vitro* and *in vivo* experiments, it can be concluded that the TZFs under study are potential targets for post-translational modifications upon flg22 treatment.

3.5.2 TZFs mobility shift after flg22 elicitation is due to phosphorylation

Post-translational modifications upon PAMP-treatment include phosphorylation, glycosylation, ubiquitination, acetylation and the like. Hence, to prove the proteins' phosphorylation (mobility shift) by flg22-activated MAPKs, experiments were conducted by treating the protein extracts with λ-phosphatase (known to dephosphorylate proteins). The λ-phosphatase is known to release the phosphate group from phosphorylated serine, threonine and tyrosine residue in a protein.

Protoplasts were treated with flg22 after overnight incubation and harvested after 10 mins of treatment. And then the protein extracts from one of the flg22 elicited samples were treated with λ-phosphatase. It was found that upon λ-phosphatase treatment, abrogation of the mobility shift was observed in the flg22 treated samples and was similar to the un-elicited state (**Fig.23**). But TZF9 and TZF10 have shown a different mobility also in the non-elicited protoplasts (possibly due to basal phosphorylation) and a higher mobility shift after 10 mins of flg22 treatment. This proves that the mobility shift observed in the TZFs is due to phosphorylation after PAMP elicitation.
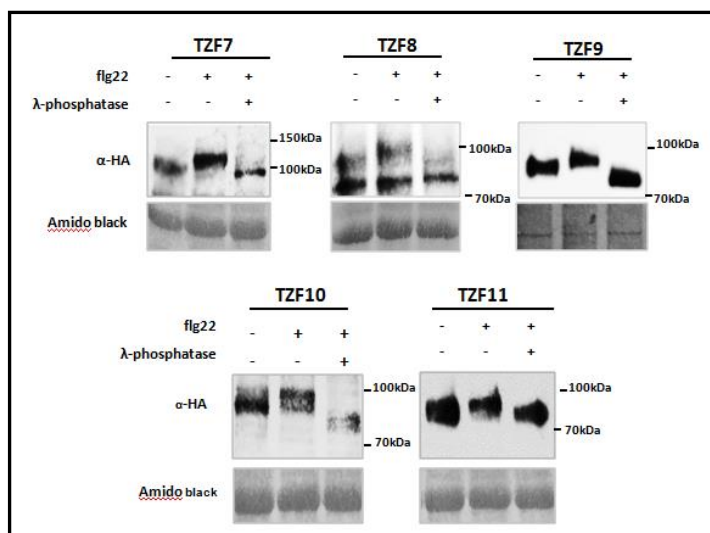
Fig.23 Phosphorylation (mobility shift) of the TZFs (TZF7-11) is abrogated after λ-phosphatase treatment. Protoplasts expressing HA tagged TZFs were lysed and protein extracts were treated with flg22 and λ-phosphatase (as indicated with plus and dash). Protein extracts were run on SDS-PAGE gel and blotted against α-HA antibody. TZF proteins show reduced mobility after flg22 treatment (10 min) and abrogated shift upon λ-phosphatase treatment as compared to the untreated or water-treated samples (indicated with dash). Amido black staining of the membrane is used as the loading control.

3.5.3 TZFs interact with MPK3, MPK4 and MPK6

Direct interaction of the TZFs with the PAMP-responsive MPKs were also tested using split YFP assay and was observed that all the TZFs interact with MPK3 in the cytoplasm and nucleus (**Fig.24 (A & B)**); also in speckled structures as observed in case of TZF9 and TZF10. Interaction of the TZFs with MPK4 occurs mainly in the cytoplasm and cytoplasmic foci; also in the nucleus (in case of TZF11) (**Fig.24 (C)**). Also the interaction of TZF7-10 with MPK6 was observed mainly in the cytoplasm and cytoplasmic foci; also in the nucleus (in case of TZF10) with the exception of TZF11 (do not interact with MPK6) (**Fig.24 (D)**). Interaction of the TZFs with the unrelated MPK8 was used as negative control for the interaction study (**Fig.24 (E)**).
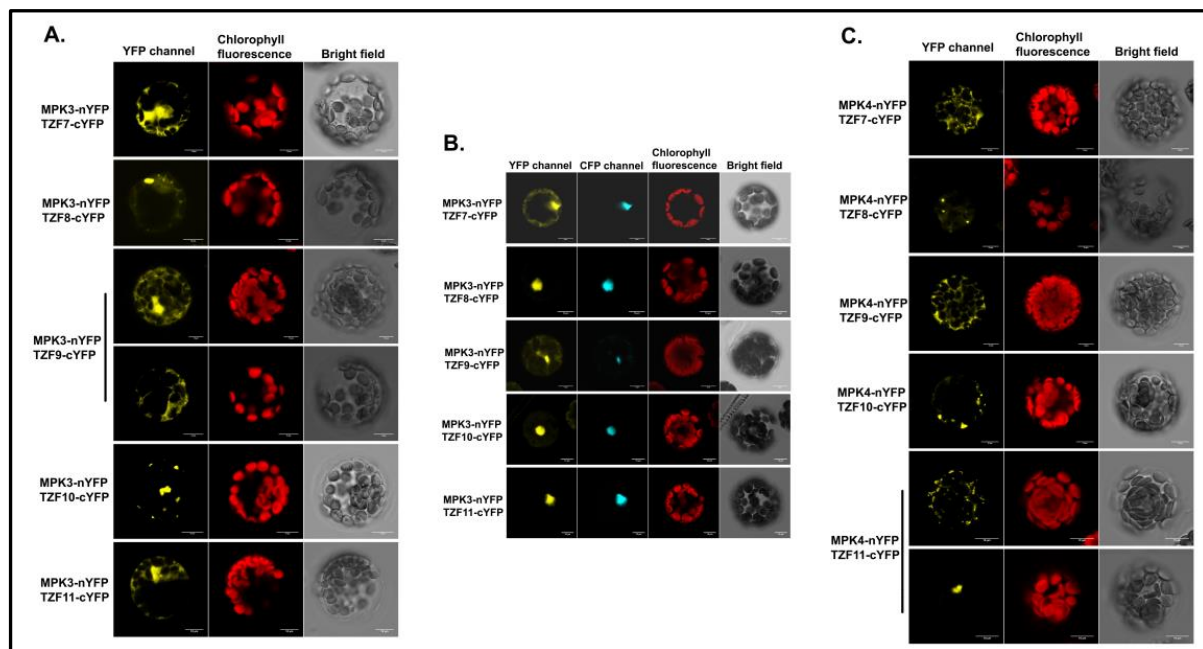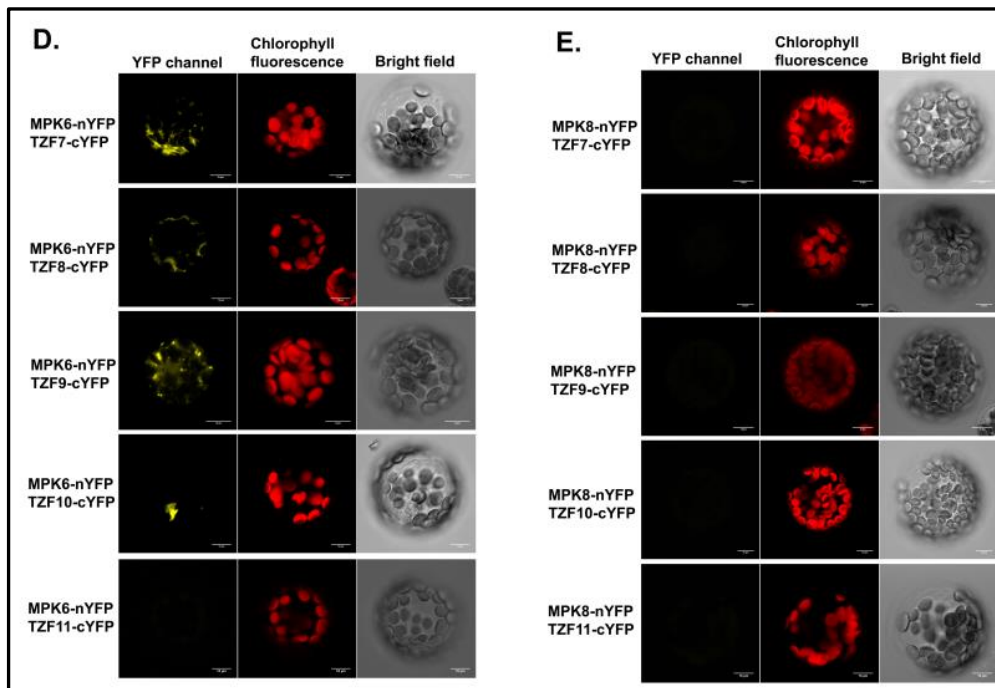
Fig.24 TZFs interact with the PAMP responsive MAPKs *in vivo.*
Visualization of *in vivo* interactions by BiFC analysis (YFP channel) by transiently expressing the respective protein fusions to N- or C-terminal YFP fragments (nYFP or cYFP, respectively) in *Arabidopsis* protoplasts. Scale bars=10 μm.
A & B. TZFs (TZF7-TZF11) and MPK3 (N-YFP-/C-YFP-tagged proteins) were pair-wise tested and observed to interact mainly in the cytoplasm and nucleus; also in cytoplasmic foci in case of TZF9 and TZF10. The nuclear interaction is represented using transfection with the ERF104 transcription factor fused to CFP (in the CFP channel).
C. TZFs (TZF7-TZF11) and MPK4 (N-YFP-/C-YFP-tagged proteins) were pair-wise tested and observed to interact mainly in the cytoplasm and cytoplasmic foci; also in the nucleus (in case of TZF11)
D. TZFs (TZF7-TZF11) and MPK6 (N-YFP-/C-YFP-tagged proteins) were pair-wise tested and interaction of TZF7-10 with MPK6 was observed mainly in the cytoplasm and cytoplasmic foci; also in the nucleus (in case of TZF10) with the exception of TZF11 (do not interact with MPK6)
E. TZFs' (TZF7-TZF11) and MPK8 (N-YFP-/C-YFP-tagged proteins) interaction were pair-wise tested and was used as a negative control

Since MPK3, MPK4 and MPK6 are PAMP activated, and the TZFs being MAPK substrates (*in vitro* kinase assay) and from *in vivo* phosphorylation assays, it can be inferred that the TZFs may contribute to cellular signaling induced by PAMPs.

3.6 TZFs' role in plant stress responses

3.6.1 T-DNA insertion mutants' screening

To study the possible role of TZFs in plant stress responses, a reverse genetics approach was used and the knock out *tzf* T-DNA insertion mutants were further characterized to check for any change in PAMP/stress responses. It involved genotyping of the T-DNA insertion lines and determination of insertion position of the T-DNA in the genome for the different lines for each of the TZFs (**Fig.25**).
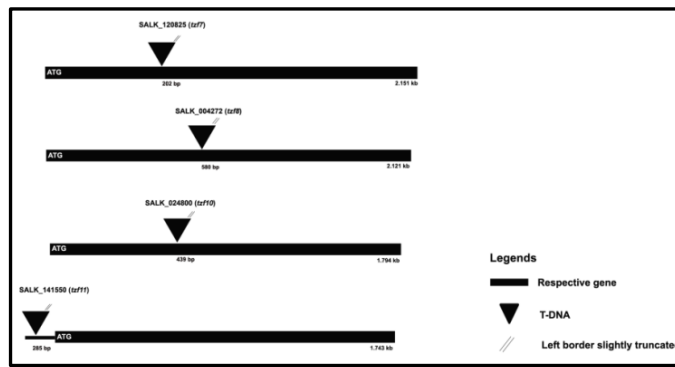
Fig.25 T-DNA insertion positions of the SALK lines of the different TZFs (TZF7/8/10/11).
Black rectangle (big) represents the coding region. Location of T-DNA insertion is depicted by black triangle and truncated left border is depicted with the slanted lines.

3.6.2 Only *tzf9* mutant shows attenuated defence response upon PAMP treatment

PAMP-induced root growth inhibition assay was performed for the single insertion mutants and also for the higher order ((double mutant, *tzf10tzf11*), quadruple (*tzf7tzf8tzf9tzf10*) and penta (*tzf7tzf8tzf9tzf10tzf11*)) mutants. As reported, that upon constant exposure to PAMP, plant development is impaired and the root growth inhibition is a quantitative effect of PAMP-mediated response in plants (Ranf, Eschen-Lippold, Pecher, Lee, & Scheel, 2011). *tzf* mutant plants and *Col-0* plants were grown in MS medium supplemented with or without flg22. The *tzf9* insertion mutant was used as a control, since it was reported to show partial attenuation in PAMP-dependent responses (Maldonado-bonilla et al., 2014). All the other TZF mutants, except *tzf9,* did not show altered phenotype (less root growth inhibition compared with the *Col-0* seedlings) (**Fig.26**).
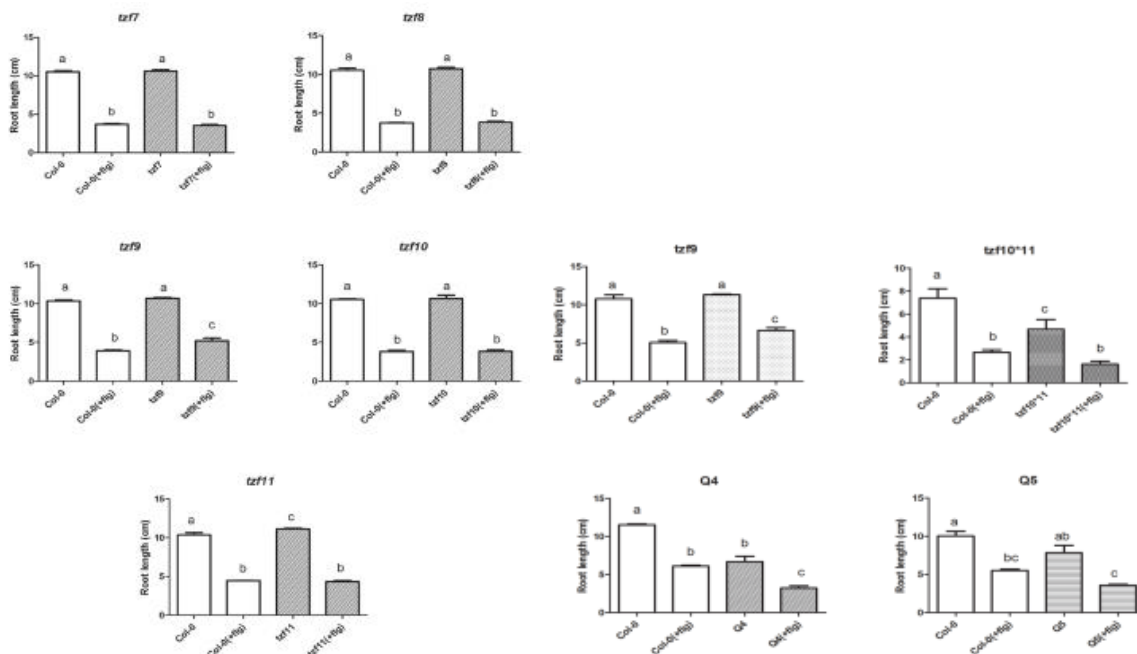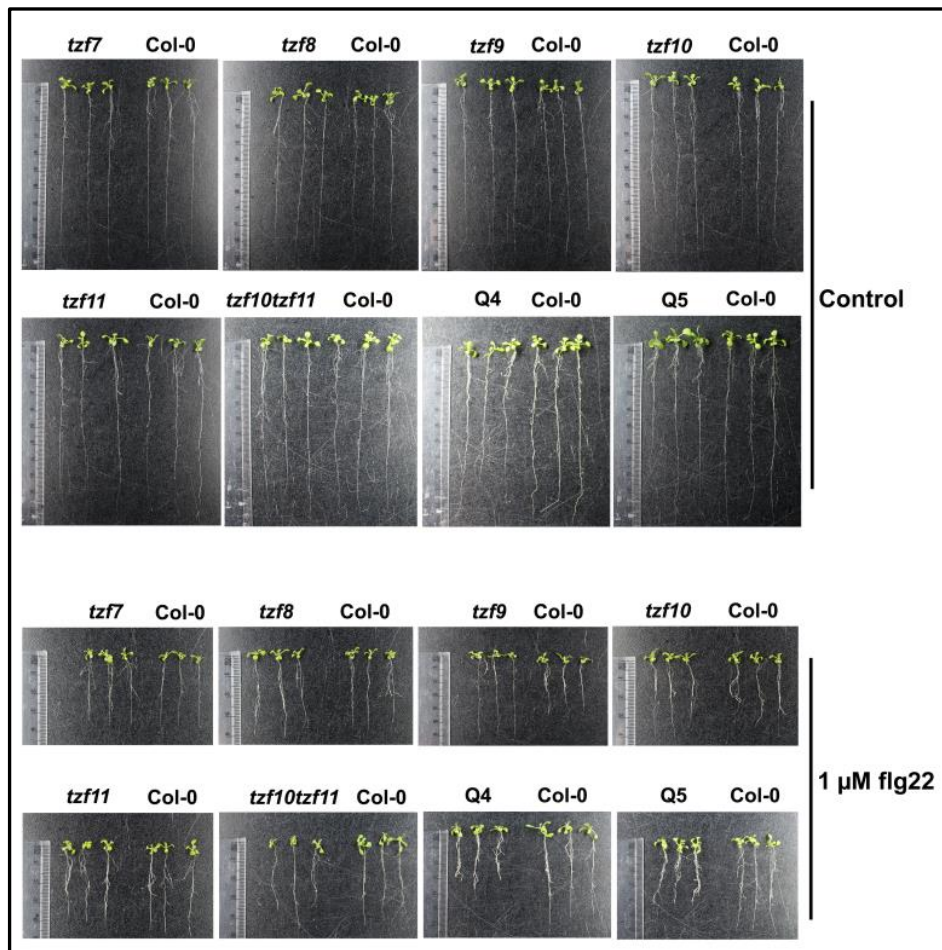
Fig.26 Phenotypic comparison of PAMP-dependent root growth inhibition.

Representative photographs of 15-day-old seedlings grown in ATS medium supplemented with or without 1 µM flg22.

The graphs depict the mean root lengths (in cm) of *Col-0* and the single insertion mutants and the higher order

mutants of the *tzfs* compared with the untreated control. The bars represent the mean ± SE of one of the two independent experiments with atleast six biological replicates. Statistical significance was evaluated by 1-way-ANOVA with Tukey's post test.

Surprisingly, no alteration in the phenotypes of the quadruple (*tzf7tzf8tzf9tzf10*) and penta (*tzf7tzf8tzf9tzf10tzf11*) mutant was observed but this may be due to opposite effects from the other TZFs or the fact that these higher order mutants already had shorter roots without PAMP treatment.

3.6.3 *tzf* mutants are sensitive to ABA

ABA response in the *tzfs* was performed based on the previous report of *tzf10*'s sensitivity to germination in the presence of abscisic acid (ABA) (AbuQamar et al., 2006). In the present study, root growth inhibition assay was performed with all the T-DNA insertion mutants. Average root length was recorded after 12 days of transfer of seedlings into plates with MS medium supplemented with or without 10 µM ABA. The higher order mutants (both quadruple and penta mutants) are more sensitive to ABA, showing severe yellowing and impaired growth of both leaves and roots (**Fig.27**). *tzf10* and the *tzf10tzf11* double mutant also showed severe yellowing of leaves in presence of ABA when compared to the wild type phenotype. Hence, *tzf10* mutant has presumably a dominant role in the sensitivity to ABA with regard to leaf yellowing in the double, quadruple and penta mutant.
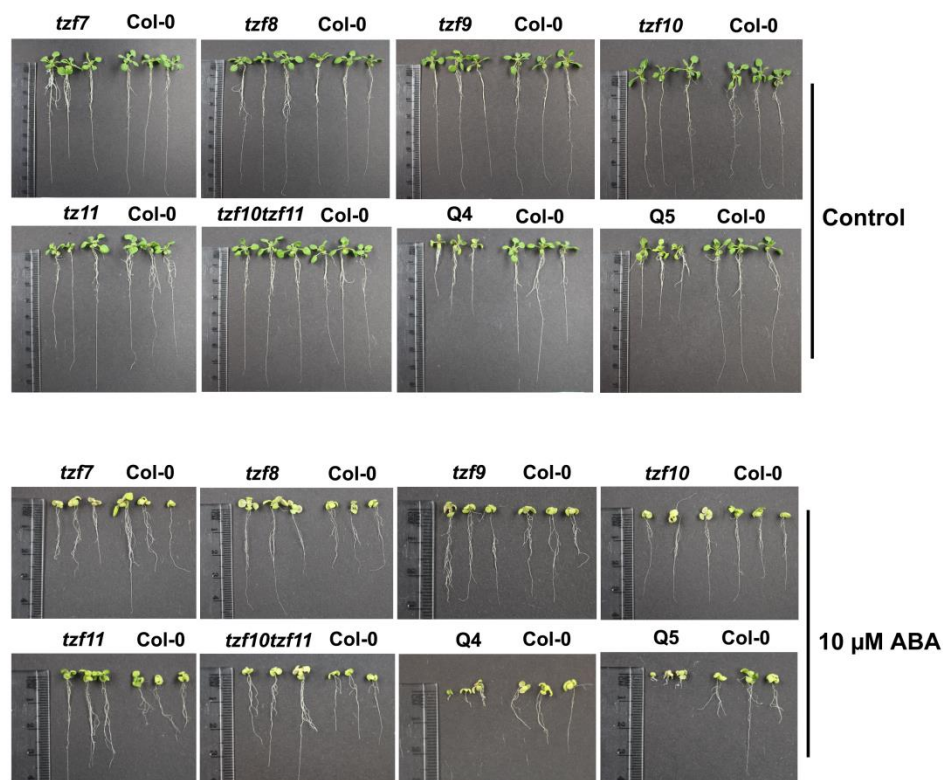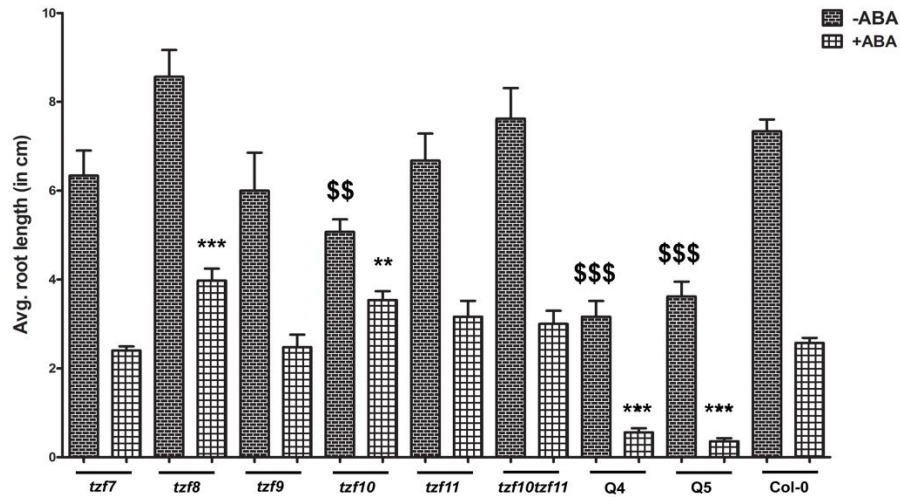
Fig.27 ABA-hypersensitive root growth inhibition of *tzf* mutants as compared to wild-type plants.
Growth of the different mutants and wild type in medium supplemented with or without 10 µM ABA. The photographs were taken after 12 d of the transfer of 5-d-old seedlings from Murashige and Skoog medium to plates lacking or containing10 µM ABA. The graphs depict the mean root lengths (in cm) of *Col-0* and the single insertion mutants and the higher order mutants of the *tzfs* compared with the untreated control. The bars represent the mean ± SE of one of the three independent experiments with atleast six biological replicates. Statistical significance was evaluated by 1-way-ANOVA ($^{\$\$}$/*P<0.05; $^{\$\$}$/**P<0.01, $^{\$\$\$}$/***P<0.001) with Dunnett's post test (compared to *Col-0* (+ABA) indicated with * and *Col-0* (-ABA) indicated with $^{\$}$).

Previous reports documented TZFs' proteins role mostly in abiotic stress responses (Blanvillain et al., 2011; Bogamuwa & Jang, 2013a; Gupta et al., 2016; Huang et al., 2011a; Kim et al., 2008; Lee et al., 2012; Z. Li & Thomas, 2007; P. C. Lin et al., 2011; Sun et al., 2007) and also TZF9 and 10, in having a role in biotic stress responses as well (AbuQamar et al., 2006; Maldonado-bonilla et al., 2014). However, in the current study, from the various experiments, it can be stated that it provides evidence of involvement of TZF7, TZF8, TZF10 and TZF11 in PTI and also in response to ABA signaling. TZFs role in ABA responses implies that the TZFs might have a role in abiotic stress responses together with biotic responses.

4 Discussion

4.1 TZFs' involvement in PAMP induced gene regulation

The molecular functions of most of the plant TZFs have not been fully characterized. However, multiple lines of evidence suggest that they play a pivotal role in regulation of gene expression through modulation of RNA metabolism and affects growth, development and stress responses in plants (Guo et al., 2009; Kim et al., 2008; Z. Kong et al., 2006; Lee et al., 2012; P. C. Lin et al., 2011; Sun et al., 2007). In the present study, gene expression analyses revealed that *TZF7-11* gene are PAMP inducible (**Fig.10**). Yet, not all the TZFs under study have shown a similar pattern of gene induction (**Fig.10 (A-E)**).

Among the previously reported gene expression analyses, AtTZF1 was identified as a sugar-sensitive gene (Price, Laxmi, St. Martin, & Jang, 2004) and reported to play a role in mediating ABA- and GA-dependent growth and stress responses by affecting gene expression (P. C. Lin et al., 2011). AtTZF2 and AtTZF3 were described to be induced by abiotic stresses such as ABA, salt, mannitol and cold (Gupta et al., 2016; Huang et al., 2011a; Lee et al., 2012). *AtTZF4*, *5* and *6* have been reported to be both ABA and GA responsive (Bogamuwa & Jang, 2013a). AtTZF10 and AtTZF11 are involved in salt stress responses (Sun et al., 2007). On the other hand, the expression of human TZF protein, tristetraprolin (hTTP/ZFP36), has been reported to be induced by insulin, serum and other growth factors (Carrick et al., 2004). The *Arabidopsis* microarray database Genevestigator, describes *TZF7*, *TZF11* transcripts to be induced by cold; and also *TZF7* transcripts to be moderately elevated by salt, osmotic stress and during senescence (Blanvillain et al., 2011). In mammals, TZF proteins have been reported to control a variety of cellular processes via regulation of gene expression at both transcriptional and post-transcriptional level (Brown, 2005) and in plants these proteins have been described to participate in multiple developmental and adaptive processes (H. Deng, Liu, Li, Xiao, & Wang, 2012; Kim et al., 2008; Z. Kong et al., 2006; Z. Li & Thomas, 2007; P. C. Lin et al., 2011; Maldonado-bonilla et al., 2014; Sun et al., 2007). However, to date no report of the TZFs under study, except of TZF9, has communicated gene regulation upon PAMP elicitation. Hence, the results obtained in the current study support the hypothesis that the TZFs are involved in PAMP induced gene regulation.

4.2 Potential involvement of the TZFs in mRNA processing

4.2.1 Sub-cellular localization of the TZFs in cytoplasmic foci

Determination of the TZFs' sub-cellular localization may provide clues to the molecular functions of these proteins. The present study revealed a varied localization pattern of the TZFs when transiently expressed in *Arabidopsis* protoplast. The TZFs (TZF7-11) localized primarily in

cytoplasmic foci and also in the cytoplasm and/or nucleus (as depicted in **Fig.11**). The percentage of distribution for each of the TZFs as calculated in the observed protoplasts was nearly 50% (depicted in the pie-diagrams in **Fig.11 (A-E)**), with the exception of TZF8 and TZF10 with 70% and 90% localization respectively in the speckled structures. The observations from the current study slightly differ from previous reports, for example: all AtTZF gene family members (TZF1-11) localized to cytoplasmic foci (M. C. Pomeranz et al., 2010b). Other reports also depicted TZF1, TZF7, TZF9 and hTTP to shuttle between the nucleus and the cytoplasm upon treatment with cold, ABA, Leptomycin B, CHX or ActD (Blanvillain et al., 2011; Maldonado-bonilla et al., 2014; Phillips, Ramos, & Blackshear, 2002; M. C. Pomeranz et al., 2010b). Yet, other reports documented GhZFP1 (Cotton Zinc-finger Protein 1), OsTZF2 (Rice Tandem Zinc Finger 2), TZF1,TZF4 and TZF11 to be localized in the nucleus solely (Guo et al., 2009; Kim et al., 2008; Z. Kong et al., 2006; Sun et al., 2007). OsTZF1 (Rice Tandem Zinc Finger 1) was reported to localize in the nucleus and also in cytoplasmic foci (which increases in number upon treatment with ABA and salt) (A. et al., 2013).

The discrepancies in the various reports of the TZFs might result from different experimental setups. However, eventhough likely due to experimental setup differences, the localization patterns observed were similar in case of TZF9 when GFP was fused to either its C or N terminus (**Supplementary Fig.S1.2**). Additionally, generation of stable *Arabidopsis* lines expressing the fusion proteins at low levels can be used to indicate that the sub-cellular localizations observed in Arabidopsis protoplast are not artifacts caused by over-expression. The correct localization of mRNAs is important during development and, hence, localization of the TZFs in the nucleus (although a minor fraction) might suggest a role in processing of pre-mRNAs in the nucleus which is required for the recruitment of RNA-binding proteins determining the RNA's eventual localization in the cytoplasm (Giorgi & Moore, 2007). On the other hand, AtTZFs are nucleocytoplasmic shuttling proteins due to the presence of a leucine-rich nuclear export signal (NES) (D. Wang et al., 2008b) and this shuttling of the TZFs was reported to occur due to treatment with cold, ABA, Leptomycin B, CHX or ActD (Blanvillain et al., 2011; Maldonado-bonilla et al., 2014; M. C. Pomeranz et al., 2010b). The minor fraction of the TZFs localized in the nucleus in the present study might be a result of the stress on the protoplasts due to handling. As reported, hTTP is known to shuttle between the cytoplasm and the nucleus NES dependent manner, which describes its potential secondary role in transcriptional regulation (Phillips et al., 2002). Likewise, the same can be predicted with regard to TZF7 and TZF9, which were shown to shuttle between the cytoplasm and the nucleus (Blanvillain et al., 2011; Maldonado-bonilla et al., 2014). Also, UPF3, a shuttle protein operating in NMD, involves both nuclear-localized steps and a cytoplasmic-localized translation termination coupled step

(Shirley, Ford, Rachel Richards, Albertini, & Culbertson, 2002). In the present study, the TZFs localized primarily in cytoplasmic foci. Since hTTP and AtTZF1, have been shown to play dual roles in both transcriptional and post-transcriptional regulation (Phillips et al., 2002; M. C. Pomeranz et al., 2010b; Qu et al., 2014), the same can be hypothesized for the TZFs under study (those with both nuclear and cytoplasmic foci localization).

4.2.2 TZFs co-localize with P body and siRNA body markers

In the present study, TZF7-11 co-localized with various P body markers (DCP1, DCP2, XRN4, PARN and AGO1). However, the association observed was partial as depicted in **Fig.12 (A-E)**. Quantification of the proportion of TZF labeled bodies co-localizing with different P body markers is shown in the bar graphs in **Fig.12 (A-E).** The results obtained indicated that TZF7 co-localized with the markers *viz.* DCP1, DCP2, XRN4, PARN, AGO1 ranging from 10-70% average percent co-localization. Likewise, TZF8 showed nearly 30-60%, TZF9 nearly 40-70%, TZF10 and TZF11 each with about 30-50% average percent co-localization. In previous reports, similar co-localization patterns were observed. AtTZF1, 4, 5, 6 and 9, as well as rice OsTZF1 co-localized with the P body markers AGO1, DCP1, DCP2 and XRN4 (A. et al., 2013; Bogamuwa & Jang, 2013b; Maldonado-bonilla et al., 2014; M. C. Pomeranz et al., 2010b), supporting the results obtained in the present study. This co-localization of the TZFs with the P body markers suggests that the TZFs might be involved in the regulatory functions of P bodies, mainly comprising the RNA decay machinery. In this context, it has been reported that P bodies assemble when the 5′→3′ decay system is overloaded with RNA substrates or when mRNA decay is impaired (Cougot et al., 2004; Sheth & Parker, 2003).

On the other hand, TZF protein accumulating in cytoplasmic foci distinct to P bodies, might suggest co-localization with siRNA bodies, a second class of cytoplasmic granules (Jouannet et al., 2012b; Kumakura et al., 2009). Indeed, in **Fig.13 (A & B)**, the TZFs (TZF7-11) were observed to have partial association with the siRNA body markers, SGS3 and UPF1 (UPF1 in the present study is used as siRNA marker as this was reported to be equally associated with both siRNA and P bodies (Moreno et al., 2013)). The bar graphs in **Fig.13 (A & B)** depict the quantification of the proportion of TZF labeled bodies co-localizing with the two siRNA body markers. The results obtained indicated that TZF7 co-localized with the markers *viz.* SGS3 and UPF1 with nearly 50% average percent co-localization. Likewise, average co-localization percent in TZF8 was nearly 70%, TZF9 and TZF11 each with about 30-50%, TZF10 about 40-50%. No report till date has documented association of TZFs with siRNA bodies. Hence, these results suggest a role of TZF proteins in PTGS.

Thus, TZF proteins might have dual roles in RNA surveillance and RNA silencing. Reports on UPF1, CCR4a and PARN co-localizing with both P- and siRNA-body markers suggested the

exchange of RNA substrates between the two RNA degradation bodies (Moreno et al., 2013) and also might suggest the prevalence of tug-of-war between RNA quality control (RQC) and PTGS for correct partitioning of aberrant RNA substrates among the RNA degradation mechanisms (Christie, Brosnan, Rothnagel, & Carroll, 2011).

On the other hand, since the AtTZF proteins share high sequence homologies in their TZF regions and have similar sub-cellular localization patterns, each AtTZF protein may also have a similar molecular function with a distinct role in response to various developmental and environmental cues. AtTZF1, AtTZF9 and OsTZF1 can bind RNA *in vitro* (A. et al., 2013; Maldonado-bonilla et al., 2014; M. C. Pomeranz et al., 2010b). AtTZF1 can also bind to DNA *in vitro* (M. C. Pomeranz et al., 2010b) and can trigger mRNA decay in a sequence specific manner. *In vivo*, AtTZF1 was shown to be involved in the decay of AU rich elements (ARE)-containing mRNAs (Qu et al., 2014). AtTZF2 and AtTZF3 were reported to have RNase activity *in vitro* (Lee et al., 2012) and AtTZF7 was reported to bind DNA (Blanvillain et al., 2011). The Mammalian TTP binds class II AREs with the consensus sequence of UUAUUUAUU (Perry J. Blackshear et al., 2003). Hence, TZFs' association with the cytoplasmic mRNP granules might suggest RNA or DNA binding activities also for the other TZFs (TZF8, TZF10 and TZF11).

4.2.3 TZFs interact with SG components

An interesting observation in the present study was that the TZFs associated partially with the SG components, PAB2 and PAB8, even without any stress stimulus (as shown in **Fig.14 (B & E)**). This finding differs from the previously reported TZFs' (TZF1, TZF4, TZF5 and TZF6) association with SG components only after heat stress (Bogamuwa & Jang, 2013b; M. C. Pomeranz et al., 2010b). Rice OsTZF1 also co-localized with SG markers and ABA and salt treatment enhanced the assembly of cytoplasmic foci, indicating a stress-inducible SG assembly (A. et al., 2013). As also shown in **Fig.14** (**A & D), right panel**, cytoplasmic PAB2 and PAB8 are aggregating in granules upon heat stress (**Fig.14** (**A & D), left panel**). Additionally, co-localization analyses of the TZFs with the PABs revealed that cytoplasmic granules were formed regardless of heat treatment (**Fig.14 (B & E)**).The quantification of the association indicated that in all the cases (be it with PAB2 or PAB8 co-transformation with the TZFs) (**Fig.14 (C & F)**), heat stress induced higher rates of average percent co-localization (except that in TZF7 and PAB2, association after heat treatment decreased nearly 10%). For the rest other associations, increment was nearly 10-50%. This might suggest that heat stress induced an increment in the association of the TZFs with the PABs or an increased PABs' aggregation after heat treatment.

Based on the results obtained, it can be hypothesized that the TZFs are involved in recruiting target mRNAs bound to PABs into the granule structures. Hence, to ascertain the nature of the PAB containing structures under basal conditions, triple localization experiments were

conducted. These experiments revealed that, when DCP1, a P body marker was co-expressed, the partially associated TZFs and PABs were also associated with DCP1 both with and without heat stress (partial association) (**Fig.15 (A & B)**). Thus, it can be speculated that the non heat inducible granule formation in the PABs in the presence of TZFs recruits the PABs into P bodies influencing their functions.

The association of the TZFs with the PABs and the altered localization of the PABs in the presence of the TZFs also suggest that they might interact with each other. Split YFP experiments revealed that PABs do interact with all the five TZFs in the cytoplasm and notably also in foci (**Fig.17 (A & B)**). These interactions were also observed after heat stress with increment in the number of speckles, suggesting further formation of stress granules containing TZF-PAB complexes. Additionally, inclusion of DCP1 in the split YFP assay revealed that the speckled split-YFP signals resulting from interaction between the PABs and the TZFs co-localize with CFP-labeled DCP1 (**Fig.18 (A & B)**). However, from split-YFP-based interaction assays, this interaction between the TZFs and the PABs was independent of direct interaction of DCP1 with TZFs or PABs (**Fig.19 (A & B)**).

TTP has been reported to localize in P bodies and SG, transiently docking with one another during arsenite treatment (Nancy Kedersha et al., 2005). In yeast, SG form in conjunction and partially overlap with, P bodies (Brengues & Parker, 2007; Buchan, Muhlrad, & Parker, 2008; Grousl et al., 2009; Hoyle, Castelli, Campbell, Holmes, & Ashe, 2007). It is interesting to note that P bodies and SG share many protein components (eIF4E, XRN1 and FAST) and the same mRNA species (Hoyle et al., 2007; Nancy Kedersha et al., 2005). And, SG interaction with P bodies results in exchange of mRNPs suggesting a cytoplasmic mRNP cycle (Parker & Sheth, 2007). Some reports state that P bodies form first, followed by SG formation, which initially co-localize with pre-existing P bodies (Buchan et al., 2008; Hoyle et al., 2007). But not all SG in mammalian cells have been reported to form in association with P bodies (Mollet et al., 2008), although other reports suggest that SG and P bodies may form with similar kinetics (Nancy Kedersha et al., 2005; Ohn, Kedersha, Hickman, Tisdale, & Anderson, 2008). In *Arabidopsis*, it has been reported from localization analyses of marker proteins that P body, SG and Heat Shock Protein (HSP) structures are morphologically and physically distinct; having different kinetics for their formation and harbouring characteristic proteins (Weber, Nover, & Fauth, 2008b).

As reported, mRNAs within P bodies can return to translation (Bhattacharyya, Habermacher, Martine, Closs, & Filipowicz, 2006; Brengues, Teixeira, & Parker, 2005) or accumulate within a SG. This implies the role of P bodies in mRNP sorting: whether an mRNA is stored, degraded, or

returns to translation. Also, SG are formed due to overexpression of RNA-binding proteins that repress translation (De Leeuw et al., 2007; Gilks, 2004; Nancy Kedersha et al., 2005; Wilczynska, A., Aigueperse, C., Kress, M., Dautry, F., Weil, D., 2005) and additionally, many signaling proteins recruited to SGs also influence their assembly transiently (Nancy Kedersha, Ivanov, & Anderson, 2013b). Heat stress results in translational reprogramming of the housekeeping mRNPs (Belanger, Brodl, & Ho, 2006) and sequestering of these mRNPs to P Bodies and SGs might result in a change in gene expression patterns resulting from changed environmental conditions. As reported, cytoplasmic siRNA bodies also form SG under heat-shock conditions (Jouannet et al., 2012b). Hence, based on the results obtained in the current study, from both co-localization and interaction assays, it can be hypothesized that TZFs might tether into different cytoplasmic granule structures based on the environmental conditions and thereby, might either influence their functions or play a potential role in post-transcriptional regulation (similar to the functions of the P bodies, siRNA bodies and SG).

4.3 TZFs are MAPK substrates

4.3.1 TZFs' possible involvement in PTI

Previous studies described TZF7 and TZF9 as targets of PAMP activated MAPKs, MPK3 and MPK6 (Feilner et al., 2005; Hoehenwarter et al., 2013; Lassowskat et al., 2014). In the present study, TZF7 was validated to be a MAPK substrate by both *in vitro* (kinase assays **Fig.21**) and *in vivo* approaches (phospho shift assays and BiFC assays **Fig.22-24**). Similar experiments conducted on TZF8, TZF10 and TZF11, revealed that these are also phospho-targets of MPKs (**Fig.21-24**). In *in vitro* kinase assays, TZF7, TZF8, TZF10 and TZF11 were observed to be substrates of MPK3/4/6 with the exception of TZF10 being the substrate of MPK3 and MPK4, but not MPK6 (**Fig.21**). TZF9 was confirmed to be an MPK3/6 substrate and interaction studies revealed its interaction with MPK3 and MPK6 in both the cytoplasm and the nucleus (Maldonado-bonilla et al., 2014). However, TZF10 was previously reported to be phosphorylated *in vitro* by the calcium-dependent protein kinase, CPK3 (Kanchiswamy et al., 2010), but till date CPK3 activation by flg22 was not shown.

Bimolecular fluorescence complementation (BiFC) assays were performed in protoplasts to determine the *in vivo* phosphorylation of TZFs by MAPKs, co-expressing TZFs (TZF7-11) and MPKs (**Fig.24**). Interaction was observed primarily in the cytoplasm, cytoplasmic foci and in some cases, also in the nucleus (**Fig.24 (A-E)**). No reconstituted YFP signals were seen in the negative controls used for the BiFC assays, highlighting the specificity of the TZF-MPK interactions. In a second approach, based on western blot, phosphorylation-dependent mobility shifts upon elicitation with flg22 were monitored in protoplast transiently expressing epitope-

tagged TZFs (**Fig.22**). In elicited samples, a reduced mobility of the TZF proteins was observed (**Fig.22**), which was abolished after λ-phosphatase treatment of the extracted proteins, indicating that the band shifts were solely based on phosphorylation (**Fig.23**). As shown in **Fig.23,** TZF9 and TZF10 have shown a different mobility also in the non-elicited protoplasts (possibly due to basal phosphorylation) and a higher mobility shift after 10 min of flg22 treatment. Together with this observation and the previous report of TZF10 being phosphorylated by CPK3 (Kanchiswamy et al., 2010), it raises the possibility that both TZF9 and TZF10 might be phosphorylated by other kinases as well. Additionally, P body components such as the mRNA decapping complex proteins, DCP1 and VCS and the exoribonuclease, XRN4, are reported to be phosphorylated by MPKs (Lassowskat et al., 2014; Jun Xu & Chua, 2012). In the current study, the TZFs co-localize with the various P body components and have been validated to be MAPK substrates. It might be hypothesized that MAPKs affect post-transcriptional gene regulation through elements of mRNA processing in P bodies. Hence, the results suggest TZFs' phospho-modification after PAMP treatment by cellular kinases and also hints at their contribution to cellular signaling induced by PAMPs. This opens up a future research on identification and mapping of the phospho-sites of the TZFs to elucidate the impact of phosphorylation on TZF's function.

4.3.2 TZF localization is altered upon PAMP elicitation

PAMP/flg22 elicitation was applied to analyze for changes in size, quantity or distribution of the speckled structures within the cell. In the present study, TZFs' localization was observed primarily in cytoplasmic foci in transiently expressed TZFs in protoplasts (**Fig.11**) and flg22 treatment induced changes in the cytoplasmic foci within 15 mins (**Fig.20**). However, different patterns of transient reduction or fusion or reappearance of the TZF-labeled speckled structures were observed as shown in **Fig.20 (A-E)** and in the summarized **Table.20 (F)**. In TZF7, about 67% of the protoplasts were responsive to flg22 treatment and have shown changes in localization. Likewise, 77% of TZF8, and TZF9, 10 and 11 with 88% of localization changes in the observed protoplasts upon flg22 treatment. These results were in contrast to the previously reported PAT1 relocalization to P bodies after MAPK phosphorylation as part of cellular reprogramming (Roux et al., 2015). Yet, in another report, treatment of mesophyll protoplasts with cycloheximide led to a marked reduction in size, whereas different stress conditions (hypoxia, heat stress) led to an increase in the size and number of DCP1-containing cytoplasmic foci (Goeres et al., 2007b; Weber et al., 2008b). In additional studies, upon treatment with cold, ABA, Leptomycin B, CHX or ActD, led to relocalization of TZF1, TZF7 and TZF9 from cytoplasmic foci to the nucleus (Blanvillain et al., 2011; Maldonado-bonilla et al., 2014; M. C. Pomeranz et al., 2010b).

Generally, in plants and mammalian cells, treatment with cycloheximide inhibits the assembly of P bodies and also prevents the formation of SGs (Nancy Kedersha et al., 2005; Weber et al., 2008b). In the present study, the results suggest that PAMP elicitation alters the localization of the TZFs from cytoplasmic foci to the cytoplasm to mediate defense-related functions instead of involving TZFs in the RNA decay pathway. Previous reports state that formation of P bodies is dependent on the availability of targeted mRNAs and these P bodies substantially decrease in size and number or disappear when the amount of mRNA to be decayed is reduced. The changes in the size and number of P bodies depends on the status of the cellular translation machinery (since the mechanisms of translation and degradation of mRNA compete with each other) (Caponigro & Parker, 1996; Khanna & Kiledjian, 2004; Ramirez, Vilela, Berthelot, & McCarthy, 2002; Schwartz & Parker, 2000; Sheth & Parker, 2003; Teixeira, Sheth, Valencia-Sanchez, Brengues, & Parker, 2005). Hence, taken together, it can be speculated that phosphorylation state is a determinant for the protein to localize within or outside of the cytoplasmic foci. However, it should be taken into account that, since all the experiments were performed in protoplast, it may not reflect the *in planta* situation resulting from slight changes in the environmental conditions. Thus, it would be important to confirm the results obtained using stable transgenic lines.

4.4 TZFs' role in plant stress responses

In the present context, similar sub-cellular localization patterns in the TZFs (TZF7-11) were observed suggesting each TZF may have a similar molecular function. To gain insight in TZFs' function, a reverse genetic approach was used applying PAMP and ABA treatment. ABA was used as an additional treatment since ABA plays a crucial role in drought, cold, etc. stresses.

Upon constant exposure to PAMP, plant development is impaired and root growth is inhibited (Ranf et al., 2011). This effect was used to obtain a quantitative effect of PAMP-mediated response in plants. From the PAMP-induced root growth inhibition assay, only for *tzf9* mutant, a statistically significant growth phenotype compared with *Col-0* was observed (less root growth inhibition). For all the other tested TZF single mutants as well as the quadruple (*tzf7tzf8tzf9tzf10*) and penta (*tzf7tzf8tzf9tzf10tzf11*) mutants, no growth phenotype was observed (**Fig.26**). The higher order mutants (quadruple and penta mutants) containing additional TZF mutations may suppress the growth phenotype of *tzf9* mutation. As previously reported, besides late responses such as PAMP induced growth arrest, *tzf9* knockout mutant was attenuated in PAMP-induced early signaling events, with reduced ROS accumulation, MAPK activation and expression of two PAMP-responsive genes, *FRK1* and *NHL10* after flg22 treatment. Additionally, *tzf9* mutant has

shown enhanced susceptibility to *Pseudomonas syringae* pv. *tomato* DC3000 (Maldonado-bonilla et al., 2014).

It is well established that ABA induces seed dormancy and hence, results in suppressed or delayed germination of seeds (AbuQamar et al., 2006; Saez et al., 2006). In the present context, root growth inhibition assays were performed and the *tzf* mutants depicted more sensitivity to ABA with severe yellowing and impaired growth of both leaves and roots (**Fig.27**). In comparison with *Col-0*, *tzf10* and the *tzf10tzf11* double mutants developed strongly enhanced yellowing of leaves in presence of ABA. Hence, it might suggest that *tzf10* mutant has presumably a dominant role in the sensitivity to ABA with regard to leaf yellowing in the double, quadruple and penta mutant.

Previous reports documented TZF proteins' crucial roles in response to environmental cues. AtTZF1 was reported as a positive regulator of ABA/sugar responses and a negative regulator of GA responses and its overexpression resulted in late flowering and enhanced tolerance to cold and drought stress (P. C. Lin et al., 2011). *AtTZF2* and *AtTZF3* expression is induced by ABA and abiotic stresses such as salt, mannitol and cold (Huang et al., 2011b; Lee et al., 2012). Also, AtTZF3 is described as a negative regulator of seed germination in the presence of NaCl and ABA (Gupta et al., 2016). AtTZF4, AtTZF5 and AtTZF6 act as negative regulators of light-dependent seed germination, loss-of-function mutants are characterized by reduced levels of ABA and elevated levels of GA (Bogamuwa & Jang, 2013b; Kim et al., 2008). AtTZF6 is involved in embryogenesis (Z. Li & Thomas, 2007) and AtTZF7 (OXS2) is described to have multiple roles in regulating vegetative growth, to activate stress tolerance and to involve in stress-induced flowering (Blanvillain et al., 2011). Both AtTZF10 and AtTZF11 act as positive regulators of salt tolerance (Sun et al., 2007) and *zfar1* or *tzf10* mutants are more susceptible to the necrotrophic pathogen, *Botrytis cinerea*, and are also hypersensitive to ABA in germination assays (AbuQamar et al., 2006). In rice, *OsTZF1* expression is positively regulated by polyethylene glycol and ABA, and its overexpression conferred hypersensitivity to ABA (Cheng Zhang et al., 2012). Furthermore, it is involved in seed germination, seedling growth, leaf senescence, and oxidative-stress tolerance (A. et al., 2013; Z. Kong et al., 2006). GhZFP1, a CCCH-type zinc finger protein from cotton, confers enhanced tolerance to salt stress and fungal disease resistance to *Rhizoctonia solani* (Guo et al., 2009).

The previous reports on the TZF proteins illustrate their role mostly in abiotic stress responses and also TZF9 and 10, and GhZFP1 having a role in biotic stress responses as well (AbuQamar et al., 2006; Guo et al., 2009; Maldonado-bonilla et al., 2014). The current study provides

evidence of involvement of TZF7, TZF8, TZF10 and TZF11 in PTI and also in response to ABA signaling, implying that the TZFs might have a role in abiotic stress responses.

5. Summary

PAMP induced gene expression and phosphorylation by the PAMP-responsive MAPKs of the TZFs (TZF7-11), indicates possible roles of TZFs in cellular signaling triggered by PAMPs. Transient expression of the TZFs in *Arabidopsis* mesophyll protoplasts showed localization of the TZFs in cytoplasm and/or nucleus, with a high percentage of the TZFs in cytoplasmic foci. The nature of the foci was evaluated with established marker proteins of P-body, siRNA body and SG. Strong-to-partial co-localization of the TZFs was observed with the respective markers. Surprisingly, co-expression with TZFs caused constitutive stress granule formation of PAB2 and PAB8 even in the absence of stress, which hints at a possible recruitment of the target mRNAs bound to PABs by the TZFs via interaction, thereby resulting in a change in the functions of the PABs at room temperature. As such, TZFs' association with the different markers suggests a potential role of all the five TZFs under study in post-transcriptional regulation (i.e. mRNA decay/storage or translational arrest; see pictorial representation in **Fig.28**). Upon PAMP elicitation, changes in the localization of the TZFs (disappearance or reappearance after transient reduction at an early time point or fusion until a certain time point of the TZFs compartmentalized in cytoplasmic foci) was observed, suggesting an alteration in the functions of the TZFs (possibly decreased rate of translational arrest, which is otherwise occurring in the cytoplasmic foci). Mutant analysis indicates that the quadruple and the penta mutants show hypersensitive responses to abscisic acid (ABA) induced root growth inhibition, with TZF10 being the dominant player with respect to the severe yellowing of leaves in the presence of ABA. And only *tzf9* was observed to have attenuated PAMP induced defense responses.
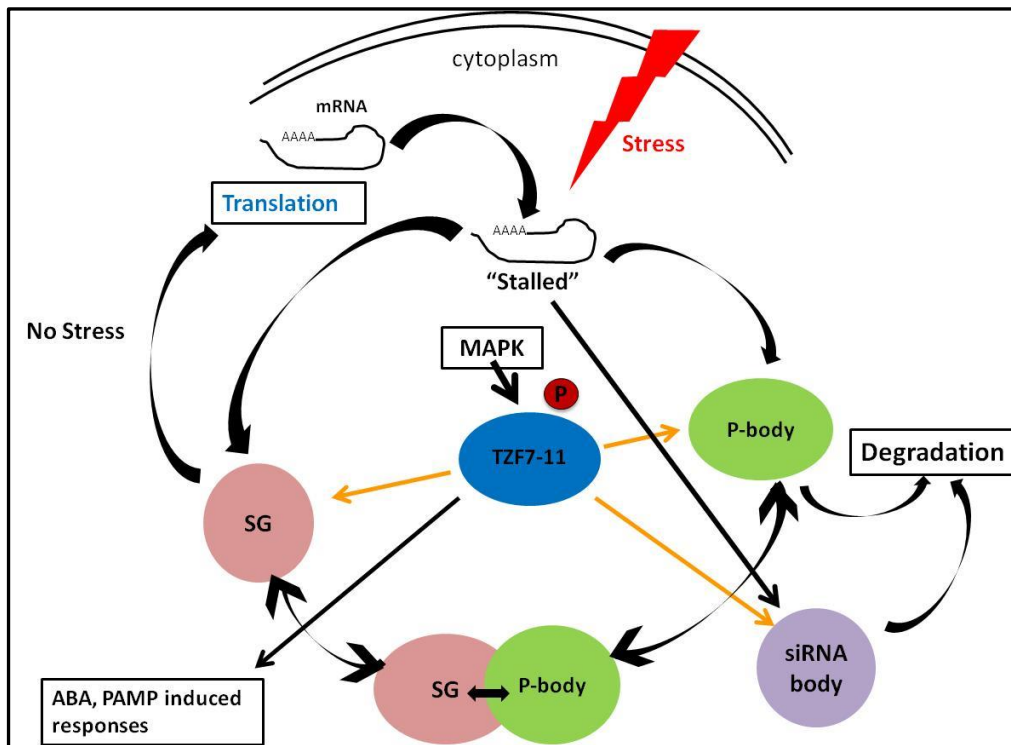
Fig.28 Involvement of TZF7-11 in post-transcriptional regulation.

The model above shows involvement of the TZFs in post-transcriptional regulation as depicted by TZFs' association with the different marker proteins (as shown with arrows in orange) (i.e. the stalled or repressed mRNAs due to the presence of stress, might either be degraded in P bodies/siRNA bodies or the repressed mRNAs might be stored in the stress granules until the stress is released to further enter the translational machinery to be translated). On the other hand, TZFs' are being phosphorylated by PAMP-responsive MAPKs (shown by both *in vitro* and *in vivo* experiments) and organizational changes with regard to the change in the number and (or) distribution of the speckled structures was observed in the TZFs. Mutant analysis have shown ABA/PAMP induced growth responses in the TZFs.

6. References

A., J., K., M., D., T., S., K., M., A., E., Y., … K., Y.-S. (2013). OsTZF1, a CCCH-tandem zinc finger protein, confers delayed senescence and stress tolerance in rice by regulating stress-related genes. *Plant Physiology*. https://doi.org/10.1104/pp.112.205385

AbuQamar, S., Chen, X., Dhawan, R., Bluhm, B., Salmeron, J., Lam, S., … Mengiste, T. (2006). Expression profiling and mutant analysis reveals complex regulatory networks involved in Arabidopsis response to Botrytis infection. *Plant Journal*, *48*(1), 28–44. https://doi.org/10.1111/j.1365-313X.2006.02849.x

Ahrens, S., Zelenay, S., Sancho, D., Hanč, P., Kjær, S., Feest, C., … Schulz, O. (2012). F-Actin Is an Evolutionarily Conserved Damage-Associated Molecular Pattern Recognized by DNGR-1, a Receptor for Dead Cells. *Immunity*. https://doi.org/10.1016/j.immuni.2012.03.008

Ahuja, I., Kissen, R., & Bones, A. M. (2012). Phytoalexins in defense against pathogens. *Trends in Plant Science*. https://doi.org/10.1016/j.tplants.2011.11.002

Albert, M. (2013). Peptides as triggers of plant defence. *Journal of Experimental Botany*. https://doi.org/10.1093/jxb/ert275

Altenbach, D., & Robatzek, S. (2007). Pattern Recognition Receptors: From the Cell Surface to Intracellular Dynamics. *Molecular Plant-Microbe Interactions*. https://doi.org/10.1094/mpmi-20-9-1031

Amrani, N., Ghosh, S., Mangus, D. A., & Jacobson, A. (2008). Translation factors promote the formation of two states of the closed-loop mRNP. *Nature*. https://doi.org/10.1038/nature06974

Anderson, P., & Kedersha, N. (2006). RNA granules. *Journal of Cell Biology*. https://doi.org/10.1083/jcb.200512082

Anderson, P., & Kedersha, N. (2009). RNA granules: Post-transcriptional and epigenetic modulators of gene expression. *Nature Reviews Molecular Cell Biology*. https://doi.org/10.1038/nrm2694

Andreasson, E., & Ellis, B. (2010). Convergence and specificity in the Arabidopsis MAPK nexus. *Trends in Plant Science*. https://doi.org/10.1016/j.tplants.2009.12.001

Andreasson, E., Jenkins, T., Brodersen, P., Thorgrimsen, S., Petersen, N. H. T., Zhu, S., … Mundy, J. (2005). The MAP kinase substrate MKS1 is a regulator of plant defense responses. *EMBO Journal*. https://doi.org/10.1038/sj.emboj.7600737

Andrei, M. A., Ingelfinger, D., Heintzmann, R., Achsel, T., Rivera-Pomar, R., & Lührmann, R. (2005). A role for eIF4E and eIF4E-transporter in targeting mRNPs to mammalian processing bodies. *RNA*. https://doi.org/10.1261/rna.2340405

Arnaud, D., Déjardin, A., Leplé, J. C., Lesage-Descauses, M. C., & Pilate, G. (2007). Genome-wide analysis of LIM gene family in populus trichocarpa, arabidopsis thaliana, and oryza sativa. *DNA Research*. https://doi.org/10.1093/dnares/dsm013

Asai, T., Tena, G., Plotnikova, J., Willmann, M. R., Chiu, W. L., Gomez-Gomez, L., … Sheen, J. (2002). Map kinase signalling cascade in Arabidopsis innate immunity. *Nature*. https://doi.org/10.1038/415977a

Ausubel, F. M. (2005). Are innate immune signaling pathways in plants and animals conserved? *Nature Immunology*. https://doi.org/10.1038/ni1253

Bartels, S., Lori, M., Mbengue, M., Verk, M. Van, Klauser, D., Hander, T., … Boller, T. (2013). The family of peps and their precursors in arabidopsis: Differential expression and localization but similar induction of pattern-Triggered immune responses. *Journal of Experimental Botany*, *64*, 5309–5321. https://doi.org/10.1093/jxb/ert330

Bashkirov, V. I., Scherthan, H., Solinger, J. A., Buerstedde, J. M., & Heyer, W. D. (1997). A mouse cytoplasmic exoribonuclease (mXRN1p) with preference for G4 tetraplex substrates. *Journal of Cell Biology*. https://doi.org/10.1083/jcb.136.4.761

Beck, M., Komis, G., Müller, J., Menzel, D., & Šamaj, J. (2010). Arabidopsis Homologs of Nucleus- and Phragmoplast-Localized Kinase 2 and 3 and Mitogen-Activated Protein Kinase 4 Are Essential for Microtubule Organization . *The Plant Cell*. https://doi.org/10.1105/tpc.109.071746

Bednarek, P. (2012). Chemical warfare or modulators of defence responses - the function of secondary metabolites in plant immunity. *Current Opinion in Plant Biology*. https://doi.org/10.1016/j.pbi.2012.03.002

Belanger, F. C., Brodl, M. R., & Ho, T. H. (2006). Heat shock causes destabilization of specific mRNAs and destruction of endoplasmic reticulum in barley aleurone cells. *Proceedings of the National Academy of Sciences*. https://doi.org/10.1073/pnas.83.5.1354

Belostotsky, D. (2004). MRNA turnover meets RNA interference. *Molecular Cell*. https://doi.org/10.1016/j.molcel.2004.11.010

Belostotsky, D. A., & Sieburth, L. E. (2009). Kill the messenger: mRNA decay and plant development. *Current Opinion in Plant Biology*. https://doi.org/10.1016/j.pbi.2008.09.003

Benschop, J. J., Mohammed, S., O'Flaherty, M., Heck, A. J. R., Slijper, M., & Menke, F. L. H. (2007). Quantitative Phosphoproteomics of Early Elicitor Signaling in Arabidopsis . *Molecular & Cellular Proteomics*. https://doi.org/10.1074/mcp.m600429-mcp200

Bethke, G., Unthan, T., Uhrig, J. F., Poschl, Y., Gust, A. A., Scheel, D., & Lee, J. (2009). Flg22 regulates the release of an ethylene response factor substrate from MAP kinase 6 in Arabidopsis thaliana via ethylene signaling. *Proceedings of the National Academy of Sciences*. https://doi.org/10.1073/pnas.0810206106

Bevilacqua, A., Ceriani, M. C., Capaccioli, S., & Nicolin, A. (2003). Post-transcriptional regulation of gene expression by degradation of messenger RNAs. *Journal of Cellular Physiology*. https://doi.org/10.1002/jcp.10272

Bhattacharyya, S. N., Habermacher, R., Martine, U., Closs, E. I., & Filipowicz, W. (2006). Relief of microRNA-Mediated Translational Repression in Human Cells Subjected to Stress. *Cell*. https://doi.org/10.1016/j.cell.2006.04.031

Bigeard, J., Colcombet, J., & Hirt, H. (2015). Signaling mechanisms in pattern-triggered immunity (PTI). *Molecular Plant*, *8*(4), 521–539. https://doi.org/10.1016/j.molp.2014.12.022

Blackshear, P. J. (2002). Tristetraprolin and other CCCH tandem zinc-finger proteins in the regulation of mRNA turnover. *Biochemical Society Transactions*. https://doi.org/10.1042/bst0300945

Blackshear, Perry J., Lai, W. S., Kennington, E. A., Brewer, G., Wilson, G. M., Guan, X., & Zhou, P. (2003). Characteristics of the interaction of a synthetic human tristetraprolin tandem zinc finger peptide with AU-rich element-containing RNA substrates. *Journal of Biological Chemistry*.

https://doi.org/10.1074/jbc.M301290200

Blanvillain, R., Wei, S., Wei, P., Kim, J. H., & Ow, D. W. (2011). Stress tolerance to stress escape in plants: Role of the OXS2 zinc-finger transcription factor family. *EMBO Journal*, *30*(18), 3812–3822. https://doi.org/10.1038/emboj.2011.270

Bogamuwa, S., & Jang, J. C. (2013a). The Arabidopsis tandem CCCH zinc finger proteins AtTZF4, 5 and 6 are involved in light-, abscisic acid- and gibberellic acid-mediated regulation of seed germination. *Plant, Cell and Environment*, *36*(8), 1507–1519. https://doi.org/10.1111/pce.12084

Bogamuwa, S., & Jang, J. C. (2013b). The Arabidopsis tandem CCCH zinc finger proteins AtTZF4, 5 and 6 are involved in light-, abscisic acid- and gibberellic acid-mediated regulation of seed germination. *Plant, Cell and Environment*, *36*, 1507–1519. https://doi.org/10.1111/pce.12084

Böhm, H., Albert, I., Oome, S., Raaymakers, T. M., Van den Ackerveken, G., & Nürnberger, T. (2014). A Conserved Peptide Pattern from a Widespread Microbial Virulence Factor Triggers Pattern-Induced Immunity in Arabidopsis. *PLoS Pathogens*. https://doi.org/10.1371/journal.ppat.1004491

Boller, T., & Felix, G. (2009). A Renaissance of Elicitors: Perception of Microbe-Associated Molecular Patterns and Danger Signals by Pattern-Recognition Receptors. *Annual Review of Plant Biology*, *60*, 379–406. https://doi.org/10.1146/annurev.arplant.57.032905.105346

Brengues, M., & Parker, R. (2007). Accumulation of Polyadenylated mRNA, Pab1p, eIF4E, and eIF4G with P-Bodies in Saccharomyces cerevisiae . *Molecular Biology of the Cell*. https://doi.org/10.1091/mbc.e06-12-1149

Brengues, M., Teixeira, D., & Parker, R. (2005). Cell biology: Movement of eukaryotic mRNAs between polysomes and cytoplasmic processing bodies. *Science*. https://doi.org/10.1126/science.1115791

Brown, R. S. (2005). Zinc finger proteins: Getting a grip on RNA. *Current Opinion in Structural Biology*. https://doi.org/10.1016/j.sbi.2005.01.006

Buchan, J. R., Muhlrad, D., & Parker, R. (2008). P bodies promote stress granule assembly in Saccharomyces cerevisiae. *Journal of Cell Biology*. https://doi.org/10.1083/jcb.200807043

Cao, Y., Liang, Y., Tanaka, K., Nguyen, C. T., Jedrzejczak, R. P., Joachimiak, A., & Stacey, G. (2014). The kinase LYK5 is a major chitin receptor in Arabidopsis and forms a chitin-induced complex with related kinase CERK1. *ELife*. https://doi.org/10.7554/eLife.03766

Caponigro, G., & Parker, R. (1996). mRNA turnover in yeast promoted by the MATα1 instability element. *Nucleic Acids Research*. https://doi.org/10.1093/nar/24.21.4304

Carrick, D. M., Lai, W. S., & Blackshear, P. J. (2004). The tandem CCCH zinc finger protein tristetraprolin and its relevance to cytokine mRNA turnover and arthritis. *Arthritis Research and Therapy*. https://doi.org/10.1186/ar1441

Carthew, R. W., & Sontheimer, E. J. (2009). Origins and Mechanisms of miRNAs and siRNAs. *Cell*. https://doi.org/10.1016/j.cell.2009.01.035

Chai, G., Hu, R., Zhang, D., Qi, G., Zuo, R., Cao, Y., … Zhou, G. (2012). Comprehensive analysis of CCCH zinc finger family in poplar (Populus trichocarpa). *BMC Genomics*. https://doi.org/10.1186/1471-2164-13-253

Chantarachot, T., & Bailey-Serres, J. (2018). Polysomes, Stress Granules, and Processing Bodies: A Dynamic Triumvirate Controlling Cytoplasmic mRNA Fate and Function. *Plant Physiology*. https://doi.org/10.1104/pp.17.01468

Chen, C. Y. A., & Shyu, A. Bin. (1995). AU-rich elements: characterization and importance in mRNA degradation. *Trends in Biochemical Sciences*. https://doi.org/10.1016/S0968-0004(00)89102-1

Chen, C. Y. A., & Shyu, A. Bin. (2013). Deadenylation and P-bodies. *Advances in Experimental Medicine and Biology*. https://doi.org/10.1007/978-1-4614-5107-5-11

Chen, C. Y., Gherzi, R., Ong, S. E., Chan, E. L., Raijmakers, R., Pruijn, G. J. M., … Karin, M. (2001). AU binding proteins recruit the exosome to degrade ARE-containing mRNAs. *Cell*. https://doi.org/10.1016/S0092-8674(01)00578-5

Chen, X. (2008). A Silencing Safeguard: Links between RNA Silencing and mRNA Processing in Arabidopsis. *Developmental Cell*. https://doi.org/10.1016/j.devcel.2008.05.012

Chen, X. (2012). Small RNAs in development - insights from plants. *Current Opinion in Genetics and Development*. https://doi.org/10.1016/j.gde.2012.04.004

Chiba, Y., & Green, P. J. (2009). mRNA degradation machinery in plants. *Journal of Plant Biology*. https://doi.org/10.1007/s12374-009-9021-2

Chiba, Y., Johnson, M. A., Lidder, P., Vogel, J. T., Van Erp, H., & Green, P. J. (2004). AtPARN is an essential poly(A) ribonuclease in Arabidopsis. *Gene*. https://doi.org/10.1016/j.gene.2003.11.028

Chinchilla, D., Shan, L., He, P., de Vries, S., & Kemmerling, B. (2009). One for all: the receptor-associated kinase BAK1. *Trends in Plant Science*. https://doi.org/10.1016/j.tplants.2009.08.002

Chinchilla, D., Zipfel, C., Robatzek, S., Kemmerling, B., Nürnberger, T., Jones, J. D. G., … Boller, T. (2007). A flagellin-induced complex of the receptor FLS2 and BAK1 initiates plant defence. *Nature*, *448*(July), 497–500. https://doi.org/10.1038/nature05999

Christie, M., Brosnan, C. A., Rothnagel, J. A., & Carroll, B. J. (2011). RNA Decay and RNA Silencing in Plants: Competition or Collaboration? *Frontiers in Plant Science*. https://doi.org/10.3389/fpls.2011.00099

Cougot, N., Babajko, S., & Séraphin, B. (2004). Cytoplasmic foci are sites of mRNA decay in human cells. *Journal of Cell Biology*. https://doi.org/10.1083/jcb.200309008

Cowan, M. M. (1999). Plant products as antimicrobial agents. *Clinical Microbiology Reviews*.

Cui, H., Tsuda, K., & Parker, J. E. (2014). Effector-Triggered Immunity: From Pathogen Perception to Robust Defense. *Annual Review of Plant Biology*. https://doi.org/10.1146/annurev-arplant-050213-040012

Dalmay, T., Hamilton, A., Rudd, S., Angell, S., & Baulcombe, D. C. (2000). An RNA-dependent RNA polymerase gene in arabidopsis is required for posttranscriptional gene silencing mediated by a transgene but not by a virus. *Cell*. https://doi.org/10.1016/S0092-8674(00)80864-8

Dang, Y., Kedersha, N., Low, W. K., Romo, D., Gorospe, M., Kaufman, R., … Liu, J. O. (2006). Eukaryotic initiation factor 2α-independent pathway of stress granule induction by the natural product pateamine A. *Journal of Biological Chemistry*. https://doi.org/10.1074/jbc.M606149200

De Alba, A. E. M., Moreno, A. B., Gabriel, M., Mallory, A. C., Christ, A., Bounon, R., … Maizel, A. (2015). In plants, decapping prevents RDR6-dependent production of small interfering RNAs from endogenous mRNAs. *Nucleic Acids Research*. https://doi.org/10.1093/nar/gkv119

De, J., Lai, W. S., Thorn, J. M., Goldsworthy, S. M., Liu, X., Blackwell, T. K., & Blackshear, P. J. (1999). Identification of four CCCH zinc finger proteins in Xenopus, including a novel vertebrate protein with four zinc fingers and severely restricted expression. *Gene*. https://doi.org/10.1016/S0378-1119(98)00617-9

De Leeuw, F., Zhang, T., Wauquier, C., Huez, G., Kruys, V., & Gueydan, C. (2007). The cold-inducible RNA-binding protein migrates from the nucleus to cytoplasmic stress granules by a methylation-dependent mechanism and acts as a translational repressor. *Experimental Cell Research*. https://doi.org/10.1016/j.yexcr.2007.09.017

Decker, C. J., & Parker, R. (1993). A turnover pathway for both stable and unstable mRNAs in yeast: Evidence for a requirement for deadenylation. *Genes and Development*. https://doi.org/10.1101/gad.7.8.1632

Deng, H., Liu, H., Li, X., Xiao, J., & Wang, S. (2012). A CCCH-Type Zinc Finger Nucleic Acid-Binding Protein Quantitatively Confers Resistance against Rice Bacterial Blight Disease. *Plant Physiology*. https://doi.org/10.1104/pp.111.191379

Deng, X., & Cao, X. (2017). Roles of pre-mRNA splicing and polyadenylation in plant development. *Current Opinion in Plant Biology*, *35*, 45–53. https://doi.org/10.1016/j.pbi.2016.11.003

Dodds, P. N., & Rathjen, J. P. (2010). Plant immunity: Towards an integrated view of plantâ€" pathogen interactions. *Nature Reviews Genetics*. https://doi.org/10.1038/nrg2812

DuBois, R. N., McLane, M. W., Ryder, K., Lau, L. F., & Nathans, D. (1990). A growth factor-inducible nuclear protein with a novel cysteine/histidine repetitive sequence. *Journal of Biological Chemistry*.

Dupressoir, A., Morel, A. P., Barbot, W., Loireau, M. P., Corbo, L., & Heidmann, T. (2001). Identification of four families of yCCR4- and Mg2+ -dependent endonuclease-related proteins in higher eukaryotes, and characterization of orthologs of yCCR4 with a conserved leucine-rich repeat essential for hCAFI/hPOP2 binding. *BMC Genomics*. https://doi.org/10.1186/1471-2164-2-9

Dyson, M. R., Shadbolt, S. P., Vincent, K. J., Perera, R. L., & McCafferty, J. (2004). Production of soluble mammalian proteins in Escherichia coli: Identification of protein features that correlate with successful expression. *BMC Biotechnology*. https://doi.org/10.1186/1472-6750-4-32

Eschen-Lippold, L., Bethke, G., Palm-Forster, M. A. T., Pecher, P., Bauer, N., Glazebrook, J., … Lee, J. (2012). MPK11—a fourth elicitor-responsive mitogen-activated protein kinase in Arabidopsis thaliana. *Plant Signaling & Behavior*. https://doi.org/10.4161/psb.21323

Eulalio, A., Behm-Ansmant, I., & Izaurralde, E. (2007). P bodies: At the crossroads of post-transcriptional pathways. *Nature Reviews Molecular Cell Biology*. https://doi.org/10.1038/nrm2080

Feilner, T., Hultschig, C., Lee, J., Meyer, S., Immink, R. G. H., Koenig, A., … Kersten, B. (2005). High Throughput Identification of Potential Arabidopsis Mitogen-activated Protein Kinases Substrates . *Molecular & Cellular Proteomics*. https://doi.org/10.1074/mcp.m500007-mcp200

Felix, G., Duran, J. D., Volko, S., & Boller, T. (1999). Plants have a sensitive perception system for the most conserved domain of bacterial flagellin. *Plant Journal*. https://doi.org/10.1046/j.1365-

313X.1999.00265.x

Ferraiuolo, M. A., Basak, S., Dostie, J., Murray, E. L., Schoenberg, D. R., & Sonenberg, N. (2005). A role for the eIF4E-binding protein 4E-T in P-body formation and mRNA decay. *Journal of Cell Biology*. https://doi.org/10.1083/jcb.200504039

Fontana, M. F., & Vance, R. E. (2011). Two signal models in innate immunity. *Immunological Reviews*. https://doi.org/10.1111/j.1600-065X.2011.01037.x

Franks, T. M., & Lykke-Andersen, J. (2008). The Control of mRNA Decapping and P-Body Formation. *Molecular Cell*, *32*(5), 605–615. https://doi.org/10.1016/j.molcel.2008.11.001

FREEMONT, P. S. (1993). The RING Finger: A Novel Protein Sequence Motif Related to the Zinc Finger. *Annals of the New York Academy of Sciences*. https://doi.org/10.1111/j.1749-6632.1993.tb32280.x

Frei dit Frey, N., Garcia, A. V., Bigeard, J., Zaag, R., Bueso, E., Garmier, M., … Hirt, H. (2014). Functional analysis of Arabidopsis immune-related MAPKs uncovers a role for MPK3 as negative regulator of inducible defences. *Genome Biology*. https://doi.org/10.1186/gb-2014-15-6-r87

Fritz-Laylin, L. K., Krishnamurthy, N., Tör, M., Sjölander, K. V., & Jones, J. D. G. (2005). Phylogenomic Analysis of the Receptor-Like Proteins of Rice and Arabidopsis. *Plant Physiology*. https://doi.org/10.1104/pp.104.054452

Gao, M., Liu, J., Bi, D., Zhang, Z., Cheng, F., Chen, S., & Zhang, Y. (2008). MEKK1, MKK1/MKK2 and MPK4 function together in a mitogen-activated protein kinase cascade to regulate innate immunity in plants. *Cell Research*, *18*(12), 1190–1198. https://doi.org/10.1038/cr.2008.300

Garneau, N. L., Wilusz, J., & Wilusz, C. J. (2007). The highways and byways of mRNA decay. *Nature Reviews Molecular Cell Biology*, *8*(February), 113–126. https://doi.org/10.1038/nrm2104

Gasciolli, V., Mallory, A. C., Bartel, D. P., & Vaucheret, H. (2005). Partially redundant functions of arabidopsis DICER-like enzymes and a role for DCL4 in producing trans-Acting siRNAs. *Current Biology*. https://doi.org/10.1016/j.cub.2005.07.024

Gazzani, S., Lawrenson, T., Woodward, C., Headon, D., & Sablowski, R. (2004). A link between mRNA turnover and RNA interference in Arabidopsis. *Science*. https://doi.org/10.1126/science.1101092

Gilks, N. (2004). Stress Granule Assembly Is Mediated by Prion-like Aggregation of TIA-1. *Molecular Biology of the Cell*. https://doi.org/10.1091/mbc.e04-08-0715

Giorgi, C., & Moore, M. J. (2007). The nuclear nurture and cytoplasmic nature of localized mRNPs. *Seminars in Cell and Developmental Biology*. https://doi.org/10.1016/j.semcdb.2007.01.002

Giraldo, M. C., Dagdas, Y. F., Gupta, Y. K., Mentlak, T. A., Yi, M., Martinez-Rocha, A. L., … Valent, B. (2013). Two distinct secretion systems facilitate tissue invasion by the rice blast fungus Magnaporthe oryzae. *Nature Communications*. https://doi.org/10.1038/ncomms2996

Goeres, D. C., Van Norman, J. M., Zhang, W., Fauver, N. A., Spencer, M. Lou, & Sieburth, L. E. (2007a). Components of the Arabidopsis mRNA Decapping Complex Are Required for Early Seedling Development . *The Plant Cell*, *19*(5), 1549–1564. https://doi.org/10.1105/tpc.106.047621

Goeres, D. C., Van Norman, J. M., Zhang, W., Fauver, N. A., Spencer, M. Lou, & Sieburth, L. E. (2007b). Components of the Arabidopsis mRNA Decapping Complex Are Required for Early Seedling

Development . *The Plant Cell*. https://doi.org/10.1105/tpc.106.047621

Gómez-Gómez, L., & Boller, T. (2000). FLS2: An LRR receptor-like kinase involved in the perception of the bacterial elicitor flagellin in Arabidopsis. *Molecular Cell*. https://doi.org/10.1016/S1097-2765(00)80265-8

Gomperts, M., Pascall, J. C., & Brown, K. D. (1990). The nucleotide sequence of a cDNA encoding an EGF-inducible gene indicates the existence of a new family of mitogen-induced genes. *Oncogene*.

Grefen, C., Donald, N., Hashimoto, K., Kudla, J., Schumacher, K., & Blatt, M. R. (2010). A ubiquitin-10 promoter-based vector set for fluorescent protein tagging facilitates temporal stability and native protein distribution in transient and stable expression studies. *Plant Journal*. https://doi.org/10.1111/j.1365-313X.2010.04322.x

Grousl, T., Ivanov, P., Frydlova, I., Vasicova, P., Janda, F., Vojtova, J., … Hasek, J. (2009). Robust heat shock induces eIF2 -phosphorylation-independent assembly of stress granules containing eIF3 and 40S ribosomal subunits in budding yeast, Saccharomyces cerevisiae. *Journal of Cell Science*. https://doi.org/10.1242/jcs.045104

Guan, Y., Meng, X., Khanna, R., LaMontagne, E., Liu, Y., & Zhang, S. (2014). Phosphorylation of a WRKY Transcription Factor by MAPKs Is Required for Pollen Development and Function in Arabidopsis. *PLoS Genetics*. https://doi.org/10.1371/journal.pgen.1004384

Guo, Y. H., Yu, Y. P., Wang, D., Wu, C. A., Yang, G. D., Huang, J. G., & Zheng, C. C. (2009). GhZFP1, a novel CCCH-type zinc finger protein from cotton, enhances salt stress tolerance and fungal disease resistance in transgenic tobacco by interacting with GZIRD21A and GZIPR5. *New Phytologist*, *183*(1), 62–75. https://doi.org/10.1111/j.1469-8137.2009.02838.x

Gupta, B., Sengupta, A., & Gupta, K. (2016). Commentary: Conservation of AtTZF1, AtTZF2, and AtTZF3 homolog gene regulation by salt stress in evolutionarily distant plant species. *Frontiers in Plant Science*, *7*(June), 1–16. https://doi.org/10.3389/fpls.2016.00254

Gy, I., Gasciolli, V., Lauressergues, D., Morel, J.-B., Gombert, J., Proux, F., … Mallory, A. C. (2007). Arabidopsis FIERY1, XRN2, and XRN3 Are Endogenous RNA Silencing Suppressors . *The Plant Cell*. https://doi.org/10.1105/tpc.107.055319

Hall, T. M. T. (2005). Multiple modes of RNA recognition by zinc finger proteins. *Current Opinion in Structural Biology*. https://doi.org/10.1016/j.sbi.2005.04.004

Heese, A., Hann, D. R., Gimenez-Ibanez, S., Jones, A. M. E., He, K., Li, J., … Rathjen, J. P. (2007). The receptor-like kinase SERK3/BAK1 is a central regulator of innate immunity in plants. *Proceedings of the National Academy of Sciences*. https://doi.org/10.1073/pnas.0705306104

Herr, A. J., Molnar, A., Jones, A., & Baulcombe, D. C. (2006). Defective RNA processing enhances RNA silencing and influences flowering of Arabidopsis. *Proceedings of the National Academy of Sciences*. https://doi.org/10.1073/pnas.0606536103

Hoehenwarter, W., Thomas, M., Nukarinen, E., Egelhofer, V., Röhrig, H., Weckwerth, W., … Beckers, G. J. M. (2013). Identification of Novel in vivo MAP Kinase Substrates in Arabidopsis thaliana Through Use of Tandem Metal Oxide Affinity Chromatography . *Molecular & Cellular Proteomics*. https://doi.org/10.1074/mcp.m112.020560

Hou, S., Wang, X., Chen, D., Yang, X., Wang, M., Turrà, D., … Zhang, W. (2014). The Secreted Peptide PIP1

Amplifies Immunity through Receptor-Like Kinase 7. *PLoS Pathogens*. https://doi.org/10.1371/journal.ppat.1004331

Hoyle, N. P., Castelli, L. M., Campbell, S. G., Holmes, L. E. A., & Ashe, M. P. (2007). Stress-dependent relocalization of translationally primed mRNPs to cytoplasmic granules that are kinetically and spatially distinct from P-bodies. *Journal of Cell Biology*. https://doi.org/10.1083/jcb.200707010

Huang, P., Chung, M. S., Ju, H. W., Na, H. S., Lee, D. J., Cheong, H. S., & Kim, C. S. (2011a). Physiological characterization of the Arabidopsis thaliana Oxidation-related Zinc Finger 1, a plasma membrane protein involved in oxidative stress. *Journal of Plant Research*. https://doi.org/10.1007/s10265-010-0397-3

Huang, P., Chung, M. S., Ju, H. W., Na, H. S., Lee, D. J., Cheong, H. S., & Kim, C. S. (2011b). Physiological characterization of the Arabidopsis thaliana Oxidation-related Zinc Finger 1, a plasma membrane protein involved in oxidative stress. *Journal of Plant Research*, *124*(6), 699–705. https://doi.org/10.1007/s10265-010-0397-3

Huang, P., Ju, H. W., Min, J. H., Zhang, X., Chung, J. S., Cheong, H. S., & Kim, C. S. (2012). Molecular and physiological characterization of the arabidopsis thaliana oxidation-related zinc finger 2, a plasma membrane protein involved in ABA and salt stress response through the ABI2-mediated signaling pathway. *Plant and Cell Physiology*. https://doi.org/10.1093/pcp/pcr162

Huffaker, a., Pearce, G., & Ryan, C. a. (2006). An endogenous peptide signal in Arabidopsis activates components of the innate immune response. *Proceedings of the National Academy of Sciences*, *103*, 10098–10103. https://doi.org/10.1073/pnas.0603727103

Huffaker, A., & Ryan, C. A. (2007). Endogenous peptide defense signals in Arabidopsis differentially amplify signaling for the innate immune response. *Proceedings of the National Academy of Sciences*. https://doi.org/10.1073/pnas.0703343104

Ichimura, K., Shinozaki, K., Tena, G., Sheen, J., Henry, Y., Champion, A., … Walker, J. C. (2002). Mitogen-activated protein kinase cascades in plants: A new nomenclature. *Trends in Plant Science*. https://doi.org/10.1016/S1360-1385(02)02302-6

Isken, O., & Maquat, L. E. (2007). Quality control of eukaryotic mRNA: Safeguarding cells from abnormal mRNA function. *Genes and Development*. https://doi.org/10.1101/gad.1566807

Isken, O., & Maquat, L. E. (2008). The multiple lives of NMD factors: Balancing roles in gene and genome regulation. *Nature Reviews Genetics*. https://doi.org/10.1038/nrg2402

Iwasaki, S., Takeda, A., Motose, H., & Watanabe, Y. (2007). Characterization of Arabidopsis decapping proteins AtDCP1 and AtDCP2, which are essential for post-embryonic development. *FEBS Letters*, *581*, 2455–2459. https://doi.org/10.1016/j.febslet.2007.04.051

Jenkins, T. H., Li, J., Scutt, C. P., & Gilmartin, P. M. (2005). Analysis of members of the Silene latifolia Cys 2 /His 2 zinc-finger transcription factor family during dioecious flower development and in a novel stamen-defective mutant ssf1. *Planta*. https://doi.org/10.1007/s00425-004-1365-8

Jianming, L., & Joanne, C. (1997). A putative leucine-rich repeat receptor kinase involved in brassinosteroid signal transduction. *Cell*. https://doi.org/10.1016/S0092-8674(00)80357-8

Jones, J. D. G., & Dangl, J. L. (2006). The plant immune system. *Nature*, *444*(November), 323–329. https://doi.org/10.1038/nature05286

Jouannet, V., Moreno, A. B., Elmayan, T., Vaucheret, H., Crespi, M. D., & Maizel, A. (2012a). Cytoplasmic Arabidopsis AGO7 accumulates in membrane-associated siRNA bodies and is required for ta-siRNA biogenesis. *EMBO Journal*. https://doi.org/10.1038/emboj.2012.20

Jouannet, V., Moreno, A. B., Elmayan, T., Vaucheret, H., Crespi, M. D., & Maizel, A. (2012b). Cytoplasmic Arabidopsis AGO7 accumulates in membrane-associated siRNA bodies and is required for ta-siRNA biogenesis. *EMBO Journal*, *31*(7), 1704–1713. https://doi.org/10.1038/emboj.2012.20

Kanchiswamy, C. N., Takahashi, H., Quadro, S., Maffei, M. E., Bossi, S., Bertea, C., … Arimura, G. I. (2010). Regulation of Arabidopsis defense responses against Spodoptera littoralis by CPK-mediated calcium signaling. *BMC Plant Biology*. https://doi.org/10.1186/1471-2229-10-97

Kastenmayer, J. P., & Green, P. J. (2002). Novel features of the XRN-family in Arabidopsis: Evidence that AtXRN4, one of several orthologs of nuclear Xrn2p/Rat1p, functions in the cytoplasm. *Proceedings of the National Academy of Sciences*. https://doi.org/10.1073/pnas.97.25.13985

Kedersha, N. (2002). Evidence That Ternary Complex (eIF2-GTP-tRNAiMet)-Deficient Preinitiation Complexes Are Core Constituents of Mammalian Stress Granules. *Molecular Biology of the Cell*. https://doi.org/10.1091/mbc.01-05-0221

Kedersha, N. L., Gupta, M., Li, W., Miller, I., & Anderson, P. (1999). RNA-binding proteins TIA-1 and TIAR link the phosphorylation of eIF-2α to the assembly of mammalian stress granules. *Journal of Cell Biology*. https://doi.org/10.1083/jcb.147.7.1431

Kedersha, Nancy, Cho, M. R., Li, W., Yacono, P. W., Chen, S., Gilks, N., … Anderson, P. (2000). Dynamic shuttling of TIA-1 accompanies the recruitment of mRNA to mammalian stress granules. *Journal of Cell Biology*. https://doi.org/10.1083/jcb.151.6.1257

Kedersha, Nancy, Ivanov, P., & Anderson, P. (2013a). Stress granules and cell signaling: More than just a passing phase? *Trends in Biochemical Sciences*. https://doi.org/10.1016/j.tibs.2013.07.004

Kedersha, Nancy, Ivanov, P., & Anderson, P. (2013b). Stress granules and cell signaling: More than just a passing phase? *Trends in Biochemical Sciences*, *38*(10), 494–506. https://doi.org/10.1016/j.tibs.2013.07.004

Kedersha, Nancy, Stoecklin, G., Ayodele, M., Yacono, P., Lykke-Andersen, J., Fitzler, M. J., … Anderson, P. (2005). Stress granules and processing bodies are dynamically linked sites of mRNP remodeling. *Journal of Cell Biology*. https://doi.org/10.1083/jcb.200502088

Kerényi, Z., Mérai, Z., Hiripi, L., Benkovics, A., Gyula, P., Lacomme, C., … Silhavy, D. (2008). Inter-kingdom conservation of mechanism of nonsense-mediated mRNA decay. *EMBO Journal*. https://doi.org/10.1038/emboj.2008.88

Khanna, R., & Kiledjian, M. (2004). Poly(A)-binding-protein-mediated regulation of hDcp2 decapping in vitro. *EMBO Journal*. https://doi.org/10.1038/sj.emboj.7600213

Kim, D. H., Yamaguchi, S., Lim, S., Oh, E., Park, J., Hanada, A., … Choi, G. (2008). SOMNUS, a CCCH-Type Zinc Finger Protein in Arabidopsis , Negatively Regulates Light-Dependent Seed Germination Downstream of PIL5 . *The Plant Cell*. https://doi.org/10.1105/tpc.108.058859

Kimball, S. R., Horetsky, R. L., Ron, D., Jefferson, L. S., & Harding, H. P. (2003). Mammalian stress granules represent sites of accumulation of stalled translation initiation complexes. *American Journal of Physiology-Cell Physiology*. https://doi.org/10.1152/ajpcell.00314.2002

Kong, Q., Qu, N., Gao, M., Zhang, Z., Ding, X., Yang, F., … Zhang, Y. (2012). The MEKK1-MKK1/MKK2-MPK4 Kinase Cascade Negatively Regulates Immunity Mediated by a Mitogen-Activated Protein Kinase Kinase Kinase in Arabidopsis . *The Plant Cell*. https://doi.org/10.1105/tpc.112.097253

Kong, Z., Li, M., Yang, W., Xu, W., & Xue, Y. (2006). A Novel Nuclear-Localized CCCH-Type Zinc Finger Protein, OsDOS, Is Involved in Delaying Leaf Senescence in Rice. *Plant Physiology*. https://doi.org/10.1104/pp.106.082941

Kosarev, P., Mayer, K. F. X., & Hardtke, C. S. (2002). Evaluation and classification of RING-finger domains encoded by the Arabidopsis genome. *Genome Biology*.

Krol, E., Mentzel, T., Chinchilla, D., Boller, T., Felix, G., Kemmerling, B., … Hedrich, R. (2010). Perception of the Arabidopsis danger signal peptide 1 involves the pattern recognition receptor AtPEPR1 and its close homologue AtPEPR2. *Journal of Biological Chemistry*, *285*(18), 13471–13479. https://doi.org/10.1074/jbc.M109.097394

Kumakura, N., Takeda, A., Fujioka, Y., Motose, H., Takano, R., & Watanabe, Y. (2009). SGS3 and RDR6 interact and colocalize in cytoplasmic SGS3/RDR6-bodies. *FEBS Letters*, *583*(8), 1261–1266. https://doi.org/10.1016/j.febslet.2009.03.055

Kunze, G., Zipfel, C., Robatzek, S., Niehaus, K., Boller, T., & Felix, G. (2004). The N Terminus of Bacterial Elongation Factor Tu Elicits Innate Immunity in Arabidopsis Plants. *The Plant Cell*. https://doi.org/10.1105/tpc.104.026765

Laity, J. H., Lee, B. M., & Wright, P. E. (2001). Zinc finger proteins: New insights into structural and functional diversity. *Current Opinion in Structural Biology*, *11*, 39–46. https://doi.org/10.1016/S0959-440X(00)00167-6

Lampard, G. R., MacAlister, C. A., & Bergmann, D. C. (2008). Arabidopsis stomatal initiation is controlled by MAPK-mediated regulation of the bHLH SPEECHLESS. *Science*. https://doi.org/10.1126/science.1162263

Lange, H., Zuber, H., Sement, F. M., Chicher, J., Kuhn, L., Hammann, P., … Gagliardi, D. (2014). The RNA Helicases AtMTR4 and HEN2 Target Specific Subsets of Nuclear Transcripts for Degradation by the Nuclear Exosome in Arabidopsis thaliana. *PLoS Genetics*. https://doi.org/10.1371/journal.pgen.1004564

Lassowskat, I., Böttcher, C., Eschen-lippold, L., Scheel, D., & Lee, J. (2014). Sustained mitogen-activated protein kinase activation reprograms defense metabolism and phosphoprotein profile in Arabidopsis thaliana, *5*(October), 1–20. https://doi.org/10.3389/fpls.2014.00554

Law, J. A., & Jacobsen, S. E. (2010). Establishing, maintaining and modifying DNA methylation patterns in plants and animals. *Nature Reviews Genetics*. https://doi.org/10.1038/nrg2719

Lee, S. J., Jung, H. J., Kang, H., & Kim, S. Y. (2012). Arabidopsis zinc finger proteins AtC3H49/AtTZF3 and AtC3H20/AtTZF2 are involved in ABA and JA responses. *Plant and Cell Physiology*, *53*(4), 673–686. https://doi.org/10.1093/pcp/pcs023

Lejeune, F., Li, X., & Maquat, L. E. (2003). Nonsense-mediated mRNA decay in mammalian cells involves decapping, deadenylating, and exonucleolytic activities. *Molecular Cell*. https://doi.org/10.1016/S1097-2765(03)00349-6

Li, B., Jiang, S., Yu, X., Cheng, C., Chen, S., Cheng, Y., … Shan, L. (2015a). Phosphorylation of Trihelix

Transcriptional Repressor ASR3 by MAP KINASE4 Negatively Regulates Arabidopsis Immunity. *The Plant Cell*. https://doi.org/10.1105/tpc.114.134809

Li, B., Jiang, S., Yu, X., Cheng, C., Chen, S., Cheng, Y., … Shan, L. (2015b). Phosphorylation of Trihelix Transcriptional Repressor ASR3 by MAP KINASE4 Negatively Regulates Arabidopsis Immunity. *The Plant Cell*.

Li, J., Wen, J., Lease, K. a., Doke, J. T., Tax, F. E., & Walker, J. C. (2002). BAK1, an Arabidopsis LRR receptor-like protein kinase, interacts with BRI1 and modulates brassinosteroid signaling. *Cell*, *110*, 213–222. https://doi.org/10.1016/S0092-8674(02)00812-7

Li, Z., & Thomas, T. L. (2007). PEI1, an Embryo-Specific Zinc Finger Protein Gene Required for Heart-Stage Embryo Formation in Arabidopsis. *The Plant Cell*. https://doi.org/10.2307/3870596

Liebrand, T. W. H., van den Burg, H. A., & Joosten, M. H. A. J. (2014). Two for all: Receptor-associated kinases SOBIR1 and BAK1. *Trends in Plant Science*. https://doi.org/10.1016/j.tplants.2013.10.003

Lijavetzky, D., Carbonero, P., & Vicente-Carbajosa, J. (2003). Genome-wide comparative phylogenetic analysis of the rice and Arabidopsis Dof gene families. *BMC Evolutionary Biology*. https://doi.org/10.1186/1471-2148-3-17

Lin, P. C., Pomeranz, M. C., Jikumaru, Y., Kang, S. G., Hah, C., Fujioka, S., … Jang, J. C. (2011). The Arabidopsis tandem zinc finger protein AtTZF1 affects ABA- and GA-mediated growth, stress and gene expression responses. *Plant Journal*, *65*(2), 253–268. https://doi.org/10.1111/j.1365-313X.2010.04419.x

Lin, W., Lu, D., Gao, X., Jiang, S., Ma, X., Wang, Z., … Shan, L. (2013). Inverse modulation of plant immune and brassinosteroid signaling pathways by the receptor-like cytoplasmic kinase BIK1. *Proceedings of the National Academy of Sciences*. https://doi.org/10.1073/pnas.1302154110

Lin, Wenwei, Li, B., Lu, D., Chen, S., Zhu, N., He, P., & Shan, L. (2014). Tyrosine phosphorylation of protein kinase complex BAK1/BIK1 mediates Arabidopsis innate immunity . *Proceedings of the National Academy of Sciences*. https://doi.org/10.1073/pnas.1318817111

Liu, P.-L., Xie, L.-L., Li, P.-W., Mao, J.-F., Liu, H., Gao, S.-M., … Gong, J.-Q. (2016). Duplication and Divergence of Leucine-Rich Repeat Receptor-Like Protein Kinase (LRR-RLK) Genes in Basal Angiosperm Amborella trichopoda. *Frontiers in Plant Science*. https://doi.org/10.3389/fpls.2016.01952

Liu, T., Liu, Z., Song, C., Hu, Y., Han, Z., She, J., … Chai, J. (2012). Chitin-induced dimerization activates a plant immune receptor. *Science*. https://doi.org/10.1126/science.1218867

Liu, Y., & Zhang, S. (2004). Phosphorylation of 1-Aminocyclopropane-1-Carboxylic Acid Synthase by MPK6, a Stress-Responsive Mitogen-Activated Protein Kinase, Induces Ethylene Biosynthesis in Arabidopsis. *The Plant Cell*. https://doi.org/10.1105/tpc.104.026609

Liu, Z., Wu, Y., Yang, F., Zhang, Y., Chen, S., Xie, Q., … Zhou, J.-M. (2013). BIK1 interacts with PEPRs to mediate ethylene-induced immunity. *Proceedings of the National Academy of Sciences*, *110*(15), 6205–6210. https://doi.org/10.1073/pnas.1215543110

Lykke-Andersen, J., & Wagner, E. (2005). Recruitment and activation of mRNA decay enzymes by two ARE-mediated decay activation domains in the proteins TTP and BRF-1. *Genes and Development*, *19*, 351–361. https://doi.org/10.1101/gad.1282305

Ma, Y., Walker, R. K., Zhao, Y., & Berkowitz, G. a. (2012). Linking ligand perception by PEPR pattern recognition receptors to cytosolic Ca2+ elevation and downstream immune signaling in plants. *Proceedings of the National Academy of Sciences*, *109*, 19852–19857. https://doi.org/10.1073/pnas.1205448109

Macho, A. P., & Zipfel, C. (2014). Plant PRRs and the activation of innate immune signaling. *Molecular Cell*, *54*(2), 263–272. https://doi.org/10.1016/j.molcel.2014.03.028

Macho, A. P., & Zipfel, C. (2015). Targeting of plant pattern recognition receptor-triggered immunity by bacterial type-III secretion system effectors. *Current Opinion in Microbiology*. https://doi.org/10.1016/j.mib.2014.10.009

Maldonado-Bonilla, L. D. (2014). Composition and function of P bodies in Arabidopsis thaliana. *Frontiers in Plant Science*, *5*(May), 1–11. https://doi.org/10.3389/fpls.2014.00201

Maldonado-bonilla, L. D., Eschen-lippold, L., Gago-zachert, S., Tabassum, N., Bauer, N., Scheel, D., & Lee, J. (2014). The Arabidopsis Tandem Zinc Finger 9 Protein Binds RNA and Mediates Pathogen-Associated Molecular Pattern-Triggered Immune Responses, *55*(2), 412–425. https://doi.org/10.1093/pcp/pct175

Maldonado-Bonilla, L. D., Eschen-Lippold, L., Gago-Zachert, S., Tabassum, N., Bauer, N., Scheel, D., & Lee, J. (2014). The arabidopsis tandem zinc finger 9 protein binds RNA and mediates pathogen-associated molecular pattern-triggered immune responses. *Plant and Cell Physiology*, *55*(2), 412–425. https://doi.org/10.1093/pcp/pct175

Mangus, D. A., Evans, M. C., & Jacobson, A. (2003). Poly(A)-binding proteins: Multifunctional scaffolds for the post-transcriptional control of gene expression. *Genome Biology*, *4*(7), 1–14. https://doi.org/10.1186/gb-2003-4-7-223

Mao, G., Meng, X., Liu, Y., Zheng, Z., Chen, Z., & Zhang, S. (2011). Phosphorylation of a WRKY Transcription Factor by Two Pathogen-Responsive MAPKs Drives Phytoalexin Biosynthesis in Arabidopsis . *The Plant Cell*. https://doi.org/10.1105/tpc.111.084996

Matzke, M. A., & Mosher, R. A. (2014). RNA-directed DNA methylation: An epigenetic pathway of increasing complexity. *Nature Reviews Genetics*. https://doi.org/10.1038/nrg3683

Mazroui, R. (2002). Trapping of messenger RNA by Fragile X Mental Retardation protein into cytoplasmic granules induces translation repression. *Human Molecular Genetics*. https://doi.org/10.1093/hmg/11.24.3007

Mazroui, Rachid, Sukarieh, R., Bordeleau, M.-E., Kaufman, R. J., Northcote, P., Tanaka, J., … Pelletier, J. (2006). Inhibition of Ribosome Recruitment Induces Stress Granule Formation Independently of Eukaryotic Initiation Factor 2α Phosphorylation. *Molecular Biology of the Cell*. https://doi.org/10.1091/mbc.e06-04-0318

Medzhitov, R., & Janeway, C. A. (2002). Decoding the patterns of self and nonself by the innate immune system. *Science*. https://doi.org/10.1126/science.1068883

Mello, C. C., Schubert, C., Draper, B., Zhang, W., Lobel, R., & Priess, J. R. (1996). The PIE-1 protein and germline specification in C. elegans embryos. *Nature*. https://doi.org/10.1038/382710a0

Melotto, M., Underwood, W., & He, S. Y. (2008). Role of Stomata in Plant Innate Immunity and Foliar Bacterial Diseases. *Annual Review of Phytopathology*.

https://doi.org/10.1146/annurev.phyto.121107.104959

Meng, X., Xu, J., He, Y., Yang, K.-Y., Mordorski, B., Liu, Y., & Zhang, S. (2013). Phosphorylation of an ERF Transcription Factor by Arabidopsis MPK3/MPK6 Regulates Plant Defense Gene Induction and Fungal Resistance . *The Plant Cell*. https://doi.org/10.1105/tpc.112.109074

Meng, X., & Zhang, S. (2013). MAPK Cascades in Plant Disease Resistance Signaling. *Annual Review of Phytopathology*. https://doi.org/10.1146/annurev-phyto-082712-102314

Meyer, S., Temme, C., & Wahle, E. (2004). Messenger RNA turnover in eukaryotes: Pathways and enzymes. *Critical Reviews in Biochemistry and Molecular Biology*. https://doi.org/10.1080/10409230490513991

Miller, J., McLachlan, A. D., & Klug, A. (2001). Repetitive zinc-binding domains in the protein transcription factor IIIA from Xenopus oocytes. *Journal of Trace Elements in Experimental Medicine*. https://doi.org/10.1002/jtra.1022

Mokas, S., Mills, J. R., Garreau, C., Fournier, M.-J., Robert, F., Arya, P., … Mazroui, R. (2009). Uncoupling Stress Granule Assembly and Translation Initiation Inhibition. *Molecular Biology of the Cell*. https://doi.org/10.1091/mbc.e08-10-1061

Mollet, S., Cougot, N., Wilczynska, A., Dautry, F., Kress, M., Bertrand, E., & Weil, D. (2008). Translationally Repressed mRNA Transiently Cycles through Stress Granules during Stress. *Molecular Biology of the Cell*. https://doi.org/10.1091/mbc.e08-05-0499

Molnar, A., Melnyk, C., & Baulcombe, D. C. (2011). Silencing signals in plants: A long journey for small RNAs. *Genome Biology*. https://doi.org/10.1186/gb-2010-11-12-219

Moore, M. J. (2005). From birth to death: The complex lives of eukaryotic mRNAs. *Science*. https://doi.org/10.1126/science.1111443

Moore, M., & Ullman, C. (2003). Recent developments in the engineering of zinc finger proteins. *Briefings in Functional Genomics and Proteomics*. https://doi.org/10.1093/bfgp/1.4.342

Moreno, A. B., De Alba, A. E. M., Bardou, F., Crespi, M. D., Vaucheret, H., Maizel, A., & Mallory, A. C. (2013). Cytoplasmic and nuclear quality control and turnover of single-stranded RNA modulate post-transcriptional gene silencing in plants. *Nucleic Acids Research*. https://doi.org/10.1093/nar/gkt152

Morris, E. R., & Walker, J. C. (2003). Receptor-like protein kinases: The keys to response. *Current Opinion in Plant Biology*. https://doi.org/10.1016/S1369-5266(03)00055-4

Mosavi, L. K., Cammett, T. J., Desrosiers, D. C., & Peng, Z. (2004). The ankyrin repeat as molecular architecture for protein recognition. *Protein Science*. https://doi.org/10.1110/ps.03554604

Mourrain, P., Béclin, C., Elmayan, T., Feuerbach, F., Godon, C., Morel, J. B., … Vaucheret, H. (2000). Arabidopsis SGS2 and SGS3 genes are required for posttranscriptional gene silencing and natural virus resistance. *Cell*. https://doi.org/10.1016/S0092-8674(00)80863-6

Muench, D. G., Zhang, C., & Dahodwala, M. (2012). Control of cytoplasmic translation in plants. *Wiley Interdisciplinary Reviews: RNA*. https://doi.org/10.1002/wrna.1104

Muhlrad, D., & Parker, R. (1994). Premature translational termination triggers mRNA decapping. *Nature*.

https://doi.org/10.1038/370578a0

Mur, L. A. J., Kenton, P., Lloyd, A. J., Ougham, H., & Prats, E. (2008). The hypersensitive response; The centenary is upon us but how much do we know? In *Journal of Experimental Botany*. https://doi.org/10.1093/jxb/erm239

Nagarajan, V. K., Jones, C. I., Newbury, S. F., & Green, P. J. (2013). XRN 5'→3' exoribonucleases: Structure, mechanisms and functions. *Biochimica et Biophysica Acta - Gene Regulatory Mechanisms*. https://doi.org/10.1016/j.bbagrm.2013.03.005

Nakagawa, T., Kurose, T., Hino, T., Tanaka, K., Kawamukai, M., Niwa, Y., … Kimura, T. (2007). Development of series of gateway binary vectors, pGWBs, for realizing efficient construction of fusion genes for plant transformation. *Journal of Bioscience and Bioengineering*. https://doi.org/10.1263/jbb.104.34

Nam, K. H., & Li, J. (2002). BRI1/BAK1, a receptor kinase pair mediating brassinosteroid signaling. *Cell*, *110*, 203–212. https://doi.org/10.1016/S0092-8674(02)00814-0

Nie, X. F., Maclean, K. N., Kumar, V., McKay, I. A., & Bustin, S. A. (1995). ERF-2, the human homologue of the murine Tis11d early response gene. *Gene*. https://doi.org/10.1016/0378-1119(94)00696-P

Nitta, Y., Ding, P., & Zhang, Y. (2014). Identification of additional MAP kinases activated upon PAMP treatment. *Plant Signaling and Behavior*. https://doi.org/10.4161/15592324.2014.976155

O'Brien, J. A., Daudi, A., Butt, V. S., & Bolwell, G. P. (2012). Reactive oxygen species and their role in plant defence and cell wall metabolism. *Planta*. https://doi.org/10.1007/s00425-012-1696-9

Ohn, T., Kedersha, N., Hickman, T., Tisdale, S., & Anderson, P. (2008). A functional RNAi screen links O-GlcNAc modification of ribosomal proteins to stress granule and processing body assembly. *Nature Cell Biology*. https://doi.org/10.1038/ncb1783

Parker, R., & Sheth, U. (2007). P Bodies and the Control of mRNA Translation and Degradation. *Molecular Cell*. https://doi.org/10.1016/j.molcel.2007.02.011

Pedley, K. F., & Martin, G. B. (2005). Role of mitogen-activated protein kinases in plant immunity. *Current Opinion in Plant Biology*. https://doi.org/10.1016/j.pbi.2005.07.006

Peng, X., Zhao, Y., Cao, J., Zhang, W., Jiang, H., Li, X., … Cheng, B. (2012). CCCH-type zinc finger family in maize: Genome-wide identification, classification and expression profiling under abscisic acid and drought treatments. *PLoS ONE*. https://doi.org/10.1371/journal.pone.0040120

Petersen, M., Brodersen, P., Naested, H., Andreasson, E., Lindhart, U., Johansen, B., … Mundy, J. (2000). Arabidopsis MAP kinase 4 negatively regulates systemic acquired resistance. *Cell*. https://doi.org/10.1016/S0092-8674(00)00213-0

Phillips, R. S., Ramos, S. B. V., & Blackshear, P. J. (2002). Members of the tristetraprolin family of tandem CCCH zinc finger proteins exhibit CRM1-dependent nucleocytoplasmic shuttling. *Journal of Biological Chemistry*. https://doi.org/10.1074/jbc.M111457200

Pitzschke, A. (2015). Modes of MAPK substrate recognition and control. *Trends in Plant Science*. https://doi.org/10.1016/j.tplants.2014.09.006

Poethig, R. S., Peragine, A., Yoshikawa, M., Hunter, C., Willmann, M., & Wu, G. (2006). The function of

RNAi in plant development. In *Cold Spring Harbor Symposia on Quantitative Biology*. https://doi.org/10.1101/sqb.2006.71.030

Pomeranz, M. C., Hah, C., Lin, P.-C., Kang, S. G., Finer, J. J., Blackshear, P. J., & Jang, J.-C. (2010a). The Arabidopsis Tandem Zinc Finger Protein AtTZF1 Traffics between the Nucleus and Cytoplasmic Foci and Binds Both DNA and RNA. *Plant Physiology*. https://doi.org/10.1104/pp.109.145656

Pomeranz, M. C., Hah, C., Lin, P.-C., Kang, S. G., Finer, J. J., Blackshear, P. J., & Jang, J.-C. (2010b). The Arabidopsis Tandem Zinc Finger Protein AtTZF1 Traffics between the Nucleus and Cytoplasmic Foci and Binds Both DNA and RNA. *Plant Physiology*, *152*(1), 151–165. https://doi.org/10.1104/pp.109.145656

Pomeranz, M., Lin, P., Finer, J., & Jang, J. (2010). AtTZF gene family localizes to cytoplasmic foci, *5*(2), 190–192. https://doi.org/10.1104/pp.109.145656.n

Popescu, S. C., Popescu, G. V., Bachan, S., Zhang, Z., Gerstein, M., Snyder, M., & Dinesh-Kumar, S. P. (2009). MAPK target networks in Arabidopsis thaliana revealed using functional protein microarrays. *Genes and Development*. https://doi.org/10.1101/gad.1740009

Price, J., Laxmi, A., St. Martin, S. K., & Jang, J.-C. (2004). Global Transcription Profiling Reveals Multiple Sugar Signal Transduction Mechanisms in Arabidopsis. *The Plant Cell*. https://doi.org/10.1105/tpc.104.022616

Pruitt, R. N., Joe, A., Zhang, W., Feng, W., Stewart, V., Schwessinger, B., … Ronald, P. C. (2017). A microbially derived tyrosine-sulfated peptide mimics a plant peptide hormone. *New Phytologist*. https://doi.org/10.1111/nph.14609

Qu, J., Kang, S. G., Wang, W., Musier-Forsyth, K., & Jang, J. C. (2014). The Arabidopsis thaliana tandem zinc finger 1 (AtTZF1) protein in RNA binding and decay. *Plant Journal*. https://doi.org/10.1111/tpj.12485

Ramachandran, V., & Chen, X. (2008). Small RNA metabolism in Arabidopsis. *Trends in Plant Science*. https://doi.org/10.1016/j.tplants.2008.03.008

Ramirez, C. V., Vilela, C., Berthelot, K., & McCarthy, J. E. G. (2002). Modulation of eukaryotic mRNA stability via the cap-binding translation complex eIF4F. *Journal of Molecular Biology*. https://doi.org/10.1016/S0022-2836(02)00162-6

Ranf, S. (2017). Sensing of molecular patterns through cell surface immune receptors. *Current Opinion in Plant Biology*. https://doi.org/10.1016/j.pbi.2017.04.011

Ranf, S., Eschen-Lippold, L., Pecher, P., Lee, J., & Scheel, D. (2011). Interplay between calcium signalling and early signalling elements during defence responses to microbe- or damage-associated molecular patterns. *Plant Journal*, *68*(1), 100–113. https://doi.org/10.1111/j.1365-313X.2011.04671.x

Reverdatto, S. V., Dutko, J. A., Chekanova, J. A., Hamilton, D. A., & Belostotsky, D. A. (2004). mRNA deadenylation by PARN is essential for embryogenesis in higher plants. *RNA*. https://doi.org/10.1261/rna.7540204

Rice, W., Nakano, T., Suzuki, K., Fujimura, T., & Shinshi, H. (2006). Genome-Wide Analysis of the ERF Gene Family. *Gene*. https://doi.org/10.1104/pp.105.073783.currently

Rodriguez, M. C., Petersen, M., & Mundy, J. (2010). Mitogen-activated protein kinase signaling in plants. *Annu Rev Plant Biol*. https://doi.org/10.1146/annurev-arplant-042809-112252

Roux, M. E., Rasmussen, M. W., Palma, K., Lolle, S., Regue, A. M., Bethke, G., … Petersen, M. (2015). The mRNA decay factor PAT1 functions in a pathway including MAP kinase 4 and immune receptor SUMM2. *The EMBO Journal*. https://doi.org/10.15252/embj.201488645

Ryan, C. a., Huffaker, A., & Yamaguchi, Y. (2007). New insights into innate immunity in Arabidopsis. *Cellular Microbiology*, *9*(June), 1902–1908. https://doi.org/10.1111/j.1462-5822.2007.00991.x

Ryan, C. A., & Pearce, G. (2003). Systemins: A functionally defined family of peptide signals that regulate defensive genes in Solanaceae species. *Proceedings of the National Academy of Sciences*. https://doi.org/10.1073/pnas.1934788100

Rymarquis, L. A., Souret, F. F., & Green, P. J. (2011). Evidence that XRN4, an Arabidopsis homolog of exoribonuclease XRN1, preferentially impacts transcripts with certain sequences or in particular functional categories. *RNA*. https://doi.org/10.1261/rna.2467911

Saez, A., Robert, N., Maktabi, M. H., Schroeder, J. I., Serrano, R., & Rodriguez, P. L. (2006). Enhancement of Abscisic Acid Sensitivity and Reduction of Water Consumption in Arabidopsis by Combined Inactivation of the Protein Phosphatases Type 2C ABI1 and HAB1. *Plant Physiology*. https://doi.org/10.1104/pp.106.081018

Sasabe, M., Kosetsu, K., Hidaka, M., Murase, A., & Machida, Y. (2011). Arabidopsis thaliana MAP65-1 and MAP65-2 function redundantly with MAP65-3/PLEIADE in cytokinesis downstream of MPK4. *Plant Signaling and Behavior*. https://doi.org/10.4161/psb.6.5.15146

Schoenberg, D. R., & Maquat, L. E. (2012). Regulation of cytoplasmic mRNA decay. *Nature Reviews Genetics*. https://doi.org/10.1038/nrg3160

Schumann, U., Prestele, J., O'Geen, H., Brueggeman, R., Wanner, G., & Gietl, C. (2007). Requirement of the C 3 HC 4 zinc RING finger of the Arabidopsis PEX10 for photorespiration and leaf peroxisome contact with chloroplasts . *Proceedings of the National Academy of Sciences*. https://doi.org/10.1073/pnas.0610402104

Schwartz, D. C., & Parker, R. (2000). mRNA Decapping in Yeast Requires Dissociation of the Cap Binding Protein, Eukaryotic Translation Initiation Factor 4E. *Molecular and Cellular Biology*. https://doi.org/10.1128/mcb.20.21.7933-7942.2000

Schweingruber, C., Rufener, S. C., Zünd, D., Yamashita, A., & Mühlemann, O. (2013). Nonsense-mediated mRNA decay - Mechanisms of substrate mRNA recognition and degradation in mammalian cells. *Biochimica et Biophysica Acta - Gene Regulatory Mechanisms*. https://doi.org/10.1016/j.bbagrm.2013.02.005

Sen, G. L., & Blau, H. M. (2005). Argonaute 2/RISC resides in sites of mammalian mRNA decay known as cytoplasmic bodies. *Nature Cell Biology*. https://doi.org/10.1038/ncb1265

Seong, S. Y., & Matzinger, P. (2004). Hydrophobicity: An ancient damage-associated molecular pattern that initiates innate immune responses. *Nature Reviews Immunology*. https://doi.org/10.1038/nri1372

Seydoux, G., Mello, C. C., Pettitt, J., Wood, W. B., Priess, J. R., & Fire, A. (1996). Repression of gene expression in the embryonic germ lineage of C. elegans. *Nature*. https://doi.org/10.1038/382713a0

Sheth, U., & Parker, R. (2003). Decapping and decay of messenger RNA occur in cytoplasmic processing bodies. *Science*. https://doi.org/10.1126/science.1082320

Sheth, U., & Parker, R. (2006). Targeting of Aberrant mRNAs to Cytoplasmic Processing Bodies. *Cell*. https://doi.org/10.1016/j.cell.2006.04.037

Shirley, R. L., Ford, A. S., Rachel Richards, M., Albertini, M., & Culbertson, M. R. (2002). Nuclear import of Upf3p is mediated by importin-α/-β and export to the cytoplasm is required for a functional nonsense-mediated mRNA decay pathway in yeast. *Genetics*.

Shiu, S.-H., & Bleecker, A. B. (2001). Plant Receptor-Like Kinase Gene Family: Diversity, Function, and Signaling. *Science Signaling*, *2001*(113), re22–re22. https://doi.org/10.1126/stke.2001.113.re22

Shiu, Shin-Han, Karlowski, W. M., Pan, R., Tzeng, Y.-H., Mayer, K. F. X., & Li, W.-H. (2004). Comparative Analysis of the Receptor-Like Kinase Family in Arabidopsis and Rice. *The Plant Cell*. https://doi.org/10.1105/tpc.020834

Shoemaker, C. J., & Green, R. (2012). Translation drives mRNA quality control. *Nature Structural and Molecular Biology*. https://doi.org/10.1038/nsmb.2301

Sinha, A. K., Jaggi, M., Raghuram, B., & Tuteja, N. (2011). Mitogen-activated protein kinase signaling in plants under abiotic stress. *Plant Signaling and Behavior*. https://doi.org/10.4161/psb.6.2.14701

Smertenko, A. P. (2006). Control of the AtMAP65-1 interaction with microtubules through the cell cycle. *Journal of Cell Science*. https://doi.org/10.1242/jcs.03051

Souret, F. F., Kastenmayer, J. P., & Green, P. J. (2004). AtXRN4 degrades mRNA in Arabidopsis and its substrates include selected miRNA targets. *Molecular Cell*, *15*, 173–183. https://doi.org/10.1016/j.molcel.2004.06.006

Stael, S., Kmiecik, P., Willems, P., Van Der Kelen, K., Coll, N. S., Teige, M., & Van Breusegem, F. (2015). Plant innate immunity - sunny side up? *Trends in Plant Science*. https://doi.org/10.1016/j.tplants.2014.10.002

Suarez-Rodriguez, M. C., Adams-Phillips, L., Liu, Y., Wang, H., Su, S.-H., Jester, P. J., … Krysan, P. J. (2007). MEKK1 Is Required for flg22-Induced MPK4 Activation in Arabidopsis Plants. *Plant Physiology*. https://doi.org/10.1104/pp.106.091389

Sun, J., Jiang, H., Xu, Y., Li, H., Wu, X., Xie, Q., & Li, C. (2007). The CCCH-type zinc finger proteins AtSZF1 and AtSZF2 regulate salt stress responses in Arabidopsis. *Plant and Cell Physiology*, *48*(8), 1148–1158. https://doi.org/10.1093/pcp/pcm088

Takatsuji, H., Mori, M., Benfey, P. N., Ren, L., & Chua, N. H. (1992). Characterization of a zinc finger DNA-binding protein expressed specifically in Petunia petals and seedlings. *The EMBO Journal*. https://doi.org/10.1002/j.1460-2075.1992.tb05047.x

Takatsuji, Hiroshi. (1999). Zinc-finger proteins: The classical zinc finger emerges in contemporary plant science. *Plant Molecular Biology*. https://doi.org/10.1023/A:1006184519697

Taylor, G. a, Lai, W. S., Oakey, R. J., Seldin, M. F., Shows, T. B., Eddy, R. L., & Blackshear, P. J. (1991). The human TTP protein: sequence, alignment with related proteins, and chromosomal localization of the mouse and human genes. *Nucleic Acids Research*, *19*(12), 3454.

Teixeira, D., Sheth, U., Valencia-Sanchez, M. A., Brengues, M., & Parker, R. (2005). Processing bodies require RNA for assembly and contain nontranslating mRNAs. *RNA*. https://doi.org/10.1261/rna.7258505

Tena, G., Boudsocq, M., & Sheen, J. (2011). Protein kinase signaling networks in plant innate immunity. *Current Opinion in Plant Biology*, *14*(5), 519–529. https://doi.org/10.1016/j.pbi.2011.05.006

Thompson, M. J., Lai, W. S., Taylor, G. A., & Blackshear, P. J. (1996). Cloning and characterization of two yeast genes encoding members of the CCCH class of zinc finger proteins: Zinc finger-mediated impairment of cell growth. *Gene*. https://doi.org/10.1016/0378-1119(96)00084-4

Tintor, N., Ross, a., Kanehara, K., Yamada, K., Fan, L., Kemmerling, B., … Saijo, Y. (2013). Layered pattern receptor signaling via ethylene and endogenous elicitor peptides during Arabidopsis immunity to bacterial infection. *Proceedings of the National Academy of Sciences*, *110*(March 2016), 6211–6216. https://doi.org/10.1073/pnas.1216780110

Tör, M., Lotze, M. T., & Holton, N. (2009). Receptor-mediated signalling in plants: Molecular patterns and programmes. *Journal of Experimental Botany*. https://doi.org/10.1093/jxb/erp233

Tsuda, K., & Somssich, I. E. (2015). Transcriptional networks in plant immunity. *New Phytologist*. https://doi.org/10.1111/nph.13286

Umezawa, T., Sugiyama, N., Takahashi, F., Anderson, J. C., Ishihama, Y., Peck, S. C., & Shinozaki, K. (2013). Genetics and phosphoproteomics reveal a protein phosphorylation network in the abscisic acid signaling pathway in arabidopsis thaliana. *Science Signaling*. https://doi.org/10.1126/scisignal.2003509

Unterholzner, L., & Izaurralde, E. (2004). SMG7 acts as a molecular link between mRNA surveillance and mRNA decay. *Molecular Cell*. https://doi.org/10.1016/j.molcel.2004.10.013

van Loon, L. C., Rep, M., & Pieterse, C. M. J. (2006). Significance of Inducible Defense-related Proteins in Infected Plants. *Annual Review of Phytopathology*. https://doi.org/10.1146/annurev.phyto.44.070505.143425

Virtanen, A., Henriksson, N., Nilsson, P., & Nissbeck, M. (2013). Poly(A)-specific ribonuclease (PARN): An allosterically regulated, processive and mRNA cap-interacting deadenylase. *Critical Reviews in Biochemistry and Molecular Biology*. https://doi.org/10.3109/10409238.2013.771132

Walter, M., Chaban, C., Schütze, K., Batistic, O., Weckermann, K., Näke, C., … Kudla, J. (2004). Visualization of protein interactions in living plant cells using bimolecular fluorescence complementation. *Plant Journal*. https://doi.org/10.1111/j.1365-313X.2004.02219.x

Wang, D., Guo, Y., Wu, C., Yang, G., Li, Y., & Zheng, C. (2008a). Genome-wide analysis of CCCH zinc finger family in Arabidopsis and rice. *BMC Genomics*, *9*, 1–20. https://doi.org/10.1186/1471-2164-9-44

Wang, D., Guo, Y., Wu, C., Yang, G., Li, Y., & Zheng, C. (2008b). Genome-wide analysis of CCCH zinc finger family in Arabidopsis and rice, *20*, 1–20. https://doi.org/10.1186/1471-2164-9-44

Wang, H., Ngwenyama, N., Liu, Y., Walker, J. C., & Zhang, S. (2007). Stomatal Development and Patterning Are Regulated by Environmentally Responsive Mitogen-Activated Protein Kinases in Arabidopsis . *The Plant Cell*. https://doi.org/10.1105/tpc.106.048298

Wang, P., Xue, L., Batelli, G., Lee, S., Hou, Y.-J., Van Oosten, M. J., … Zhu, J.-K. (2013). Quantitative

phosphoproteomics identifies SnRK2 protein kinase substrates and reveals the effectors of abscisic acid action. *Proceedings of the National Academy of Sciences*. https://doi.org/10.1073/pnas.1308974110

Weber, C., Nover, L., & Fauth, M. (2008a). Plant stress granules and mRNA processing bodies are distinct from heat stress granules. *Plant Journal*, *56*(4), 517–530. https://doi.org/10.1111/j.1365-313X.2008.03623.x

Weber, C., Nover, L., & Fauth, M. (2008b). Plant stress granules and mRNA processing bodies are distinct from heat stress granules. *Plant Journal*. https://doi.org/10.1111/j.1365-313X.2008.03623.x

Wells, S. E., Hillner, P. E., Vale, R. D., & Sachs, A. B. (1998). Circularization of mRNA by eukaryotic translation initiation factors. *Molecular Cell*. https://doi.org/10.1016/S1097-2765(00)80122-7

Whisenant, T. C., Ho, D. T., Benz, R. W., Rogers, J. S., Kaake, R. M., Gordon, E. A., … Bardwell, L. (2010). Computational prediction and experimental verification of new MAP kinase docking sites and substrates including Gli transcription factors. *PLoS Computational Biology*. https://doi.org/10.1371/journal.pcbi.1000908

WIDMANN, C., GIBSON, S., JARPE, M. B., & JOHNSON, G. L. (2017). Mitogen-Activated Protein Kinase: Conservation of a Three-Kinase Module From Yeast to Human. *Physiological Reviews*. https://doi.org/10.1152/physrev.1999.79.1.143

Wilczynska, A., Aigueperse, C., Kress, M., Dautry, F., Weil, D. (2005). The translational regulator CPEB1 provides a link between dcp1 bodies and stress granules. *Journal of Cell Science*. https://doi.org/10.1242/jcs.01692

Wilusz, C. J., Wormington, M., & Peltz, S. W. (2001). The cap-to-tail guide to mRNA turnover. *Nature Reviews. Molecular Cell Biology*, *2*(April), 237–246. https://doi.org/10.1038/35067025

Wirthmueller, L., Maqbool, A., & Banfield, M. J. (2013). On the front line: Structural insights into plant-pathogen interactions. *Nature Reviews Microbiology*. https://doi.org/10.1038/nrmicro3118

Xu, Juan, & Zhang, S. (2015). Mitogen-activated protein kinase cascades in signaling plant growth and development. *Trends in Plant Science*. https://doi.org/10.1016/j.tplants.2014.10.001

Xu, Jun, & Chua, N.-H. (2009). Arabidopsis Decapping 5 Is Required for mRNA Decapping, P-Body Formation, and Translational Repression during Postembryonic Development . *The Plant Cell*. https://doi.org/10.1105/tpc.109.070078

Xu, Jun, & Chua, N. H. (2011). Processing bodies and plant development. *Current Opinion in Plant Biology*, *14*(1), 88–93. https://doi.org/10.1016/j.pbi.2010.10.003

Xu, Jun, & Chua, N. H. (2012). Dehydration stress activates Arabidopsis MPK6 to signal DCP1 phosphorylation. *EMBO Journal*. https://doi.org/10.1038/emboj.2012.56

Xu, Jun, Yang, J.-Y., Niu, Q.-W., & Chua, N.-H. (2006). Arabidopsis DCP2, DCP1, and VARICOSE Form a Decapping Complex Required for Postembryonic Development . *The Plant Cell*. https://doi.org/10.1105/tpc.106.047605

Yamaguchi, Y., Huffaker, a., Bryan, a. C., Tax, F. E., & Ryan, C. a. (2010). PEPR2 Is a Second Receptor for the Pep1 and Pep2 Peptides and Contributes to Defense Responses in Arabidopsis. *The Plant Cell*, *22*(February), 508–522. https://doi.org/10.1105/tpc.109.068874

Yoine, M., Nishii, T., & Nakamura, K. (2006). Arabidopsis UPF1 RNA helicase for nonsense-mediated mRNA decay is involved in seed size control and is essential for growth. *Plant and Cell Physiology*. https://doi.org/10.1093/pcp/pcj035

Zhang, Cheng, Zhang, F., Zhou, J., Fan, Z., Chen, F., Ma, H., & Xie, X. (2012). Overexpression of a phytochrome-regulated tandem zinc finger protein gene, OsTZF1, confers hypersensitivity to ABA and hyposensitivity to red light and far-red light in rice seedlings. *Plant Cell Reports*. https://doi.org/10.1007/s00299-012-1252-x

Zhang, Cuiqin, Zhang, H., Zhao, Y., Jiang, H., Zhu, S., Cheng, B., & Xiang, Y. (2013). Genome-wide analysis of the CCCH zinc finger gene family in Medicago truncatula. *Plant Cell Reports*. https://doi.org/10.1007/s00299-013-1466-6

Zhang, J., & Zhou, J. M. (2010). Plant immunity triggered by microbial molecular signatures. *Molecular Plant*.

Zhang, T., Chen, S., & Harmon, A. C. (2016). Protein-protein interactions in plant mitogen-activated protein kinase cascades. *Journal of Experimental Botany*. https://doi.org/10.1093/jxb/erv508

Zhang, X., & Guo, H. (2017). mRNA decay in plants: both quantity and quality matter. *Current Opinion in Plant Biology*, *35*, 138–144. https://doi.org/10.1016/j.pbi.2016.12.003

Zhang, Y., & Wang, L. (2005). The WRKY transcription factor superfamily: Its origin in eukaryotes and expansion in plants. *BMC Evolutionary Biology*. https://doi.org/10.1186/1471-2148-5-1

Zipfel, C., Kunze, G., Chinchilla, D., Caniard, A., Jones, J. D. G., Boller, T., & Felix, G. (2006). Perception of the Bacterial PAMP EF-Tu by the Receptor EFR Restricts Agrobacterium-Mediated Transformation. *Cell*. https://doi.org/10.1016/j.cell.2006.03.037

Zipfel, C., Robatzek, S., Navarro, L., Oakeley, E. J., Jones, J. D. G., Felix, G., & Boller, T. (2004). Bacterial disease resistance in Arabidopsis through flagellin perception. *Nature*. https://doi.org/10.1038/nature02485

7. Appendix I

7.1 List of figures

7.2 List of tables

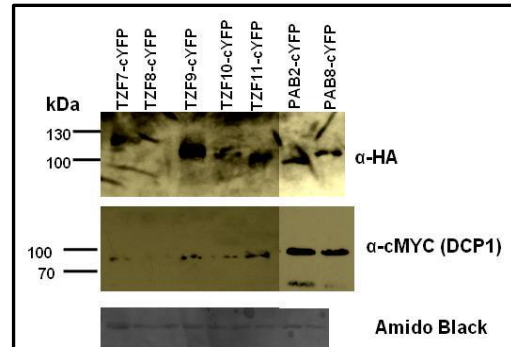# 8. Appendix II

8.1 Supplementary figures

Fig.S1.1 Western blot showing integrity of the fusion proteins.
DCP1 do not interact with the TZFs and PABs *in vivo*. Amido black staining of the membrane was used to show equal protein loading. Two sliced gels (one with the TZFs and the other with the PABs) are merged and presented together.
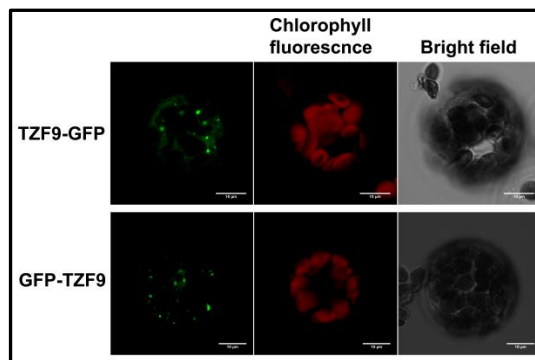

Fig.S1.2 Localization of TZF9 in cytoplasmic foci.
Representative photographs of TZF9 localizing in cytoplasmic foci when GFP was fused to either its C or N terminus as shown above. Mesophyll protoplasts were co-transfected with indicated constructs and observed by confocal microscopy 12 hrs post-transfection. Scale bars=10 μm.

8.2 Supplementary tables
Table S1.1 Conditions for qRT-PCR

Steps	Temperature (°C)	Time
Enzyme activation	95	15'
PCR cycle (40)	95	15"
	64	40"
	95	1'
Melting curve	55	30"
	95	30"

Table S1.2 PCR conditions for gene amplification (cloning)

Steps	Phase	Temperature (°C)	Time
1	Initial denaturation	98	30"
2	Denaturation	98	10"
3	Annealing	72	20"
4	Extension	72	1'
Repeat steps 2-4 (10 cycles)			
5	Denaturation	98	10"
6	Annealing	62	20"
7	Extension	72	1'
Repeat steps 5-7 (25 cycles)			
8	Final extension	72	5'
9	Final hold	14	∞

Table S1.3 Conditions for colony PCR

Steps	Phase	Temperature (°C)	Time
1	Initial denaturation	94	2'
2	Denaturation	94	15"
3	Annealing	72	30"
4	Extension	72	1'
Repeat steps 2-4 (10 cycles)			
5	Denaturation	94	15"
6	Annealing	62	30"
7	Extension	72	2'
Repeat steps 5-7 (25 cycles)			
8	Final extension	72	7'
9	Final hold	14	∞

Table S1.4 PCR conditions for genotyping

Steps	Phase	Temperature (°C)	Time
1	Initial denaturation	94	2'
2	Denaturation	94	15"
3	Annealing	70	30"
4	Extension	72	2'
Repeat steps 2-4 (15 cycles)			
5	Denaturation	94	15"
6	Annealing	55	30"
7	Extension	72	2'
Repeat steps 5-7 (25 cycles)			
8	Final extension	72	7'
9	Final hold	14	∞

Table S1.5 Antibody dilutions

Antibody	α-HA	α-His	α-GFP	α-RFP	α-myc	α-mouse	α-rabbit
Dilution	1:1000	1:3000	1:2000	1:10000	1:1000	1:10000	1:5000
Provider	Biozol	Amersham	Living Colours	Biomol	Sigma	Living colours	Biorad

Table S1.6 List of primers

SL No.	Primers	Oligonucleotide sequence	Purpose
1.	TZF7 qPCR F	5'-AAGTTGAGATCTTCGTCATCGTT-3'	Quantitative real time PCR
2	TZF7 qPCR R	5'-TGACTGGACCCATGACACAT-3'	
3	TZF8 qPCR F	5'-GGTCGGTTGAGAAAATCTCATT-3'	
4	TZF8 qPCR R	5'-TCTGCTGAGCCCATGAAAC-3'	
5	TZF9 qPCR F	5'-TGGTGAAAGAGCCACAGGA-3'	
6	TZF9 qPCR R	5'-CCACGGTCTGTTCTGTCTCC-3'	
7	TZF10 qPCR F	5'-GGTGCAGCGAGTAGAGACAA-3'	
8	TZF10 qPCR R	5'-CAATCTGCTGCTCATGGTCTA-3'	
9	TZF11 qPCR F	5'-TGGAGATGGAGATGGAATTGA-3'	
10	TZF11 qPCR R	5'-GGAAACATAAGACCCGAACG-3'	
11	AT2G41900(TZF7)-F	5'-CACCATGTGCTGTGGATCAGACCGATTA-3'	Cloning and sequencing
12	AT2G41900(TZF7)-R	5'-TCAATTCTGCTGAGCCACAAGCTG-3'	
13	AT5G12850(TZF8)-F	5'-CACCATGTGTGGTCTTGCTAAGAAGCTGGATATA-3'	
14	AT5G12850(TZF8)-R	5'-TCAGCGATCTAGGTGCAGCTGT-3'	
15	pENTR-TZF9-F	5'-CACCATGGGAGTTGATGAGCTGTC-3'	
16	pENTR-TZF9-R	5'-TCAAGCCACGGTCTGTTCTGTCTC-3'	
17	AT2G40140(TZF10)-F	5'-CACCATGTGCGGTGCAAAGAGCAAC-3'	
18	AT2G40140(TZF10)-R	5'-TTATGCCACAATCTGCTGCTCAT-3'	
19	AT3G55980(TZF11)-F	5'-CACCATGTGCAGTGGACCAAAGAGCA-3'	
20	AT3G55980(TZF11)-R	5'-TTACACCACAGTCTGCTCCTTCTCTCT-3'	
21	AT4G34110(PAB2)-F	5'-CACCATGGCGCAGGTTCAACTTCAGG-3'	
22	AT4G34110(PAB2)-R	5'-TTAAGAGAGGTTCAAGGAAGCGAGCT-3'	
23	AT1G49760(PAB8)-F	5'-CACCATGGCTCAGATTCAGCATCAGGGTC-3'	
24	AT1G49760(PAB8)-R	5'-TCAAGGTACGATGTTGTCTCCAAGAGAC-3'	
25	TZF7 internal	5'-TGAAATCTACTGAATTCAAGAAA-3'	
26	TZF8 internal	5'-TTTCGCATCAGAGAAGAA-3'	
27	TZF10 internal	5'-TTACATAATTGCCACAGG-3'	
28	TZF11 internal	5'-TCGTTTCCACTGGAAAAT-3'	
29	*tzf7*salk-F	5'-CAAAAACCCTCCCTTCTTGTC-3'	Genotyping and sequencing
30	*tzf7*salk-R	5'-ATGAAGCCAGCATTCAAACAC-3'	
31	*tzf8*-1salk-F	5'-TCAAGAATTATGTCCCATGTGG-3'	
32	*tzf8*-1salk-R	5'-ATCCAAAGTGGGTTCACTGTG-3'	

33	*tzf10*salk-F	5'-CAATTTGCGTTGCTCTTTCTC-3'	
34	*tzf10*salk-R	5'-TCTGTTCTGCCATAAACCACC-3'	
35	*tzf11*salk-F	5'-AGAAGAGTCAGCACAAGAGCG-3'	
36	*tzf11*salk-R	5'-TTCCAGTGGAAACGATGAAAG-3'	
37	M13-F	5'-GTAAAACGACGGCCAGT-3'	Sequencing
38	M13-R	5'-GGAAACAGCTATGACCATG-3'	
39	LBa1	5'-TGGTTCACGTAGTGGGCCATCG-3'	
40	LBb1.3	5'-ATTTTGCCGATTTCGGAAC-3'	

8.3 List of supplementary figures

8.4 List of supplementary tables

Acknowledgement

Curriculum Vitae

Personal Information:

Name: MANASWITA BARUAH
Nationality: Indian
Date of birth: 31.12.1989

Contact Address:

Current address: Weinberg 3, Haus Heise, Apartment 4; Halle (Saale), Germany, 06120
Phone Number: +4915157573930
Email: manaswitabaruah@gmail.com

Education Information:

Ph. D Degree: Martin Luther University; Leibniz Institute of Plant Biochemistry (October, 2014-to present)
M.Sc. Degree: Assam Agricultural University, Jorhat (August, 2012-September, 2014) Department: Agricultural Biotechnology with 7.99 (Cumulative Grade Point Average (CGPA)

B.Sc. Degree: Assam Agricultural University, Jorhat (July, 2008-June, 2012) with 7.96 CGPA
Higher Secondary: J.B. College, Jorhat (July, 2006-May, 2008) with 78.20%
High School: Don Bosco High School, Baghchung, Jorhat (January, 1994-May, 2006) with 82.8%

Halle, August 2019

Declaration

I, hereby, declare that this Ph.D. dissertation titled "Role of Tandem Zinc Finger proteins of *Arabidopsis thaliana* in plant stress responses" has been compiled by me under the guidance of Prof. Dr. Dierk Scheel and Dr. Justin Lee, IPB, Halle (Saale), Germany.

I certify that this thesis has not been previously submitted for the award of any degree, diploma, associate-ship, fellowship or its equivalent to any other University or Institution and its content was made solely based on my work as a Ph.D. student at the Martin-Luther Universität, Halle-Wittenberg. The entire work was done independently without any help from others. All citations are correct and the sources are acknowledged accordingly in the thesis references.

Halle (Saale)   Manaswita Baruah